AD_____

Award Number: DAMD17-01-1-0261

TITLE: Antibody Probes to Estrogen Receptor-α Transcript-Specific Upstream Peptides: Alternate ER-α Promoter Use and Breast Cancer Etiology/Outcome

PRINCIPAL INVESTIGATOR: Brian T. Pentecost, Ph.D.

CONTRACTING ORGANIZATION: Health Research, Inc.
Buffalo, NY 12144

REPORT DATE: May 2005

TYPE OF REPORT: Final

PREPARED FOR: U.S. Army Medical Research and Materiel Command
Fort Detrick, Maryland 21702-5012

REPORT DOCUMENTATION PAGE

Form Approved
OMB No. 0704-0188

1. REPORT DATE *(DD-MM-YYYY)*	2. REPORT TYPE	3. DATES COVERED *(From - To)*
01-05-2005	Final	1 May 2001 - 30 Apr 2005

4. TITLE AND SUBTITLE
Antibody Probes to Estrogen Receptor-α Transcript-Specific Upstream Peptides: Alternate ER-α Promoter Use and Breast Cancer Etiology/Outcome

5a. CONTRACT NUMBER

5b. GRANT NUMBER
DAMD17-01-1-0261

5c. PROGRAM ELEMENT NUMBER

6. AUTHOR(S)
Brian T. Pentecost, Ph.D.

E-Mail: Brian.Pentecost@wadsworth.org

5d. PROJECT NUMBER

5e. TASK NUMBER

5f. WORK UNIT NUMBER

7. PERFORMING ORGANIZATION NAME(S) AND ADDRESS(ES)
Health Research, Inc.
Buffalo, NY 12144

8. PERFORMING ORGANIZATION REPORT NUMBER

9. SPONSORING / MONITORING AGENCY NAME(S) AND ADDRESS(ES)
U.S. Army Medical Research and Materiel Command
Fort Detrick, Maryland 21702-5012

10. SPONSOR/MONITOR'S ACRONYM(S)

11. SPONSOR/MONITOR'S REPORT NUMBER(S)

12. DISTRIBUTION / AVAILABILITY STATEMENT
Approved for Public Release; Distribution Unlimited

13. SUPPLEMENTARY NOTES

14. ABSTRACT
Abstract follows.

15. SUBJECT TERMS
Estrogen receptor, promoter use, tissue specific regulation, gene expression regulation and control

16. SECURITY CLASSIFICATION OF:			17. LIMITATION OF ABSTRACT	18. NUMBER OF PAGES	19a. NAME OF RESPONSIBLE PERSON
a. REPORT	b. ABSTRACT	c. THIS PAGE			19b. TELEPHONE NUMBER *(include area code)*
U	U	U	UU	61	

ABSTRACT

Estrogen Receptor alpha (ER)expression correlates with a reduced incidence of breast cancer recurrence following resection of tumors. ER-protein in breast tumors increases with patient age. The project developed antibody reagents to probe expression of ER from alternate promoters taking advantage of short peptides encoded by upstream open reading frames (uORFs) in regions of the ER mRNAs that are promoter specific and not shared. We hoped that the short transcript specific peptides would act as 'Biomarkers' of promoter use.

We developed polyclonal and monoclonal reagents effective in detecting the uORF peptides of the proximal and distal ER promoter transcripts. Antisera were validated using peptides linked to Biacore chips and in western blots using fusion of the peptides to larger proteins. The small size (2000 Da) precluded direct detection in immunoblots. However, the project stalled at the point of detecting the peptide in actual tumor samples by immunochemistry. The major problem has been that the antisera cross react to other proteins giving a non-specific background. This probably relates to small sized of the peptides - providing limited numbers of antigenic features. It may be possible to use the antisera as part of the search for the peptides in cells using mass spectroscopy.

Table of Contents

INTRODUCTION

Estrogen receptor alpha (ER) plays an important role in the development and progression of breast cancer, and it is routinely used as a marker for hormone sensitivity in breast cancer patients (1). Positive ER status is a useful indicator for a first-line therapy with antiestrogens (mainly tamoxifen)(2).

ER is expressed from at least two promoters (Fig.1). The resulting transcripts from these two promoters differ only in the non-coding region upstream of the major ER open reading frame (ORF); the ER proteins from these two promoters are identical. The distal promoter is 2 KB upstream of the main translational start of the ER ORF and is spliced into nt164 of the proximal form. Both proximal and distal ER promoter transcripts have short peptide ORFs (uORFs) in the unique regions upstream of ER itself (Table 1). The proximal promoter transcript contains a 20 residue ORF which closes 50 nt upstream of the main ER ORF. We describe the peptide product of the uORF as the prox-peptide. The distal promoter transcript also contains uORFs. One of these, encoding the distal uORF peptide with 18 residues, shares 5 C-terminal codons with the prox-peptide of the proximal promoter transcript.

Our group, and others showed that ER positive MCF-7 cells mainly used proximal promoter to generate ER RNA transcripts (3). Using a new one-step, real time RT-PCR method to quantify absolute levels of the mRNAs transcribed from ER distal and prox-promoters, we were able to show that the breast tumor line MCF-7 had no detectable distal transcripts; the absolute ER prox-transcript concentration was 0.12 amol/μg total RNA. In contrast, two ER positive breast tumors had ER prox/distal mRNA concentrations of 0.0011/0.0033 and 0.0055/0.0013 amol/μg total RNA; ratios of 3.7 and 4.2 respectively (see the text of the report). It suggests that the distal ER transcript is more prevalent in breast tumors than in breast tumor cell lines. Previous studies (4) suggested that the levels of total ER protein correlated well with distal promoter usage, and ER levels in breast tumors increase greatly with patient age. Alternative promoters could have distinct tissue specificity or developmental regulation and could respond to different regulatory signals. Different controls on the alternate ER promoters may affect tumor development, response to anti-estrogen therapy. But the mechanism underlying the alternate promoter usage and the changes in ER level with age are poorly understood.

The major goal of our IDEA was to develop and test new methods for probing ER promoter use. As described above we can measure relative levels of distal and proximal promoter use by PCR on reverse transcribed RNA. However this is not a methodology that transfers easily to routine use in a Hospital lab. We had proposed that the regions of the alternate transcripts can be estimated, instead, by looking for the peptide products of short open reading frames that are distinct for the two major ER transcripts.

BODY

Development of polyclonal antisera - against the distal uORF peptide

Initial immunogens were synthetic peptides representing the translated products of the upstream open reading frames from the alternate ER promoter transcripts (see Fig 1, Table 1). The complete distal peptide (13 unique aminoacid residues, plus 5 shared with the prox-peptide) was used when attempting to make polyclonal-antisera against the distal peptide.

Peptides (5.1 umol) were conjugated at their N-terminal amine with NHS-LC-biotin II (4.1 umol, Pierce) by incubation in PBS, pH 7.4, overnight at room temperature. Solutions were stored refrigerated until use. Prior to injection, an equimolar concentration of streptavidin (based on 4 biotin binding sites per mole) was added and the solution mixed with an equal volume of adjuvant. Each rabbit received approximately 125 nmol s.c. at multiple sites. Injections were normally every four weeks, with samples for ELISA being recovered two week after injection.

The antisera from rabbits #747 and #748 to the distal peptide were able to detect immobilized distal peptide in ELISAs after 2 and more booster immunizations subsequent to the primary immunization (data not shown). The initial data showed cross reaction to a full length proximal peptide, but not against a prox peptide lacking the shared C-terminal region However, rabbit #747 showed better specificity to the distal

peptide by ELISA after a fourth boost when rabbits were euthanized and serum collected . We moved to a western blot test as a format which was more informative and which gives a measure of interaction of immune reagents with other proteins in addition to the target (= background). We used the complete distal peptide ORF fused to the C-Terminus (Fig. 2) in an over-expressed maltose binding protein (MBP, Fig. 3), these reagents were also used as alternate immunogens for monoclonal generation (see below). This approach was used so that products that were easily resolved by western blot were obtained. The native peptides are only ~2KDa and difficult to analyze by conventional SDS-PAGE and western blot, the fusion proteins are ca 40KDa).

The serum from rabbit #747 showed good specificity against distal peptide MBP fusion in Western blots (Fig. 3), this antiserum could clearly discriminate between the MBP-distal peptide fusion and MBP protein or a MBP-prox peptide fusion in a western blot. In contrast serum from rabbit #748 showed a non-specific interaction with MBP and with the prox-peptide MBP fusion. Subsequent analysis of antisera against the distal uORF peptide focused on that of rabbit #747.

Further analysis showed that the #747 antiserum at a dilution of 1:200 could detect the distal peptide at levels down to at least 25ng. This was effectively ~1.25ng of the distal peptide, given that it is ~5% of the fusion protein and we knew that we needed to be able to detect >10X lower levels to detect the peptide in cells based on crude extrapolation of our experience with antisera to the complete ER.

The next test system was detection of GFP fusions in cells transfected with DNA expression constructs. We have routinely used N-terminal GFP-fusions in studies of translational control by the uORF peptides (5, see appended paper). We typically use HeLa cells as they are easily transfected, also the cells express neither endogenous ER, nor, presumably, the uORF peptides. The Y747 antiserum had a heavy background against HeLa cells (Fig. 4 Panel 2). We therefore tried two methods two reduce the background: immunopurification on a column of a distal peptide-MBP fusion and immuno depletion on a column of HeLa protein extract. The first method was more effective. The issue of interaction of antisera with cell protein beyond the desired target has been a major problem for the project.

The background associated with the antiserum was reduced by immunopurification on a column of recombinant MBP with the distal peptide incorporated in frame as the C- terminus. Judging from the behavior of the immunopurified serum we think the major result of immunopurifcation of this Y747 antiserum was the elimination of non-specific immunoglobulin and the background was reduced because we were adding less material that the detection system (second antibody) could interact with in western blots. The model system has two advantages: first we have the confidence that the desired protein is present because of the option of probing with anti-GFP antisera. Second the 22 000 Da fusion protein is a convenient size and binds to membrane whereas the small 2000 Da peptide alone does not.

The immunopurifed Y747 antiserum still failed to detect the distal uORF-GFP fusion we have used in published studies of translational control of ER (5, also appended) though the product was detectable (though the GFP fraction) with an anti-GFP antiserum (Fig. 4). The first thought was that the antiserum was too weak for the application. A second thought was that the original coupling of peptide to carrier streptavidin was through the N-terminus of the peptide and that was similar to configuration in the MBP fusion (Fig. 2) while in the original GFP-peptide construct the link was from the C-Terminus of the peptide to the N-terminus of GFP and potentially constrained the C-terminus of the peptide with the risk of conformational problems in analysis.

We therefore made new GFP fusion constructs for both the distal and proximal constructs where the uORF peptides are C-terminal extensions of GFP (Fig. 2). Blots in Fig. 5 are of lysates of cells transfected transiently with GFP constructs. All of the transfected cell populations show a band with a commercial GFP antiserum. The size varies depending on the peptide ORF (if any) fused to the GFP ORF and on the length of any intervening sequences that become part of the final ORF, this is different for C- and N-terminal fusions. We were able to detect signal with the anti-distal Y747 anti-serum in addition to GFP in western immunoblots of cell extracts of cells transfected with the distal uORF peptide C-terminal to GFP. However, this is really too weak for any routine use and we found the most successful blots had been left overnight in antibody solutions at ~4 C indicating a weak interaction (also see later section where we included Y747

antsierum in Biacore analysis).

Clearly the data for the distal peptide polyclonal antiserum #747 show that presence of the 5 residues shared by the prox peptide did not automatically lead to cross reaction between prox and distal peptide reagents. The distal peptide was immunogenic but the resulting polyclonal antisera were weak and had difficulty in detecting the distal ORF peptide in transfected cell models. Data with the immune reagents to the distal ORF peptide indicated that antisera can be raised, but our preliminary reagents were not strong enough for use in cell analysis.

A second approach to generating immune reagents against the distal peptide was to use monoclonals (see below).

Development of polyclonal antisera - against the uORF peptide of the ER proximal promoter transcript

The first approach to making antisera against the prox-peptide was to use a C-terminal truncated prox-peptide containing only the 15 residues not shared with the distal peptide, with the shared WPAGF region (Table 1) was not included. This was done in parallel with studies described above for antisera against the full length the distal peptide and also used biotin linkage to streptavidin . In the preparation of the initial prox- and distal antiserum one goal was to understand the extent of problems arising from the shared C-terminal residues

Serum from a rabbit (#729) receiving the prox-peptide showed specificity and immunoreactivity against the immunizing peptide after preliminary immunization and two followup immunizations of immunogen by ELISA. The immune serum from rabbit #729 after the second and subsequent boosts had the best titer and specificity of all of our initial experimental animals, however, the anti serum *did not* detect a prox-peptide that was complete , ie contained the 5 residues shared with the distal peptide (Table 1) in either ELISAs or western blot tests (data not shown). Some characteristic of the complete peptide hindered immunoreactivity with the antibodies raised against only the unique regions of the prox-peptide.

We made a second attempt to develop polyclonal antisera to the proximal peptide based on experience with the first generation polyclonals and with mouse immunizations for monoclonals. The two immunogens were a raw full length prox-peptide carrying the unique and shared regions *without* linkage to any carrier and a recombinant fusion of the prox-peptide to the C-terminus of MBP. In the latter case the MBP may act as 'carrier' possibly altering presentation to the immune system. Rabbits were immunized using complete Freund's adjuvant initially. Follow up boosting was in incomplete Freund's adjuvant as approved by our IACUC.

The rabbits, Y925 & Y935, immunized with the raw peptide (unconjugated synthetic peptide) initally showed the strongest and most specific signal in the BiaCore assay (Fig. 6) in the initial test bleeds of the rabbits. There was clear discrimination for the prox peptide sector over distal sector with the sera from rabbits receiving the raw peptide. Note that BiaCore signal was limited for rabbits Y936 and Y941 that received the MBP fusion protein, and discrimination between distal and proximal peptide bound to BiaCore sectors was poor. BIAcore signal for Y941 improved following further boosting of rabbits but the failure to discriminate betwwen prox and distal peptides remained (see Fig. 13 comparing Y941 to a monoclonal).

Additional analysis by Biacore is shown in Fig. 7, this data is included to illustrate how the second generation antiserum # Y935 raised against uncoupled prox-peptide had higher affinity for its target as shown by detection of a continuing interaction on the chip in the wash phase, as compared to the signal (on the distal peptide sector) with the Y747 antiserum against the distal peptide. Y747 interaction is only seen in the loading phase (where the fluid stream contains antibody) and is lost in the wash phase (where the antibody is no longer included in the fluid).

The western blot test of antisera against recombinant MBP-uORF fusions is meaningless with the antisera raised against MBP-fusion proteins as the signal can be from antibodies against the MBP as well as uORF peptide. However, the more relevant test of western blots of GFP fusions was still useable. The first clear point from that test (Fig. 8) was that antisera against free peptides (Y925/35) were unable to detect the GFP fusion proteins, though some non-specific bands were detected. This is a paradox as Y935 and Y925

gave a strong signal in the BiaCore. We suspect we have reagents against at least two specific conformations/epitopes in the prox-peptide. One N-terminal and the other C-terminal linked into the region common to the distal uORF-encoded peptide The Y941 antiserum against the prox peptide-MBP fusion, in contrast to Y935, was readily able to detect C-terminal fusion of the prox peptide to GFP . It also was conformation sensitive as seen for Y747 (against distal -GFP fusions) as it did not detect the prox-peptide fused N-terminal to GFP.

Note that we had expended considerable effort in detecting the distal-peptide GFP fusion with antisera Y747, while, in contrast, Y941 is as easy to work with as commercial antisera against GFP, giving strong signal and low backgrounds (both to membrane and other HeLa proteins). These were re excellent preliminary characteristics. Y941 gave a specific signal with the ER uORF prox-peptide fused to the C-terminus of GFP. Its gave no signal with GFP in cells transfected with the parent pEGFP construct.

A limitation of the Y941 antiserum was that it also crossed over and detected the distal C-terminal uORF-GFP fusion, as seen in western immunoblots (Fig. 9) and the Biacore analysis included for comparison to one of the monoclonals (Fig. 13) the latter contains data for the final immunoserum obtained from the rabbit Y941 (the data in Fig. 6 is for an intermediate test bleed). We also had a successful fusion for monoclonals specific for the distal peptide by the time we had characterized Y941 and the other polyclonals against the prox-peptide. We therefore decided to use Y941 in tests of immunochemistry.

Samples from the Y941 antiserum were also cleaned up using affinity purification on a column of immobilized peptide. A urea elution had to be employed to release the high affinity fraction from the column matrix.

Monoclonal antibodies against the uORF peptide of the ER distal promoter transcript

Generation of monoclonals (mAbs) was done in association with our immunology core.
Our first attempt at fusions for mAbs using synthetic peptides against the distal and prox-uORF peptides was unsuccessful in generating clonal lines that continued to produce antibodies.
In a second attempt we focused on the distal peptide and we used the fusion of the peptide uORF to the C-terminus of maltose binding protein (MBP) (see cartoon in Fig. 2) as the immunogen in the mice used in generating hybridomas. This fusion is a recombinant protein we originally made as a screening tool.

The serum of immunized mice was assessed by the biacore assay the cell supernatants from the cloned hybridomas were tested using the Biacore 3000 (Fig. 10). The Biacore chip carried four sectors: A blank to monitor salt effects which are a problem in this technique, a sector with antibody to the mouse Fcγ which provides a measure of antibody level in samples and finally separate sectors to which synthetic prox and distal uORF peptides were attached. Interactions are detected by effects on refraction or 'plasmon resonance' The peptides on the chip did not include the MBP fraction of the immunogen. However, the signature of any antibodies to MBP without interaction with the uORF peptide regions would be signal with Fcγ sector, indicating production of mAb by the hybridoma, but no signal with the peptide sectors. The comparison of signal with the two peptide sectors gives an indication of specificity of the mAbs for the uORFs and selectivity for the immunizing distal peptide.

Multiple hybridomas from this new fusion produced immunoglobulin and interacted with the uORF peptides. Biacore analysis indicated that one clone, #204 clearly gave the strongest signal in this assay and was specific for the distal peptide. Interaction of the mAb #204 with the Biacore chip is indicated in Fig. 10A. Initial work of screening cell supernatants and the ascites fluid was done with raw material. The ascites mAb gives a strong signal with the mouse Fcγ sector and interaction is seen with the distal sector. The signal seen with the proximal sector was essentially the effect of buffer changes. The immune protein from ascites was concentrated and somewhat purified by application to and elution from an immobilized protein G (Pierce, Rockford IL). A protein G-purified fraction gives a cleaner signal in the Biacore (Fig. 10B). However note that ascites should express a single immunoglobulin. This is in contrast to the immunopurification of the Y941 antiserum where we were attempting to isolate a subset of immune molecules for the polyclonal pool. For the mAbs specificity and affinity comes from selecting the 'right'

clone.

We cannot directly analyze western immunoblots blots of the peptides as the short peptides do not bind to the blot membrane. We therefore again used fusions to GFP and MBP (Fig. 2) as test proteins. Analysis was done using a western blot panel of samples that we knew, from prior work with the polyclonals, provided a rapid survey of the effectiveness of uORF peptide antisera.

The mAb #204 detected (Fig. 11A) the distal-MBP fusion alone out of samples containing MBP, MBP-distal fusion and MBP-prox. This assay uses purified recombinant protein so this is a fairly simple test. The major points here are the specificity for the distal-MBP fusion and the lack of reactivity towards either MBP or the prox-MBP fusion ie the reactive epitope is soley associated with the uORF encoded sequence.

A more challenging test is to detect fusion protein expressed in transiently transfected mammalian tissue culture cells. A band compatible with a distal uORF fusion to the C-terminus of GFP was detected in transfected HeLa cells. The equivalent band is missing in tracks where cell were transfected with prox-GFP fusions or GFP alone. The blot was reprobed (Fig. 11B) with an anti-GFP antiserum to successfully demonstrate the presence of related GFP protein in those other tracks. However note that the mAb did interact with other HeLa proteins giving a background (Fig. 11A). This proved to be a major problem for immunochemistry.

A survey of some of the other clones from the hybridoma screen was undertaken. Culture supernatants from several clones that were positive by Biacore but not originally grown as ascites were tested. There was a strong reaction with both Prox-MBP and Distal MBP fusions by reagent from clones #25, #342 (Fig. 12A) and #349 (not shown). Any mAbs that interact with both peptides could have some utility, similar to the Y941 polyclonal. However, the signal was also found with MBP (Fig. 12B) suggesting non-specific interactions or affinity for the MBP, which was in the original mouse immunogen. This has not been pursued further. Clone #238 had a weaker signal in western immunoblots but this was specific for the distal peptide, the weakness of the signal persisted in tests against GPF fusions so we have focused on the clone #204.

Comparison of immune reagents

The Y941 rabbit polyclonal raised against the MBP-prox uORF peptide fusion which works in a number of our tests but detects both distal and prox peptides (Fig. 9 & 13). The mAb 204 has better specifity for the distal peptide but likely does not have as high affinity interaction as the rabbit polyclonal Y741. This can be seen in the greater proportional loss of signal (Fig. 13) in the wash phase of Biacore analysis where mAb #204 signal against the distal uORF sector is lost while that of the Y941 antiserum is largely resistant to this wash out. On a more anecdotal level we initially had variable success in western immunoblots with mAb #204 which we finally tracked down to effects of temperature - we were doing overnight incubations at reduced temp (14 C) while short incubations were done at room temp (25 C) and were failing.

The pair of reagents provided a useful set to move to immunochemistry

Immunochemical analysis with the anti uORF peptide antisera

The immune reagents were applied to tissue, this is demonstrated in Fig.14. We used polyclonal antisera from rabbit Y941, with and without immuopurification; the mAB #204 and a commercial antiserum, HC20 (SantaCruz Biotec), against ER protein. Methodology was established on individual sections cut from paraffin blocks, and was then applied to tissue arrays carrying ~50 samples. Deparaffinized sections were treated with hydrogen peroxide to destroy endogenous peroxidases. Blocked samples were incubated with the primary antiserum and then with a 'universal' second antibody in the Vecstain ABC system (Vector Labs, Burlingame Ca). Visualization was with the Vecstain DAB reagent kit. We have not used a counterstain. Antigen retrieval was performed for ER and mAb #204 after xylene treatment to remove paraffin wax. This was done by microwave heating in the Vector Labs citric acid-based unmasking reagent. Antigen reterieval was used with the ER antibody and with mAb 204. It is essential to

use antigen reterieval wtih the ER antiserum. Prelimenary data had indicated that the Y941 bleed 3 anti-prox-peptide did not require antigen retrieval.

Comparison of different samples is facilitated by using an array of block punches so that all sampels are processd with a specific antibody in the same way at the same time. A stark conclusion of comparing sections for the 50 or so samples from ER positive and negative tumors is that ER status does not affect the staining patterns we see with mAb#204 and with the Y941 reagents. A sample montage of four tumors is shown in Fig. 14. The patient and tumor characteristics are summarized in table 2.

Logic indicates that ER status should affect presence of the targets we are attempting to detect. This suggests that what we are seeing is interaction with other proteins. This is supported by comparison of Y941 bleed 3 with the immunopurified fraction derived from Y941 bleed 3. There is a large decrease in staining with the immunopurified fraction - a strong indication that we had eliminated some antibodies targeting proteins other than the prox-peptide. Initially at low power we thought that all staining was eliminated hwoever, there is some pattern to the staining upon inspection with a better 'scope at X600 (Fig. 15). Unfortunately this staining also was essentially identical for the ER positive and negative tumors, in addition relatively strong staining was seen in fields of #17 that appeared to be monocytes and other immune cells - an inappropriate correlation for a link to ER . The mAb #204 gave strong staining of infiltrating tumor cells in punch sections but again this did not correlate with ER status. Our pathologist commented that staining looked rather like that for cytokeratins though we note that the most prominent band seen in westerns (Fig. 11) with mAb #204 is 25 kDa, too small for the major cytokeratins.

As we close out BCRP funded studies the project seems to be failing in its ultimate goal of providing a means to discriminate between the promoter origins of ER in tumor samples. A first problem is probably a background of inappropriate staining which is preventing us from addressing the questions of are the peptides expressed and does expression correlate with promoter use. For Y941 this is partly controlled by immunopurification which should generate a monospecific immune fraction. For monoclonals that is not really feasible since there should only be one specificity and classically the solution would be to search for a better clone against the best epitope. Unfortunately we have only a limited universe of epitopes since we only have a 2000 Da peptide.

A second problem remain the question as to whether the uORF peptides actually survive in the cells. All our mechanistic data (see 5 and unpublished) indicate that the uORF of the prox promoter transcript has effects that are mediated at the protein level. However we have always been aware that the most likely mechanism underlying those effects relates to action during the act of synthesis on the ribosome. Hence the survival of the peptide beyond that time could be of no consequence to the cell. We do have an application for the antisera in future mechanistic studies of the ER uORFs using cell and in-vitro translation models. The aim would be to detect the peptides by mass spectrometry. The antisera could be used in work up of samples to enrich the fraction to be applied to the mass spectrometer. We envisage using the antisera in immuno-precipitation enrichment steps. The point being that detection of the peptides will be by the mass spec so that co- precipitation of cross reacting proteins will not be a problem in this approach.

If the entities we were aiming to detect had been a proteins of 20 kDa rather than 2 kDa peptides then we could have used western blot analysis, like many other labs in studies of other proteins, and ignored the additional 'non-specific' bands. A question we have asked in reviewing material is whether our screening approaches have led to us discarding useful reagents. The one point were we my have made an error was in not following up on the anti prox-peptide polyclonals Y935 and Y936 that showed a strong interaction with the BIAcore but failed to work well in western blot tests. There is the possibility that they would still work in an immunochemistry format, though that assumes the non-specific interactions seen in westerns could be eliminated by an immunopurification step. However, the non-specific signal with those antisera was much heavier than for Y941.

Comparative analysis of ER alternate promoter use: RNA levels

A one-step, RealTime RT-PCR method capable of quantifying absolute concentrations of the mRNAs transcribed from the distal and proximal promoters of the estrogen receptor in cell lines and tissues has been achieved. DNA templates specific for each transcript and flanking the real time RT-PCR target regions were prepared and quantitated by UV absorbance, these are used to generate standard curves. The primer pairs for analysis of transcripts from alternate ER promoters are as we previously described (3). The modified assay allows direct separate estimation of transcripts from each promoter, rather than apportioning total ER mRNA level based on a ratio of alternate transcripts.

Standard curves were constructed for the assay of promoter use in breast tumors and cell lines. The uterine tumor line Ishikawa contained 0.022 and 0.012 amol/μg total RNA of the proximal and distal transcripts, respectively. The proximal to distal transcript ratio of 1.8 is in good agreement with previously determined ratios of approximately 3 by other assays. Consistent with our previous findings, the breast tumor line MCF-7 had no detectable distal promoter; the absolute proximal promoter concentration was 0.12 amol/μg of total RNA. In contrast, two estrogen receptor positive breast tumors had proximal/distal promoter concentrations of 0.0011/0.0003 and 0.0055/ 0.0013 amol/μg total RNA – ratios of 3.7 and 4.2, respectively. These data demonstrate that the very low concentrations of the estrogen receptor promoter transcripts can be quantitated by real time RT-PCR and suggest confirmation of previous studies indicating that the distal promoter transcript is more prevalent in resected breast tumors than in breast tumor cell lines and perhaps in noncancerous tissue where approximately equal concentrations of the two promoters reportedly exist.

The ability to quantitate alternate ER absolutely and with one tube for each assay is an improvement that will allow use of smaller tumor samples compared to our earlier technique. We can now run one experimental tube (for each promoter estimation in a sample) and obtain levels from a standard curve. In prior analyses we needed to run each sample with several levels of competitor to measure ER mRNA and then run an assay to determine the relative levels of the promoters.

The methodology works well with RNA from unfixed tissue but RNA from blocks, even with crosss links reversed by heating, is not of sufficient quality to allow analysis of the many samples we accumulated from the cooperative human tissue network. As we carried out IHA and sectioned tumor blocks we had been collecting multiple thick sections for isolation of RNA. However, the assay will not work consistently with RNA from fixed blocks - the simple assay for ER exons 4-6 is more feasible but the constraints of GC content , limited selectable region from the transcript specific region coupled with size product size limits set by the degraded state of the RNA push the methodology too far.

We do not have access to significant numbers of **unfixed** (frozen) tumor samples to do an extensive study of ER promoter use. We had hoped to form a collaboration with a hospital group proposing to look at breast cells recovered by ductal lavage in the mid period of the project but they did not go ahead with setting up lavage . We did establish some of the detection limits for our methodology using Ishikawa cells (which utilize both the distal and proximal promoters). We do have another potential opportunity to collaborate in examining ER promoter use in cells recovered in the expressed milk of lactating healthy donors as part of a biomarkers study.

Preparing for potential handling of ductal lavage samples, we were able to demonstrate successful analysis on limited cell samples using a model system. The model system was the Ishikawa cell line which uses both distal and proximal promoters to generate ER transcripts. We were able to isolate RNA from 3000 cells using conventional (Trizol, Invitrogen) methodology and to assay both shared regions and promoter specific regions of ER RNA transcripts.

Our RealTime PCR assay could detect ER transcript shared regions and promoter specific regions in aliquots of the RNA from 3000 Ishikawa cells (Fig. 16). The melting curves were appropriate indicating specificity for the assay (Fig. 17). It is quite feasible to isolate sufficient cells from milk samples and our potential collaorator's lab was able to detect ER in some of the cells samples they had collected and analyzed using our ER exon 4-6 primer set.

KEY RESEARCH ACCOMPLISHMENTS

* Creation of polyclonal antiserum capable of detecting peptides derived from the upstream open reading frames in estrogen receptor transcripts.

* Creation of a hybridoma making monoclonal antibodies capable of detecting peptide encoded by the distal estrogen receptor promoter transcript.

* Application of immune reagents to tumor samples.

* Development of realtime PCR assays capable of measuring alternate estrogen promoter utilization by determining levels of alternate mRNA forms (described in year two report).

* On the downside the immune reagents are not adequate for the intended task of evaluating expression of the uORF peptides as surrogate biomarkers for promoter use in a immuno histochemical format, though we my be able to use them in a research setting coupled with Mass Spec analysis

REPORTABLE OUTCOMES

Personnel
The following individuals were the principal recipients of financial support from this award:
Lin, YiLi
Luo Mingfei
The following were supported for limited periods:
Rumpler, Mark
Prasad, Aparna
Bessette, Erin

Immune reagents
Antisera against ER uORF peptides were developed together with monoclonal antibodies agains the ER distal ER promoter uORF peptide

Publications
The following article acknowledges support by both this award and a related Concept is acknowledged. This IDEA extensively uses the GFP constructs that are the core of this paper:
Pentecost, B.T., R. Song, M. Luo, J.A. DePasquale, and M.J. Fasco. (2005) Upstream regions of the estrogen receptor alpha proximal promoter transcript regulate ER protein expression through a translational mechanism. *Mol. Cell Endocrinol.* 229, 83-94.

The following study acknowledges the current award though the relationship is tangetial and Dr Pentecost is not a primary author:
Fasco, M.J., A. Amin, B.T. Pentecost, Y. Yang, J.F. Gierthy (2003) Changes in estrogen receptor-related phenotypic changes in MCF-7 cells during prolonged exposure to tamoxifen. *Mol. Cell. Endocrinol.* 206, 33-47.

Presentations
Dr Pentecost visited with Dr K Arcaro at U Mass at Amherst and to presented a seminar mainly on the work funded in this project (Oct 29, 2002).

Abstracts
Era of Hope 2002 Fasco, Michael J., and Pentecost, Brian T. Analysis of Alternate Estrogen Receptor Promoter Use Using Novel Assays

Patents
None

Grant applications
A concept application:
Control of Estrogen Receptor Alpha (ER) expression: Mechanism for Action by a Peptide Encoded Upstream of ER in the ER Proximal Promoter transcript (BC032467) directly related to the funded IDEA was submitted to the BCRP in January 2004 by the PI but not funded.
A predoctoral support application:
Translational Control of Estrogen Receptor Alpha (ER): Mechanism for Action by a Peptide Encoded Upstream of ER in the ER Proximal Promoter transcript was submitted by student Mingfei Luo to the 2003 and 2004 BCRP competitions in May of 2003 and 2004 (BC030820, BC 044505). They were not funded.

CONCLUSIONS

An important question when developing tools is when to quit, expiration of funding is one way to define that point. In the first year of the project we developed an antiserum that worked well enough to say that development of immune reagents against our targets was possible. In the second year we developed Y941, a polyclonal raised against the prox uORF peptide which works in a number of models but detects both distal and prox peptides, as reported in the year two report. In the current report period, we have developed a monoclonal antibody reagent which specifically detects the distal uORF peptide. We consider this combination to be adequate for testing of the IDEA under which we were funded: Y941 polyclonal was proposed to give a readout for distal plus prox peptide while the mAb #204 should detect only the distal fraction. In the no-cost extension year we critically assessed the immunostaining patterns and conclude that reagents are not up to addressing the question of alternate promoter use. Indeed the future use of the antisera may in work up of cell extracts in an attempt to prove that the uORF encoded peptides are present in cells using the respective ER promoter

REFERENCES

1. **Osborne CK** 1998 Steroid hormone receptors in breast cancer management. Breast Cancer Research & Treatment 51:227-238

2. **Leclercq G** 2002 Molecular forms of the estrogen receptor in breast cancer. J Steroid Biochem Mol Biol 80:259-272

3. **Fasco MJ** 1997 Quantitation of estrogen receptor mRNA and its alternatively spliced mRNAs in breast tumor cells and tissues. Analytical Biochemistry 245:167-178

4. **Hayashi S, Imai K, Suga K, Kurihara T, Higashi Y, Nakachi K** 1997 Two promoters in expression of estrogen receptor messenger RNA in human breast cancer. Carcinogenesis 18:459-464

5. **Pentecost, B.T., Song R, Luo M, DePasquale JA, Fasco MJ** 2005 Upstream regions of the estrogen receptor alpha proximal promoter transcript regulate ER protein expression through a translational mechanism. Mol. Cell Endocrinol 229: 83-94.

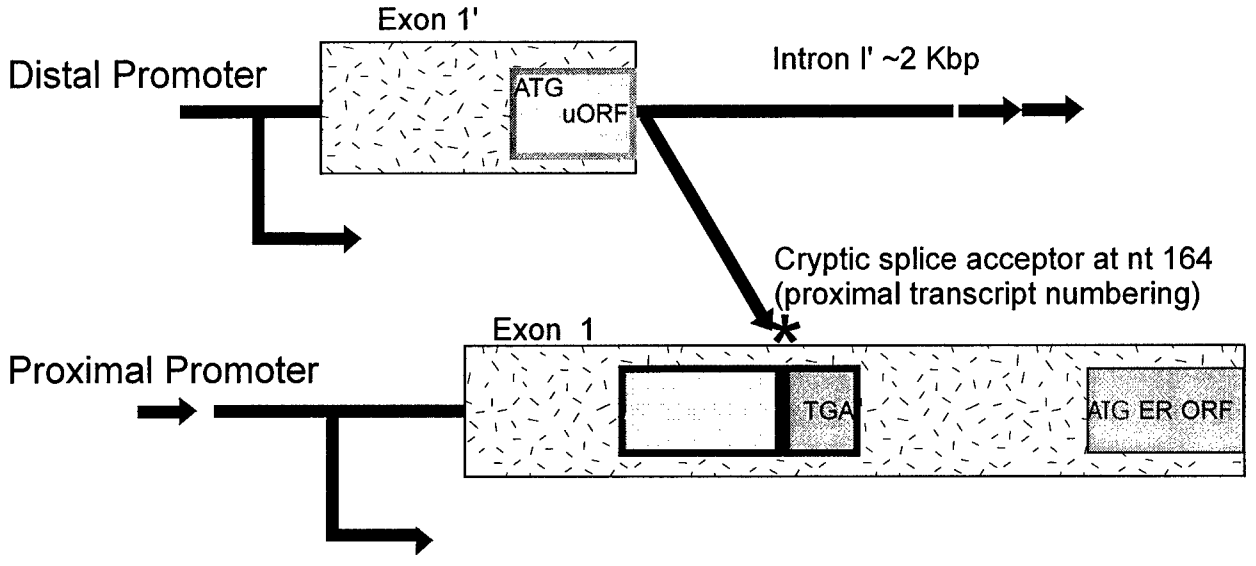

..gcgggac MetArgCysValAlaSerAsnLeuGlyLeuCysSerPheSerArg**TrpProAlaGlyPheTer**
ATGCGCTGCGTCGCCTCTAACCTCGGGCTGTGCTCTTTTTCCAG**GTGGCCCGCCGGTTTCTGA**gcc...

..caagccc MetGluHisPheTrpLysAspValLeuAspProAlaGl**yTrpProAlaGlyPheTer**
ATGGAACATTTCTGGAAAGACGTTCTTGATCCAGCAGG**GTGGCCCGCCGGTTTCTGA**gcc...

Fig. 1: The human estrogen recptor alpha is principally transcribed from two alternate promoters in human breast tumors.

The alternate mRNAs encode exactly the same protein but vary in regions 5' to the major protein open reading frame. Splicing for the distal promoter transcript occurs in a region encoding a upstram ORF in the proximal transcript. This results in differnt uORFs from the two transcripts, but they share five C-terminal codons.

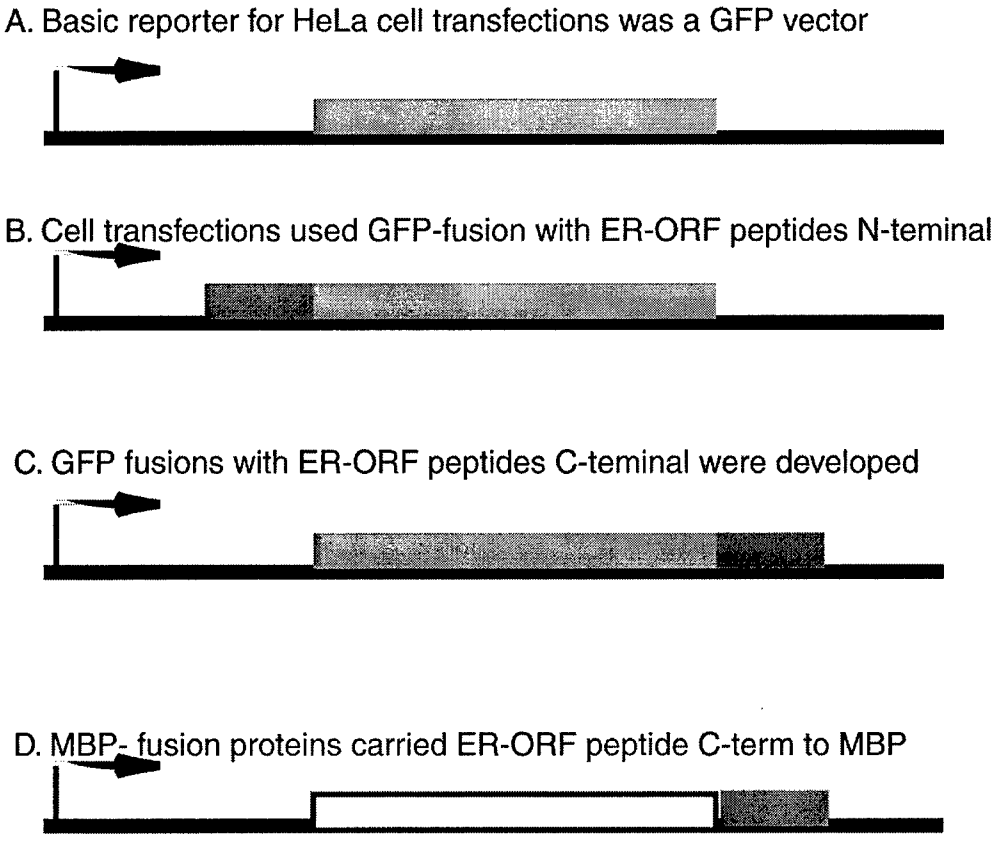

Fig. 2: Cartoon Illustrating some of the constructs designs utilized in studies

A. Our early cell reporter studies of the ER-uORF peptides utilized constructs based on Clontech's pEGFP-N1 which encodes a GFP protein expressed from a strong CMV promoter. This can be detected by its fluorescence in cells and as a protein in Western blots and immuno-histochemistry using anti-GFP antisera.

B. The majority of our cell studies utilized constructs in which the ER-uORF peptides were placed N-terminal to the GFP ORF in pEGFP-N1. The inserted fragments for the proximal and distal uORFs were included in separate constructs. The expression of the GFP fusion proteins can be detected as GFP fluorescence, GFP immuno-detectable protein in Western blots and potentially by suitable antisera against the uORF peptides

C. We created ER-uORF- GFP constructs in pEGFP-C1 after the failure of several antisera anti-ER uORF antisera to detect the relevant N-terminal GFP fusions. In these constructs the ER-uORF peptides are expressed as C-terminal extensions to GFP. The uORF peptides in the two types of GFP fusions may have differing conformations affecting detectability by antisera..

D. A tool in analyzing antisera and in making some antisera was a recombinant maltose binding protein E. coli expression system (see year one report) in which uORF peptides were expressed as a C-terminal extension of the easily purified MBP.

Rb Antiserum #747 Rb Antiserum #748

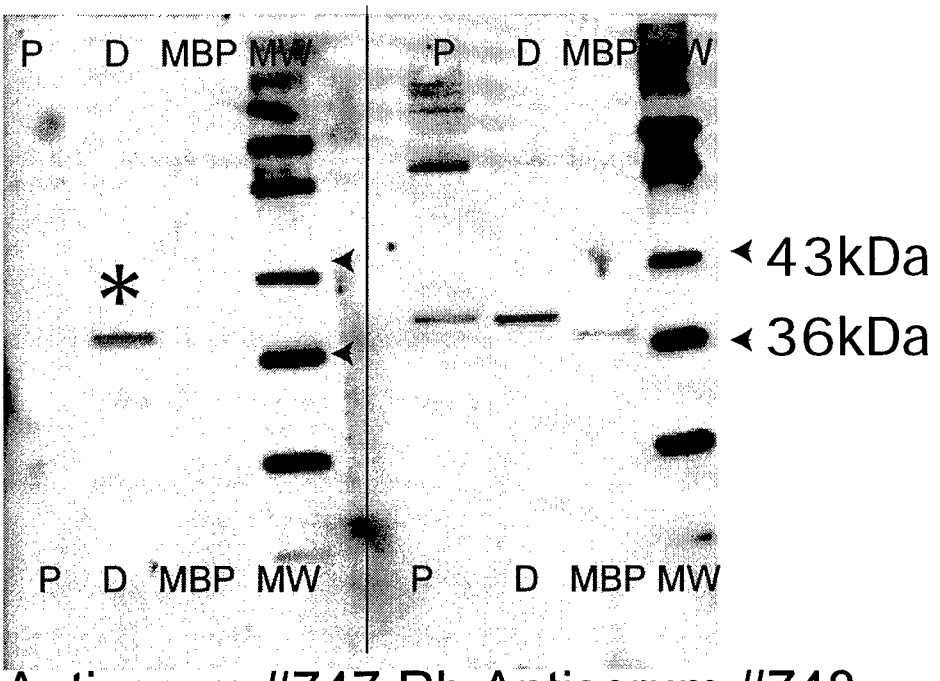

Rb Antiserum #747 Rb Antiserum #748

Fig. 3 : Analysis of Rabbit antisera against the ER distal uORF peptide

Dilutions (1:200)of antisera from two rabbits (#747, 748) immunized with synthetic peptides corresponding to ER the distal promoter transcript uORF were tested in wes tern immunoblots against 100ng purified E.coli expressed ~40kDa MBP, proxpeptide -MBP (P) and distal peptide-MBP (D) C-terminal fusions. Samples analyzed in 10% acrylamide gels (NuPage) were blotted to immobilon. blots were incubated overnight with first Ab, bands in washed blots were detected using HRP-conjugated second Ab and Pierce supersignal for chemiluminescent detection. Only the #747 antiserum gave detection specific for the distal peptide-MBP(*). The 748 antiserum cross reacted with MBP and the prox-fusion.

Fig F3 bleed4_747-748-MBP

Fig. 4: Test of distal peptide Antiserum (rabbit #747)

Panel 1: GFP Ab

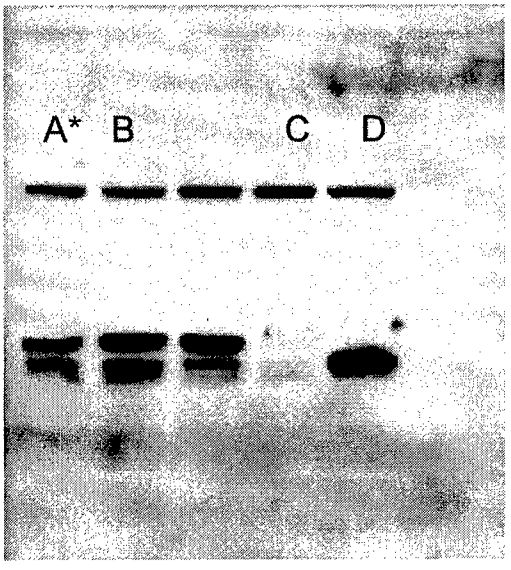

Panel 2: #747 Antiserum (distal peptide)

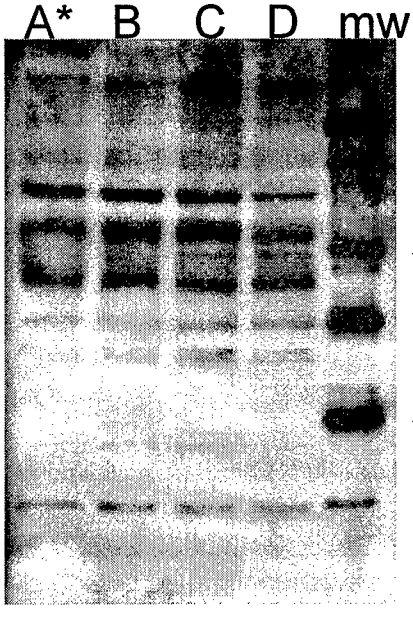

Hela cells were transfected with a GFP-distal pepide fusion construct(A); a prox peptide GFP fusion (B) or parent vector pEGFP-N1 (C). An mock transfected control HeLa was included (track D). Parallel blots were probed with antisera to GFP (Panel 1) or the distal ER upstream peptide (Panel 2, rabbit #747)

Transfected cells showed (panel 1) GFP or GFP-fusion bands at ~20-22kDa and a reference band at ~40kDa for a cotransfected reference that carries GFP fused to a 20KDa protein ORF Note that track D is blank as there was no expressed GFP in track D.

Transfected and mock transfected cells showed similar patterns of bands in Panel 2, there was 'non-specific' binding to endogenous proteins. Track A (*) is the only track that should light up withe the #747 antiserum. Note that we can see no unique band around the 23kDa size region that is identified by one of molecular weight markers (MW).

The #747 antiserum was used at 1:200 and incubated with blots overnight. Samples were run in 10% acrylamide NuPage gels and blots were to immonbilon. Chemiluiescent detection with HRP- conjugated2nd Ab was used

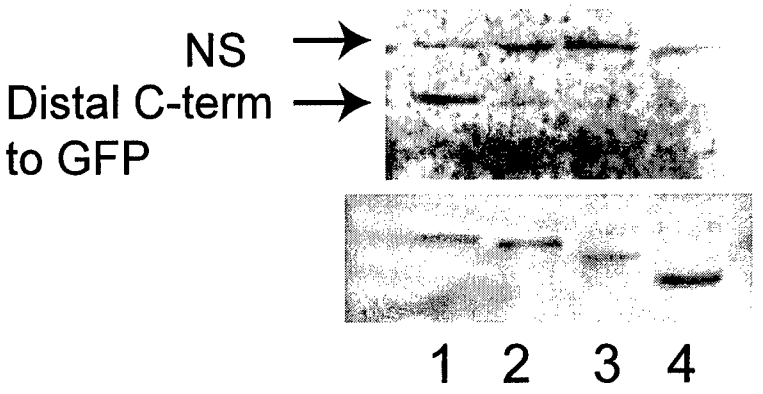

1. Distal peptide uORF fused C-terminal to GFP
2. Duplicate of transfect 1 (alternate construct)
3. Distal peptide uORF fused N-Terminal to GFP
4. GFP from parental construct pEGFPN1

(NS = non specific band)

Fig. 5: Y747 anti-serum detects ER uORF peptide C-terminal to GFP, but not N-terminal to GFP

Affinity purifed Y747 antiserum failed to detect a distal-uORF-GFP fusion in when the petide uORF was N-terminal to GFP, configuration we have routinely used instudies. The uORF placed C-terminal was detected. This was tested after consideration that the immunizing pepide had been tethered by its N-terminus to carrier for immunization and the detected form probably reflects effect of this conformation. Detection of GFPfusion by Y747was challenging and at the limit of the reagent's usable range. This likely indicates that Y747 won't detect free peptide in ER positive cells. However the studies did provide a knowledge base thatwe applied in later studies.

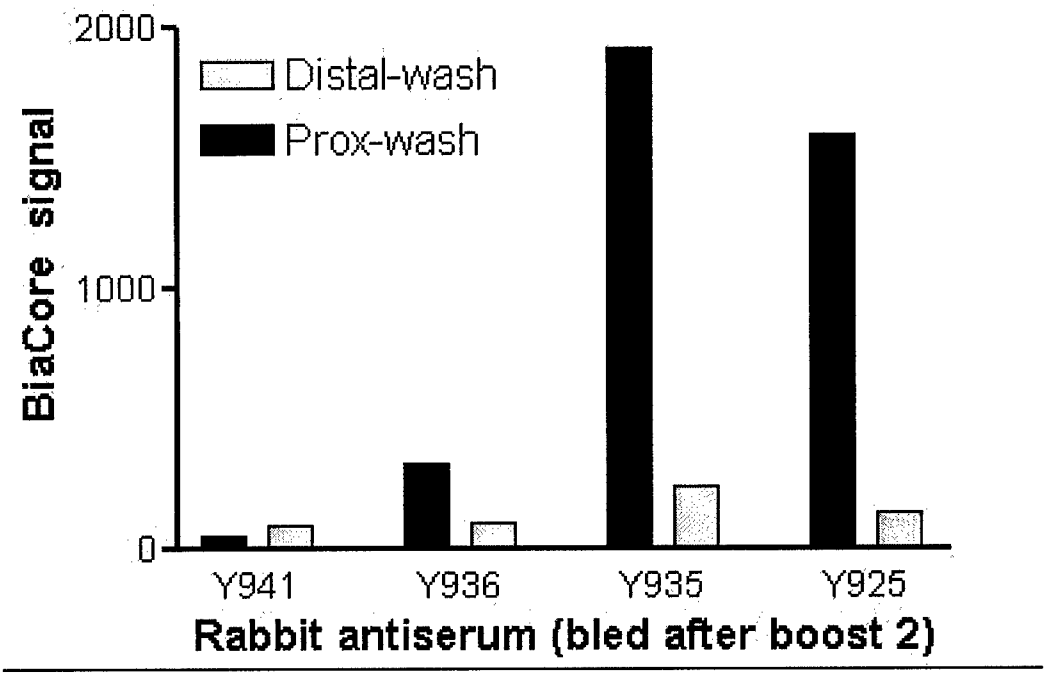

Fig. 6: Biacore analysis of antisera against the ER uROF prox-peptide

Sera were drawn and analyzed 2 weeks after the second boost in incomplete Freund's adjuvant.

Y935 and Y925 show a strong signal in the Biacore against the immobilized prox-petide with strong discrimination between the prox and distal sectors. These rabbits were immunized with the complete, but free and unconjugated, ER uORF prox peptide. Y941 and Y936 antisera, that were raised against a recombinant protein with the prox-peptide fused to the C-terminus of Maltose Binding protein, show limited activity against the imobilized distal and prox peptide with poor discrimination for immunizing prox peptide sector.
Note that Y941 antiserum had limited activity in the Biacore assay at this stage yet is the only one of the four antisera that has good activity in Western blots against GFP-proxpeptide fusions.

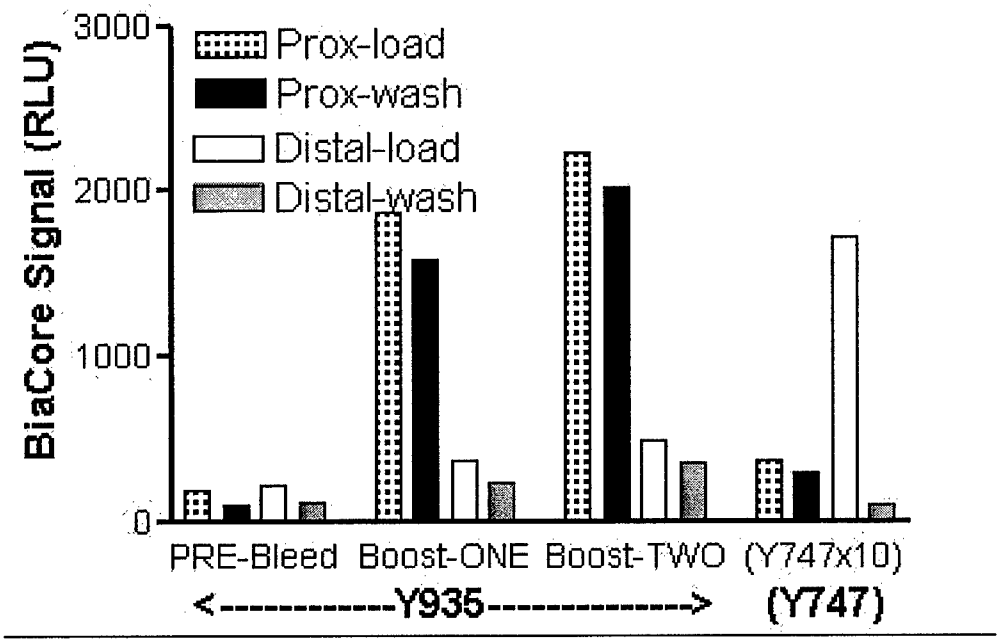

Fig. 7 : Biacore analysis for Rabbit Y935 serum

BiaCore analysis indicated that serum from Y935 developed a strong response against the immunizing prox-peptide. The serum has a high affinity component that does not disassociate during the pre-regeneration wash. That is in contrast with our earlier Y747 serum against distal peptide which is eliminated in the wash step. The Y935 serum interaction shows good discrimination for the proximal ER uORF peptide over the ER-uORF distal peptide with which it shares 5 C-terminal residues.

Note the discrepancy that Y935 has excellent signal in this assay but not in western blots.

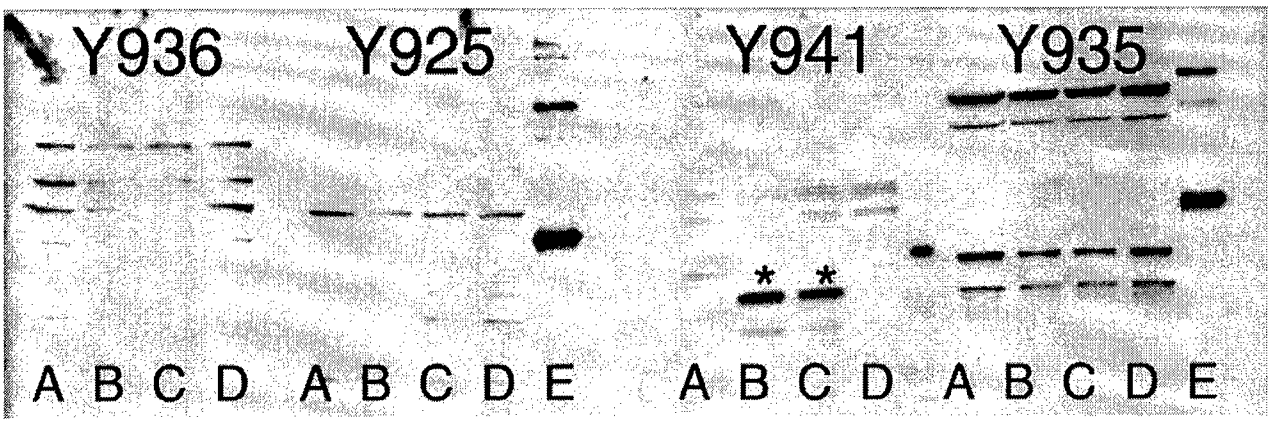

Fig. 8: Western blot assessment of Rabbit antisera against the ER uORF peptide

One of our tests for antisera is detection of GFP-fusion proteins in extracts from transiently transfected cells. This assay allows a measure of specificity for the ER distal/proximal uORF peptides versus general mammalian cell proteins. The fusions proteins run at about 20kDa in the gels and blots which makes them easy to analyze. Expression levels are likely high than for the actual peptide (in an ER expressing cell) as expression in the transfected cells is from a strong viral promoter, though only about 20% of cells get transfected. The actual uORF proteins are ~ca 2 kDA which is too small for analysis on regular gels, in addition the peptides do not bind the PVDF membrane.

Track A: GFP expression construct pEGFP-N1
Track B: GFP expression construct with prox peptide C-terminal to GFP in pEGFP-C1
Track C: Second GFP expression construct with prox peptide C-terminal to GFP in pEGFP-C1
Track D: GFP expression construct with prox peptide N-terminal to GFP in pEGFP-N1
Track E: 20 ng of the recombinant prox-MBP protein purified from E.coli (only included on blots for the rabbits immunized with un-conjugated peptides. The sera from rabbits immunized with the MBP fusion will have anti-MBP antibodies making analysis of MBP fusions in Western immunoblots irrelevant).

Y725: Bleed 2 from rabbit receiving raw peptide as immunogen
Y735: Bleed 2 from rabbit receiving raw peptide as immunogen
Y736: Bleed 2 from rabbit receiving recombinant prox-peptide-MBP fusion as immunogen
Y741: Bleed 2 from rabbit receiving recombinant prox-peptide-MBP fusion as immunogen
All sera were diluted 1:100 and detection was with the Pierce 'supersignal' chemiluminescent system.

Results: only the Y741 antiserum gives an appropriate (**) interaction with the prox-GFP protein in Western blots. The antiserum detects the Prox-peptide-GFP fusion protein in tracks B&C where the prox peptide sequence is C-terminal to the GFP ORF. However the antiserum is ineffective in detecting the prox peptide placed N-terminal to GFP in the transfected constructs. This data is in total contrast to the Biacore data.

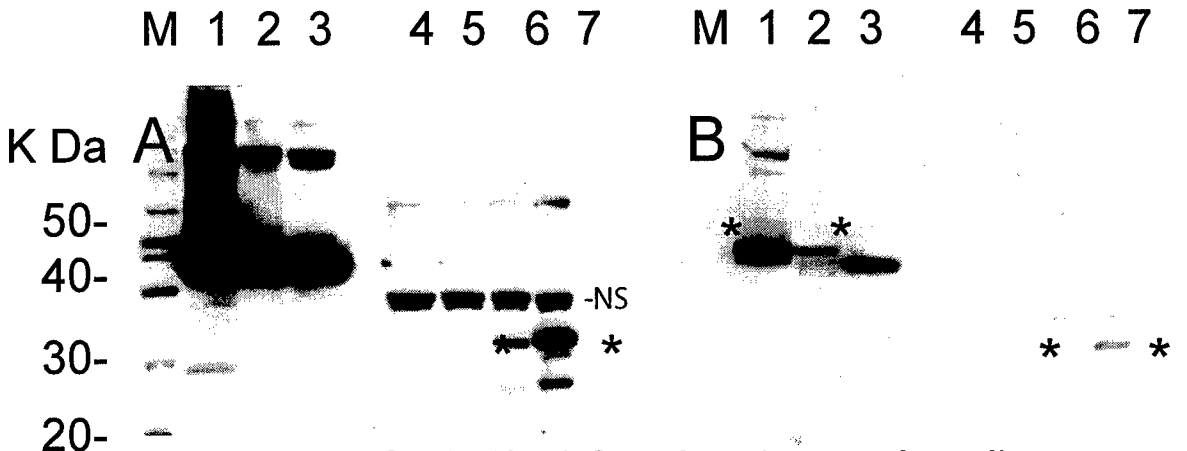

Immunopurified Y941 fraction (urea eluted)
A. Heavy exposure B. Light exposure
M: Molecular weight standards (MagicMark, Invitrogen)
NS: Non specific band
Purified maltose binding protein (MBP): Tracks:
1. Fusion of Prox-uORF to C-terminal end of MBP
2. Fusion of Distal-uORF to C-terminal end of MBP
3. Recombinant MBP

GFP-fusion transfected HeLa cells: Tracks:
4. pBSK transfected cells (no GFP vector)
5. Prox-uORF fused N-terminal to GFP
6. Prox-uORF fused C-terminal to GFP
7. Distal-uORF fused C-terminal to GFP

Fig. 9: Y941 Polyclonal antiserum raised against the Prox peptide detects both the Proximal & Distal uORF products. Similar data to this Fig was in the report last year but is included here to demonstrate differences from behavior of mAb #204. The urea eluted immunopurfied fraction of Y941 was used to probe blot a similar to that in Fig 3. In panel A, the heavy exposure, there is detection of the distal uORF fused to GFP in addition to the C-terminal Prox GFP fusion. Y941 also binds the distal MBP fusion , and is also detecing MBP in this experiment.
** is used to highlight target bands.

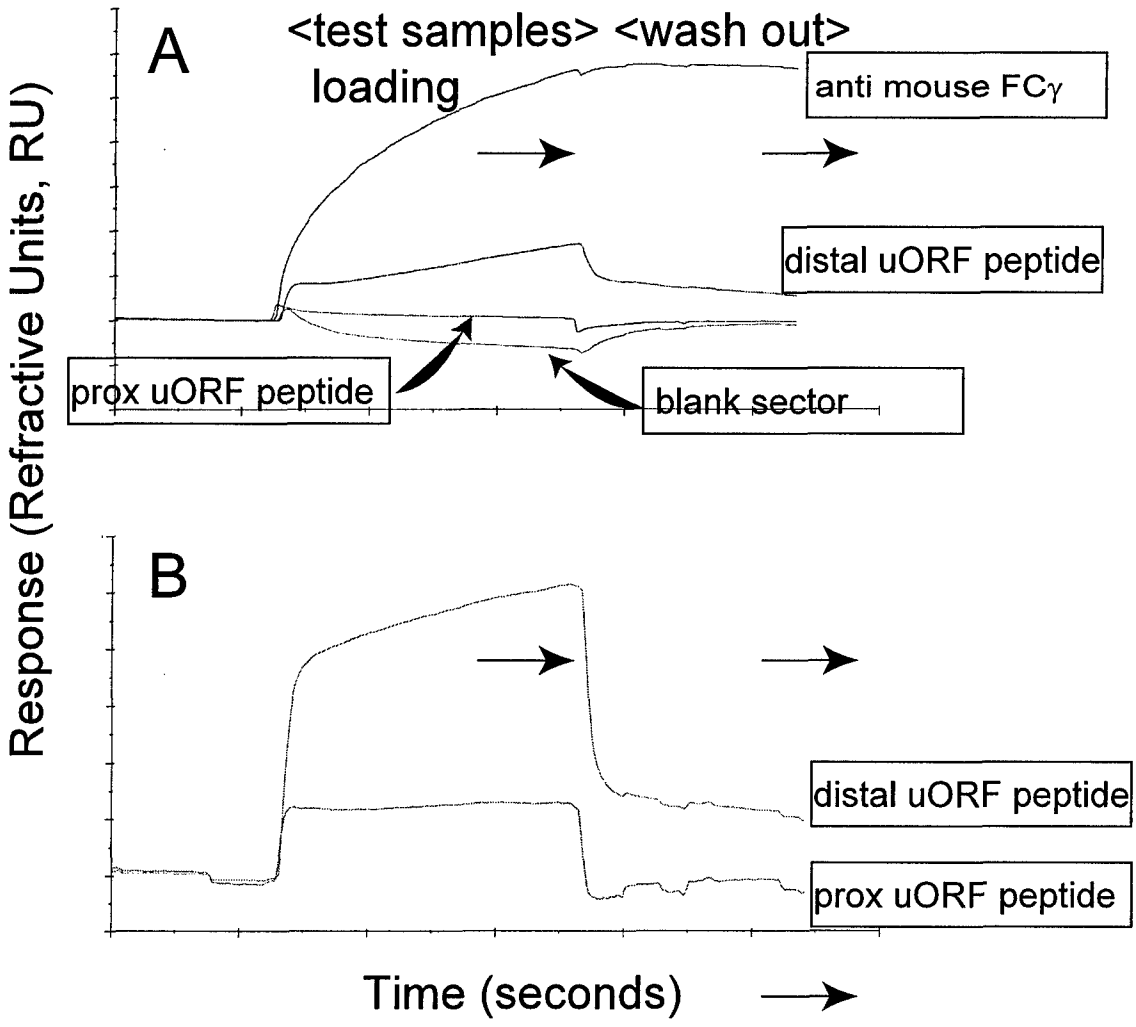

Fig. 10: Routine assesment of monclonal lines using the Biacore A Biacore chip with 4 sectors was used. Anti mouse Fcγ was coupled to one sector, this allowed estmiation of antibody level in media or ascites fluid. The Prox uORF peptide was coupled to one sector while the distal was coupled to another. The final sector was left blank to monitor salt effects.
Panel A show results for mAb #204 raw ascites fluid. There is a strong antibody signal and reaction with the Distal uORF sector. Traces are distorted; presumably due to salts and proteins in the fluid. In Panel B we used mAb#204 that had been purified on a protein G cloumn. This again shows a specfic signal with the Distal sector. The small interaction with the Prox-sector is a salt effect that is also seen with the blank sector (not shown).

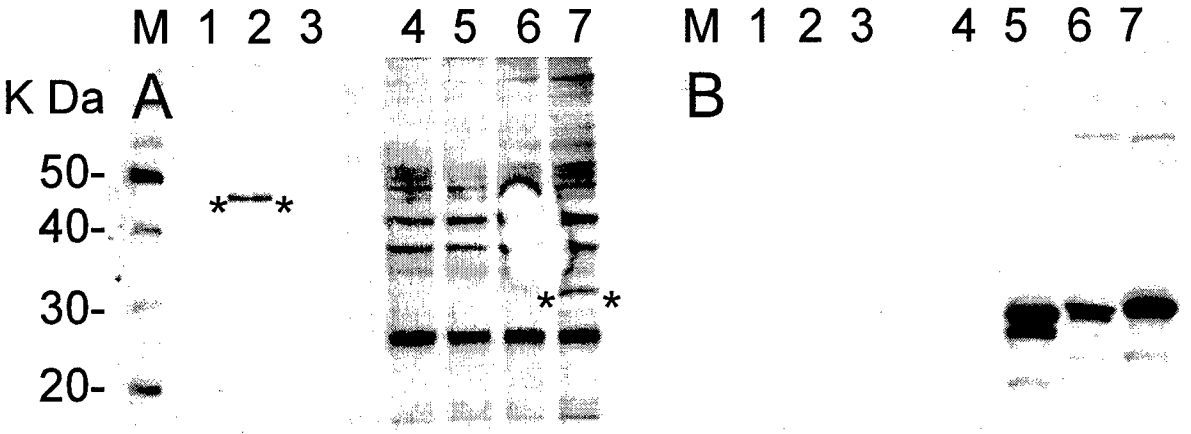

A. mAb 204 to distal uORF B. Anti-GFP (reprobe)
M: Molecular weight standards (MagicMark, Invitrogen)

Purified maltose binding protein: Tracks:
1. Fusion of Prox-uORF to the C-terminal end of MBP
2. Fusion of Distal-uORF to the C-terminal end of MBP **
3. Recombinant MBP

GFP-fusion transfected HeLa cells: Tracks:
4. pBSK transfected cells (no GFP vector)
5. Prox-uORF fused N-terminal to GFP
6. Prox-uORF fused C-terminal to GFP
7. Distal-uORF fused C-terminal to GFP

Fig. 11: mAb #204 detects the Distal uORF peptide and does not cross react to the Prox uORF peptide which shares five C-terminal residues
Specific bands interacting with the mAb 204 are indicated (**) in panel A. There is also non-specific binding to HeLa proteins. Presence of GFP proteins was confirmed by reprobing with antisera against GFP (Panel B). See Fig. 2 for a cartoon of constructs used in transfection and for overexpression of recombinant fusion proteins.

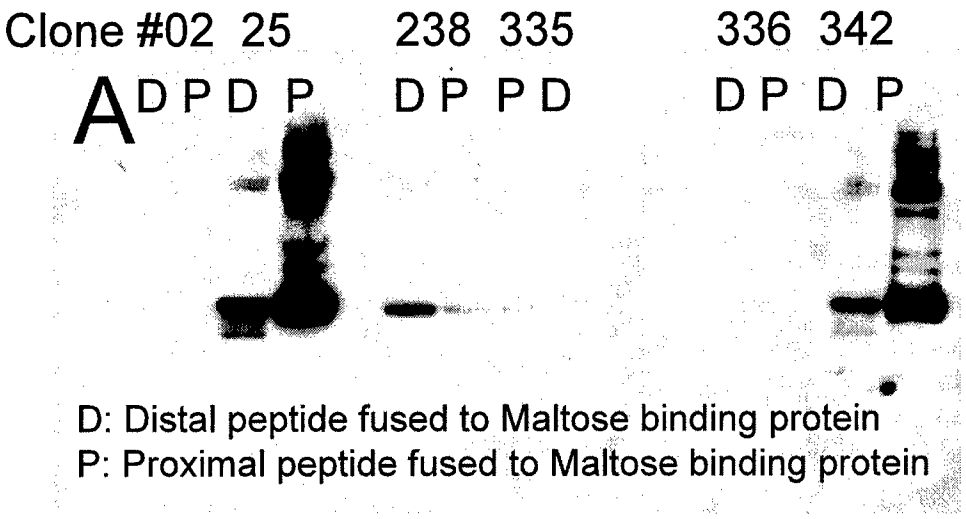

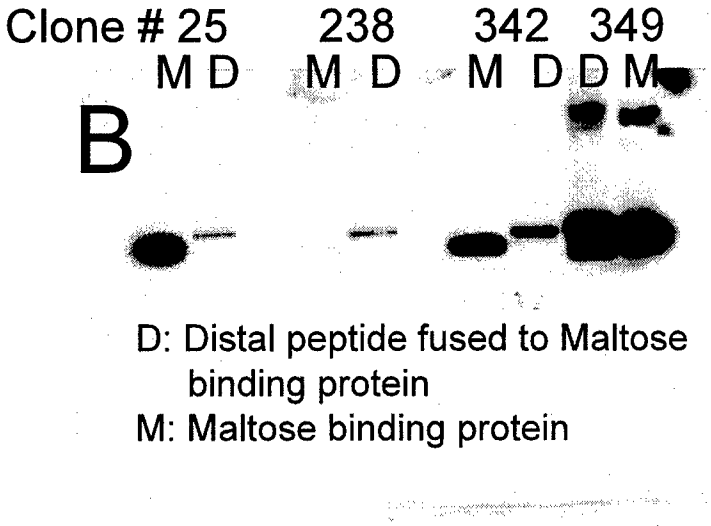

Fig. 12: Culture supernatants screened by Immunoblot for interaction with uORF peptides fused to MBP

A series of culture supernatants from the screen for mAbs against the distal uORF peptide were selected based on Biacore results and used in western immunblots against fusions of the prox and distal uORFs to maltose binding proteins (Panel A). Several of the suernatants giving brighter staining were then also tested against the unfused MBP. Most of the clones failed this test and bound MBP. Clone 238 gave distal specific signal.
Culture supernatants were used at a dilution of 1:50.

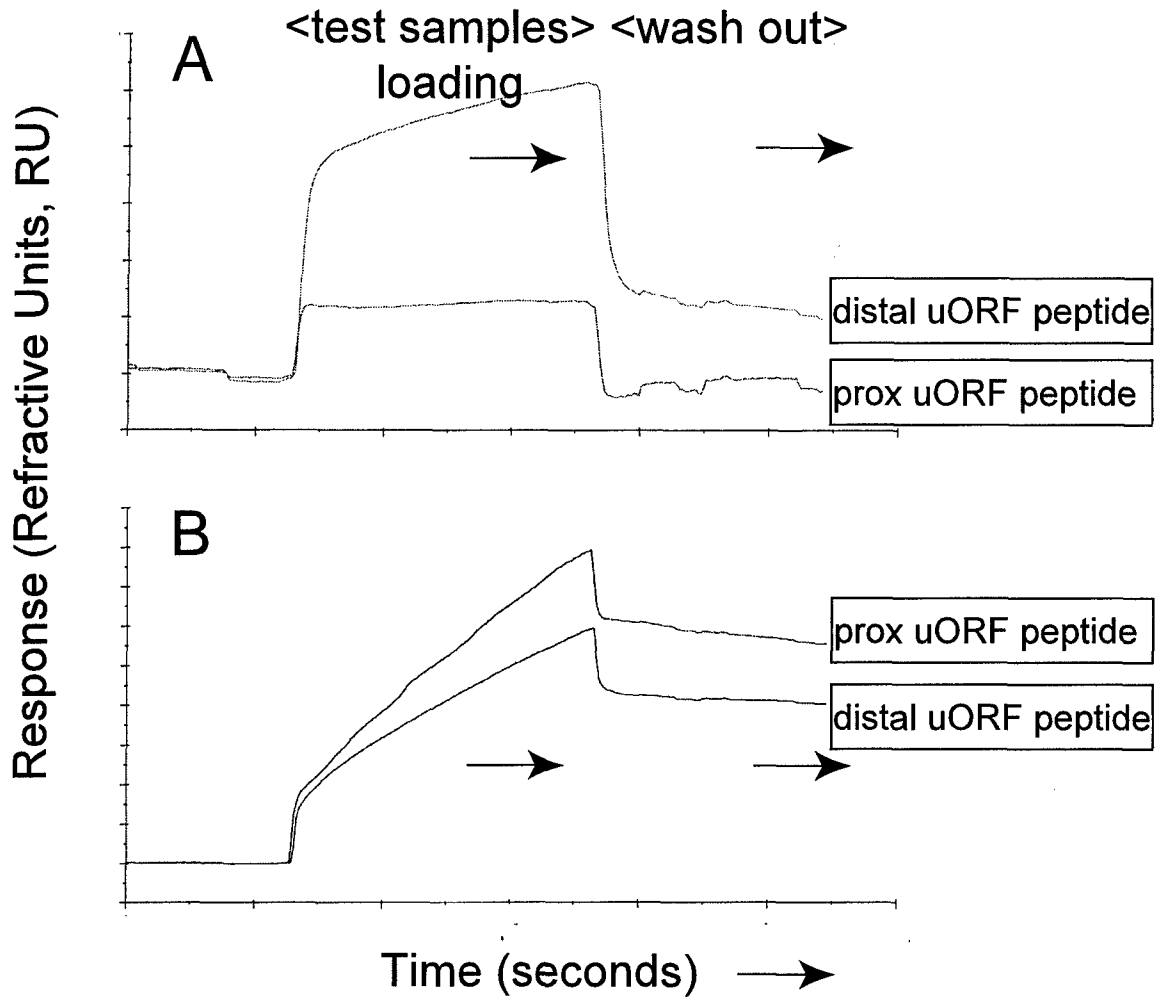

Fig. 13: The #204 mAb (Panel A) is specific for the Distal uORF peptide while the Y941 rabbit polyclonal (Panel B) against the Prox uORF peptide crossreacts with the Distal peptide.
The greater resistance of the
signal with Distal and Proximal sectors with the # 741 polyclonal to being eliminated by washing (Panel B) indicates a high affinity for the interaction than is seen for the #204 mAb in panel B.

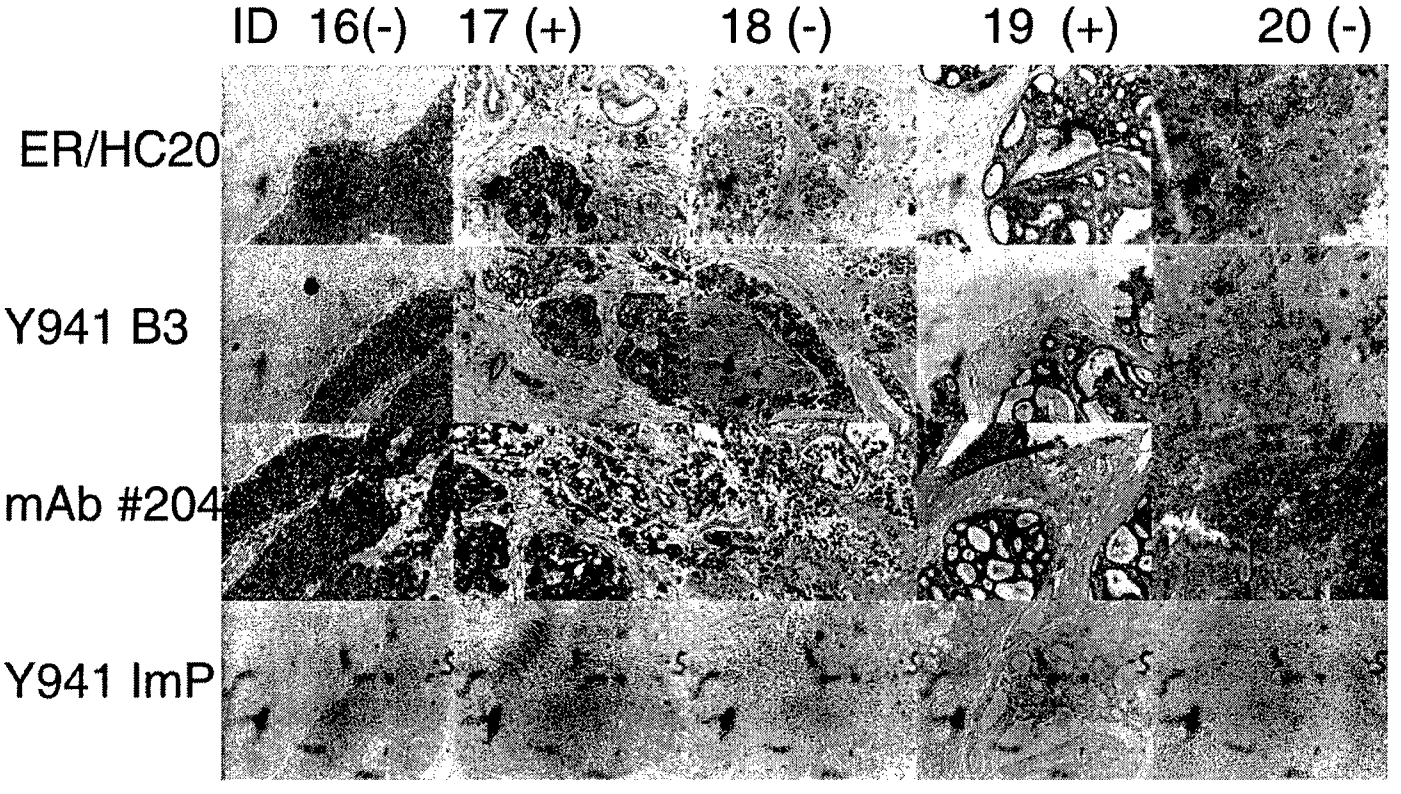

Fig. 14: Evaluation of antisera on tumor sections in arrays
Formalin fixed paraffin block punch sections were probed with the indicated antisera (left). Characteristics of the tumor samples 16-19 are described in Table 2. (+/-) indicates claimed ER status.

Anti-ER polyclonal HC20 and M-Ab 204 against the distal uORF peptide are from slides subject to antigen retrieval procedures. Both the Y941 bleed 3 antiserum and the immunpurified (ImP) fraction were used without antigen retrieval in these images. The similar marks in each of the Y941 ImP sections are artifacts of the 'scope optics and application of of 'autolevel' in photopshop.

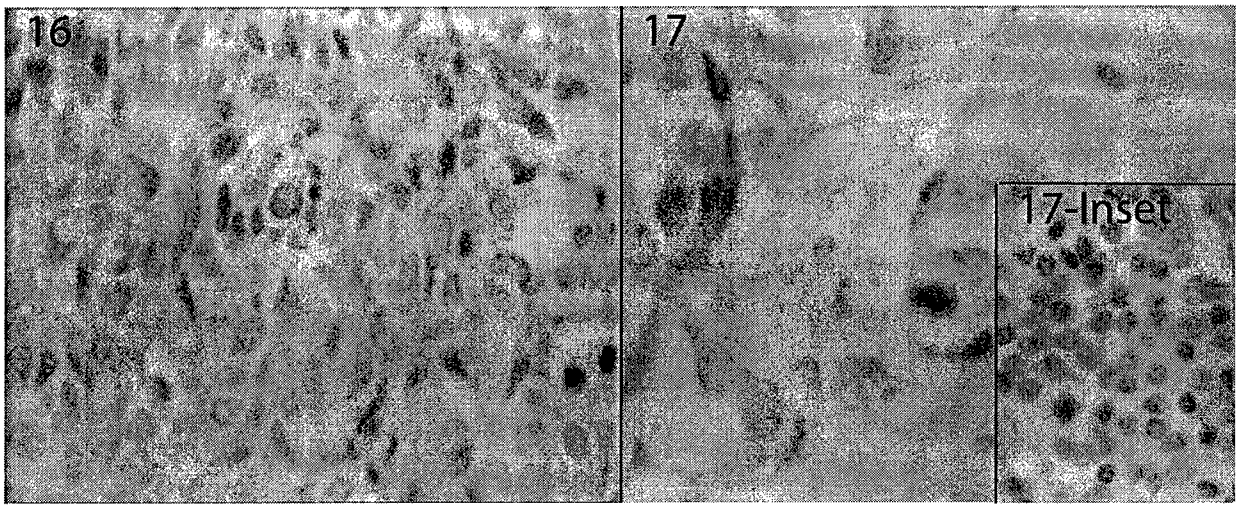

Fig. 15: Imunochem on breast tumor sections with the Immunopurified fraction from Y941 (anti prox peptide Ab) High power (600x) image of the same sections shown in Fig. 14. Tumor 16 was classified as ER neg, 17 as ER+ve (see Table 2). We saw no convincing differences.
Inset: same scale image for a lymphoid region of sample 17 showing staining of immune cells.

Note that these were 2 punch sections from an array so samples were processed identically. Slides were pre-treated with hydrogen peroxide to block endogenous peroxidase.

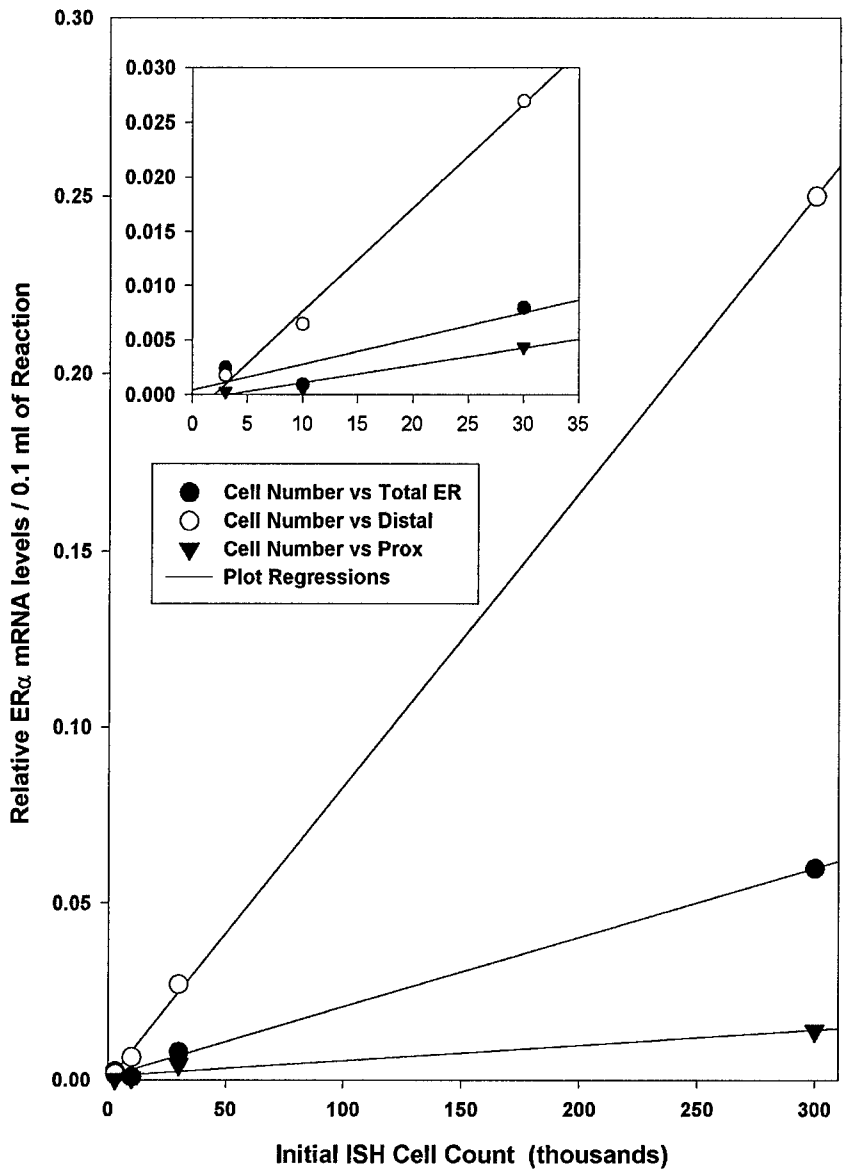

Fig. 16: Test of detection limits in ER RNA PCR

Ishikawa cells were used as a model to test the ability to analyze RNA from limited cell numbers using RealTime PCR. Ishikawa cells express ER RNAfrom both distal and proximal promoters making them a useful model. RNA was isolated from cell samples of 300K to 3000 cells. Aliquots of the RNA were analysed for total ER mRNA and the promoter specific trancripts. Fair linearity was achieved down to the smallest samples analyzed (aproximates to RNA from 1000 cells). NOTE we only used one standard curve to anlayze data. This ignores the different efficiencies of different primer sets. This is why the distal yield appears higher than total.

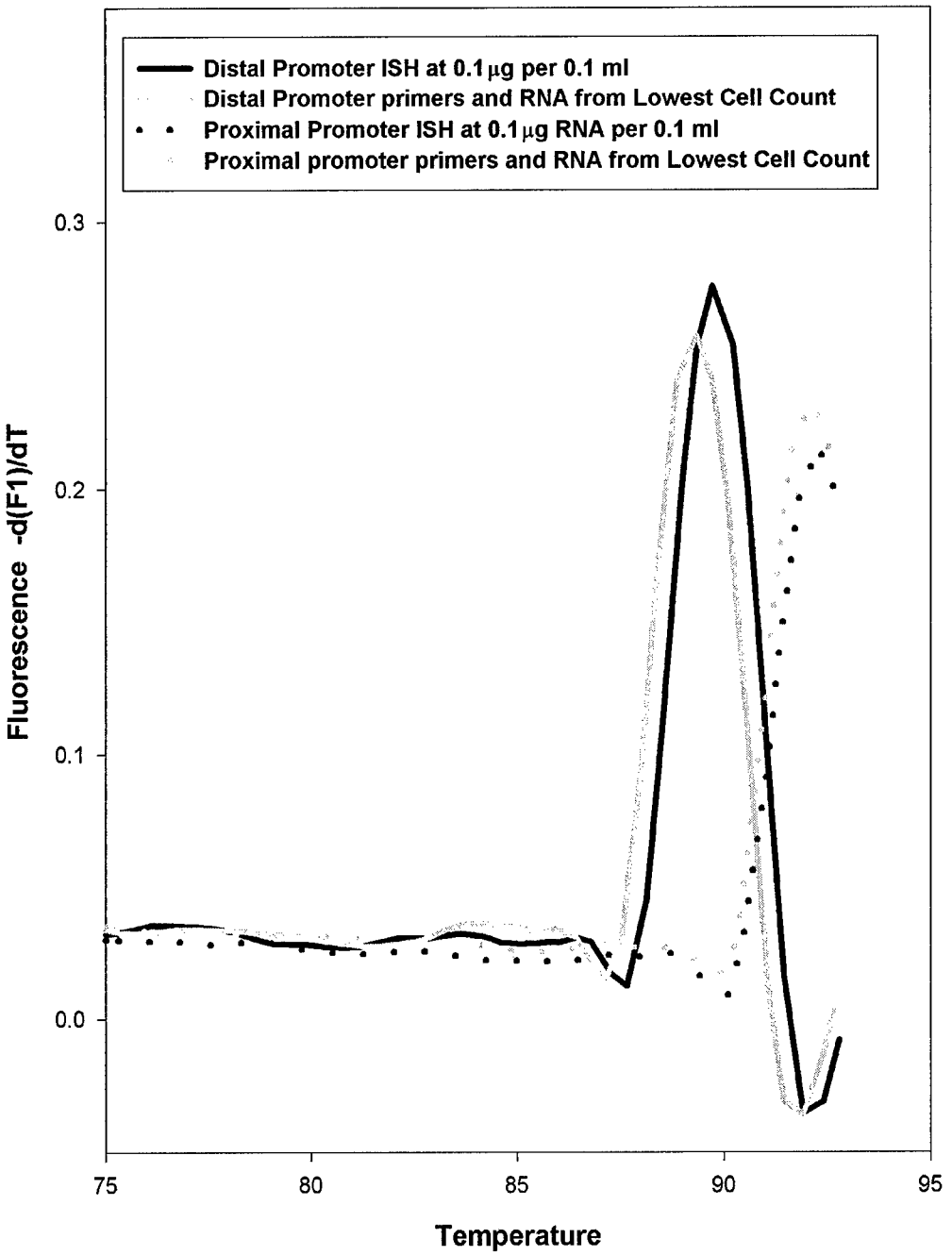

Fig. 17: Melting (denaturation) curves demonstrate the specificity of ER PCR amplification even when using only limited amounts of cells as starting material

Region	DNA Sequence and Potential Translational Product
Distal 5' uORF	MetGluHisPheTrpLysAspValLeuAspProAlaGly**TrpProAlaGlyPheTer** ..caagcccATGGAACATTTCTGGAAAGACGTTCTTGATCCAGCAGG**GTGGCCCGCCGGTTTCTGAgcc**...
Proximal 5' uORF	MetArgCysValAlaSerAsnLeuGlyLeuCysSerPheSerArg**TrpProAlaGlyPheTer** ..gcgggacATGCGCTGCGTCGCCTCTAACCTCGGGCTGTGCTCTTTTTCCAG**GTGGCCCGCCGGTTTCTGAgc**
Major ER ORF	MetThrMetThrLeuHisThrLysAlaSerGlyMetAlaLeuLeuHisGlnIle .... ccacggaccATGACCATGACCCTCCACACCAAAGCATCTGGGATGGCCCTACTGCATCAGATCCA...
Kozak Optimal Translational Start	Met ... gccgccRccATGG...

Table 1: Translational Start Regions of Estrogen Receptor Open Reading Frames

The DNA sequences and entire potential encoded peptides of alternate ER transcript upstream regions are shown together with the start region of the main ER coding region. The DNA sequences 5' of the translational starts are shown as they contribute to the relative strength of translational start sites. The five shared codons (from a common exon) of the proximal and distal transcripts are shown in bold. For comparison the optimal translational start is included; the critical elements of the ATG flanking sequences are the purine (R) at -3 and the guanine residue at +4.

ID	Age	Sex	Organ	Diagnosis	T stage	LN*	ER**	PR**	P53
16	58	F	Breast	Infiltrating duct carcinoma	T4b	1/15	-	-	-
17	37	F	Breast	Infiltrating duct carcinoma	T2	2/14	+	+	+
18	43	F	Breast	Infiltrating duct carcinoma	T2	0/13	-	-	+
19	51	F	Breast	Infiltrating duct carcinoma	T2	0/20	+	+	-
20	80	F	Breast	Medullary carcinoma	T3	4/28	-	-	+

*LN, positive lymph nodes/examined axillary lymph nodes
**ER, estrogen receptor; PR, progesterone receptor

Table 2: Reported characteristics of four tumors used to illustrate immunochemistry results

Tumor ID	Type	Age	Clinical ER	Clinical PgR	ER %MCF-7	PgR %MCF-7	Comment	Tumor	RT-PCR 28S	RT-PCR ER	RT-PCR PgR	RT-PCR Distal	RT-PCR Proximal	Dis+Prox /28S	ER/28S	PgR/28S	PgR/ER
21127	Mets to Lymph node	63			2.47%	275.00%		90%	0.0013	0.0025	0.47		0.001600	1.26	1.93	373.76	193.74
23147	Malignant	47			0.94%	65.00%		80%	0.0003	0.0009	0.11				2.80	335.91	119.99
23153	Malignant	54	Negative	Negative	0.55%	15.00%		40%	0.0001	0.0005	0.03				4.19	199.16	47.51
23155	Malignant	47	Negative	Negative	0.74%	33.00%		90%	0.0009	0.0007	0.06		0.000500	0.59	0.86	67.01	78.03
MCF-7	Cell Line		>90%	>90%					0.0011	0.0990	0.1		0.120000	112.68	92.96	93.90	1.01
23148	Malignant	47	15%		2.83%	160.00%	20% Necrosis	80%	0.0001	0.0028	0.26				45.90	4527.40	98.63
23149	Malignant	36	15%	20%	0.72%	4.45%	Weak ER Strong PgR	80%	0.0005	0.0007	0.01				1.58	16.99	10.74
23154	Malignant	60	26 fmol/mg	712 fmol/mg	2.17%	655.00%		80%	0.0007	0.0022	1.13	0.000300	0.001100	1.88	2.89	1517.55	525.85
23158	Malignant	53	90%	70%	2.88%	48.00%	Strong ER Weak PgR	100%	0.0004	0.0029	0.08		0.000900	2.50	7.92	230.14	29.07
22392	Malignant	51	90%	10%	9.95%	42.50%		90%	0.0014	0.0099	0.07	0.001300	0.005500	5.04	7.30	54.34	7.45

Table 3: Data on breast cancer samples incorporated into ERA of Hope Poster, Fall 2003

Tumor ID	28 S Values			Average	% MCF-7
21127	0	0	0		119.25%
23147	0	0	0		31.36%
23153	0	0	0		12.21%
23155	0	0	0		79.81%
MCF-7	0	0	0		
23148	0	0	0		5.73%
23149	0	0	0		42.44%
23154	0	0	0		69.95%
23158	0	0	0		33.80%
22392	0	0	0		126.76%

Tumor ID	ER Values		Average	% MCF-7
21127	0	0	0.002450	2.47%
23147	0	0	0.000935	0.94%
23153	0	0	0.000545	0.55%
23155	0	0	0.000730	0.74%
MCF-7	0.1	0.1	0.099000	
23148	0	0	0.002800	2.83%
23149	0	0	0.000715	0.72%
23154	0	0	0.002150	2.17%
23158	0	0	0.002850	2.88%
22392	0.01	0.01	0.009850	9.95%

Tumor ID	PgR Values		Average
21127	0.2	0.35	0.28
23147	0.08	0.05	0.07
23153	0.01	0.02	0.02
23155	0.04	0.03	0.03
MCF-7	0.1	0.1	0.1
23148	0.19	0.13	0.16
23149	0.01	0	0
23154	0.68	0.65	0.66
23158	0	0.05	0.05
22392	0.04	0.05	0.04

Tumor ID	Distal Promoter Values		Average	No RT	amol/0.1 ugRNA	% ISH
21127	0	0	0	0	0	-22.69%
23147	0	0	0	0	0	-2.31%
23155	0	0	0	0	0	-2.78%
MCF-7	0	0	0	0		
ISH	0.01	0.01	0.01	0	0.01	100.00%
23149	0	0	0	0.01	-0.01	-72.69%
23154	0	0	0	0	0	-2.78%
23158	0	0	0	0		
22392	0	0	0	0	0	12.04%

Tumor ID	Proximal Promoter Values		Average	No RT	amol/0.1 ugF	% ISH
21127	0.01	0	0	0.003400	0.001550	7.75%
23147	0	0	0	0.003100	-0.000750	-3.75%
23155	0	0	0	0.003200	0.000450	2.25%
MCF-7	0.12	0.12	0.12	0.002000	0.118000	590.00%
ISH	0.02	0.02	0.02	0.002000	0.020000	100.00%
23149	0	0	0	0.002200	-0.000350	-1.75%
23154	0	0	0	0.002700	0.001150	5.75%
23158	0	0	0	0.002500	0.000850	4.25%
22392	0.01	0.01	0.01	0.003000	0.005500	27.50%

ANALYSIS OF ALTERNATE ESTROGEN RECEPTOR PROMOTER USE USING NOVEL ASSAYS

Fasco, Michael J., and Pentecost, Brian T.

Wadsworth Center, New York State
Department of Health, Albany

pentecos@wadsworth.org

Estrogen Receptor alpha (ER) mRNA is primarily transcribed from two promoters. The proximal (prox) ER promoter transcribes a complete exon 1 whereas the distal promoter is 2 kb upstream in genomic DNA and splices into nt164 of the prox form. Identical ER protein is translated from both ER mRNAs because nt 164 is ~70 b upstream of the ER translational start. The two promoters may be under differing controls; their patterns of use may indicate how a breast tumor may progress and respond to drugs. We are developing assays to determine the promoter origin of ER transcripts and to test these hypotheses.

We developed a new one-step, real time RT-PCR method to quantify absolute levels of the mRNAs transcribed from ER distal and prox-promoters. Uterine Ishikawa cells contained 0.022 and 0.012 amol/μg total RNA of the prox and distal transcripts. The ratio of 1.8 is in good agreement with previously determined ratios of ~3. Consistent with our prior work, the breast tumor line MCF-7 had no detectable distal ER transcripts; the absolute ER prox-transcript concentration was 0.12 amol/μg total RNA. In contrast, two ER positive breast tumors had ER prox/distal mRNA concentrations of 0.0011/0.0003 and 0.0055/ 0.0013 amol/μg total RNA; ratios of 3.7 and 4.2, respectively. The data show that the very low levels of ER promoter transcripts can be quantitated by real time RT-PCR and suggest that the distal ER transcript is more prevalent in breast tumors than in breast tumor cell lines.

RNA-based assays are inherently challenging. We have therefore tried to develop protein based assays for alternate promoter use, despite the identity of ERs from the two promoters. The 5' region of prox-ER transcript contains a 20 amino acid (aa) residue open reading frame (uORF) besides the main ER ORF. The distal promoter transcript contains an 18 aa residue uORF, sharing five in-frame codons with the uORF in the ER prox transcript. Both uORFs terminate 50 bases 5' to the main ER translational start. From transfection studies we have evidence that the translational starts of the peptides are functional.

We propose that antisera can be made against the peptides and levels of the prox and distal peptides used as surrogate markers of ER promoter use. Rabbit polyclonal antisera were raised against the complete distal peptide, including residues shared with the prox uORF peptide. We obtained an antiserum that specifically interacts with a fusion protein of the distal peptide and maltose binding protein (MBP) in Western blots while interacting with neither MBP nor an MBP-prox-peptide fusion. This reagent will be further evaluated in test systems and tumor samples. A 15-residue prox-peptide containing unique sequences generated an antiserum with high ELISA reactivity to immunogen but the reagent failed to interact, in both ELISA and western blots, with prox-peptides containing the shared five C-terminal residues. Clearly the prox peptide has antigenic epitopes and further studies will involve use of modified immunogens and generation of mouse monoclonal antibodies.

The U.S. Army Medical Research and Materiel Command under DAMD17-01-1-0261 and New York State supported this work.

ELSEVIER

Molecular and Cellular Endocrinology 229 (2005) 83–94

MCE
Molecular and Cellular Endocrinology

www.elsevier.com/locate/mce

Upstream regions of the estrogen receptor alpha proximal promoter transcript regulate ER protein expression through a translational mechanism

B.T. Pentecost*, R. Song, M. Luo, J.A. DePasquale, M.J. Fasco

Wadsworth Center, P.O. Box 509, Albany, 12201-0509 NY, USA

Received 6 July 2004; received in revised form 19 August 2004; accepted 15 September 2004

Abstract

Estrogen receptor alpha (ER) mRNA is primarily transcribed from two promoters, the two transcripts share identical sequence encoding the same ER protein but differ in upstream regions. The 5′ region of the two transcripts contain upstream open reading frames (uORFs) encoding potential peptides of 20 and 18 amino acids. The peptides have five C-terminal residues in common. These studies were undertaken to determine if the uORFs and encoded peptides differentially affected expression of ER.

Expression of green fluorescent protein (GFP) reporter constructs containing upstream proximal promoter transcript sequences with the first 18 codons of ER fused to GFP was tested in HeLa cells. The cells expressed reduced levels of GFP as compared to the pEGFP-N1 parent vector; the effect was dependent on the presence of an intact proximal ER transcript uORF. Similar regulation by the uORF was seen in transfected MCF-7, MDA MB-231 and Ishikawa cells. Only protein expression was affected by eliminating the uORF; RNA levels were unchanged. This indicates the mechanism is translational rather than being an effect of the introduced point mutations on either mRNA stability or transcription.

Eliminating the uORF did not significantly increase expression from similar distal promoter transcript ER-GFP constructs. However, study of in-frame fusions of GFP to the entire proximal and distal uORFs and to their translational start motifs showed that the translational start region of the distal uORF was inherently better at initiating translation than the AUG environment of the proximal promoter transcript uORF. The data indicate there are regulatory properties suppressing expression from the ER translation start which are specific to the unique regions of the ER proximal promoter transcript and these are likely associated with the proximal transcript uORF peptide product.

Keywords: Estrogen receptor; Translational control; Upstream open reading frame; Alternate promoters; Alternate splicing

1. Introduction

Estrogen and its receptor systems have critical signaling and control roles in and beyond reproductive physiology (Grandien et al., 1997). Estrogen receptors are modular transcription factors with activating and DNA binding domains that can function separately. Estrogen receptors bind, principally as homodimers, to specific, distinct pseudo-palindromic DNA motifs (Lucas and Granner, 1992). Estrogen interaction with its nuclear receptors leads to modulated transcriptional action (Lucas and Granner, 1992).

Positive estrogen receptor alpha (ER) status correlates with reduced breast cancer recurrence in the first years after diagnosis and resection of breast tumors, and predicts a favorable response to adjuvant anti-estrogen therapy (Osborne, 1998). ER levels in breast tumors increase with the patient age on a population basis (Clark et al., 1984; Romain et al., 1995). The increase with age may reflect both the fraction of cells contributing to the measured ER level and the regulation of estrogen receptor expression in the tumors, including both

Abbreviations: aa: Amino acid; DMEM: Dulbecco's modified Eagle's medium; DC10: 10% DCS in DMEM; DCS: Donor calf serum; ER: Estrogen receptor alpha; GFP: Green fluorescent protein; HRP: Horse radish peroxidase; nt: Nucleotide; ORF: Open reading frame; PCR: Polymerase chain reaction; RT: Reverse transcriptase; uORF: Upstream ORF; wt-GFP: Wild type; parental GFP from pEGFP-N1

* Corresponding author. Tel.: +1 518 474 2165; fax: +1 518 486 1505.
E-mail address: pentecos@wadsworth.org (B.T. Pentecost).

0303-7207/$ – see front matter © 2004 Elsevier Ireland Ltd. All rights reserved.
doi:10.1016/j.mce.2004.09.002

transcriptional effects and reduced ER turnover due to lower circulating estradiol levels.

Several forms of the ER transcript are detected in cells. ER is expressed from more than one promoter (Keaveney et al., 1991) (Fig. 1A). Alternative ER forms exist due to exon skipping in RNA processing (Fuqua and Wolf, 1995), and this may give rise to alternate forms of ER protein in the cell (Fasco et al., 2000). The proximal ER promoter (Fig. 1A) transcribes a complete exon 1. A second promoter is located ~2 kb upstream in the genomic DNA, and sequence transcribed from an additional 5′ exon (exon 1′) is spliced into nt 164 of the proximal form (Fig. 1A). We previously determined that alternative (distal versus proximal) ER promoter usage does not affect splicing patterns outside of the 5′ noncoding region (Fasco, 1998). Promoter usage should not alter the nature of expressed ER protein, as the distal transcript splices into the shared sequence upstream of the main coding region (Fig. 1) and its translational start.

We (Fasco, 1998) and others (Hayashi et al., 1997; Weigel et al., 1995) have measured the relative levels of ER proximal and distal promoter transcripts. ER positive cell lines favor the proximal promoter, while the respective in vivo tissues appear to utilize the upstream (distal) promoter to a much greater extent. DNase hypersensitivity in promoter sites often correlates with promoter usage. The human uterine distal ER promoter was less methylated than the proximal promoter in the proliferative phase of the menstrual cycle (Hori et al., 2000), but not in the secretory phase, suggesting that promoter use could vary in normal tissue during the menstrual cycle.

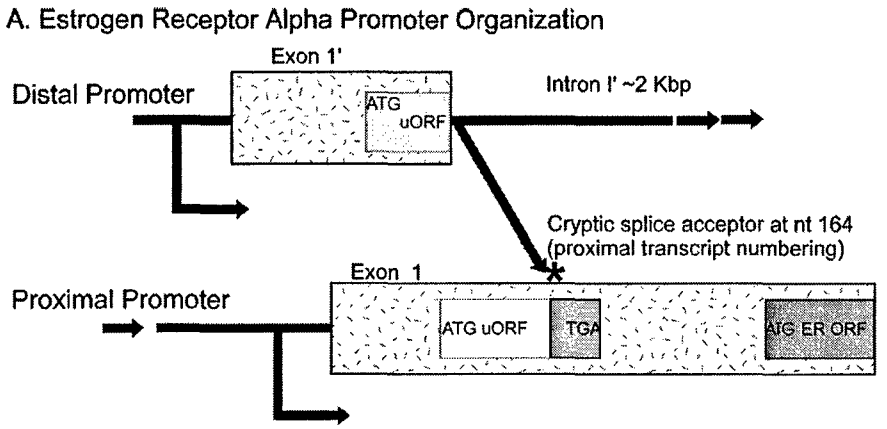

B. RNA and Related Peptide Sequences for ERα uORFs

Proximal Promoter Transcript

Distal Promoter Transcript

C. Predicted Characteristics of the ERα uORF Peptides

Peptide	Residues	Mass	pI
Distal	18	2103 Da	4.4
Proximal	20	2202 Da	8.8

Fig. 1. Estrogen receptor alpha promoter and transcript structure. (A) ER is transcribed from at least two promoters (Keaveney et al., 1991). The two transcripts (hatched boxed regions represent gene exons) share a common translational reading frame for ER (ER-ORF). The proximal promoter generates a complete exon 1. The upstream (distal) promoter generates a transcript containing an additional 5′ exon (exon 1′) that splices into the sequence transcribed from the proximal promoter at base 164 (marked with an asterisk, *) of the proximal mRNA transcript. Both 5′ regions encode short uORFs (embedded shaded boxes represent ORFs) with the potential for translational initiation in the alternate regions but which share five C-terminal residues. The unique peptide uORF regions are indicated by open or light shaded boxes. The uORF termination signal (TGA stop) is 60 bases prior to the translational start of the major ORF encoding the ER protein. Shared ORF regions are indicated by heavily shaded boxes. (B) The uORF sequences and flanking regions are indicated with the unique and shared regions boxed as in (A) the region around the translational start is numbered relative to the first nt of the initiator codon. The peptide is given in IUPAC single letter code, Ter is the terminator (stop) codon. (C) The predicted characteristics of the uORF-encoded peptides are indicated in a table.

Hayashi et al. (1997) studied the ER protein level, total mRNA level, and *relative* promoter usage in a series of breast tumors. The authors reported a positive correlation between breast tumor ER-protein expression and relative usage of the distal promoter in post-menopausal women; this correlation was not seen in pre-menopausal women. Our evaluation of their data suggests the age related increase in tumor ER levels is partly due to increasing distal promoter-dependent mRNA expression and that there is a strong correlation of age and 'yield' of ER protein per unit of mRNA expression. There is greater variability in the proximal to distal transcript ratios in pre-menopausal women, where menstrual cycle stage could differentially affect promoter usage. The controls on the two promoters must be different, since only the distal transcripts show the strong age related increase. Differential expression and regulation of ER expression from two promoters could be important in breast cancer development and progression.

The increased yield of ER per unit RNA indicates that either more ER is being made, or less is being degraded. The studies reported here indicate that the translational controls of the alternative ER transcripts may be different, with a short upstream open reading frame (uORF) in the 5′ region of the proximal transcript having an inhibitory effect on ER expression from the main downstream ER translational start.

Our studies focus on properties of the unique regions of the alternative promoter transcripts that might contribute to age related changes in ER levels. One such difference is that both transcripts have uORFs 5′ to the main ER coding region (Fig. 1). A uORF is a feature of the regions of some mRNAs located 5′ to the sequences encoding the recognized protein product. They consist of a translational start site (generally AUG) and a run of codons that ends in one of the recognized termination codons (typically UGA). The basic scanning model of eukaryotic translation (Kozak, 1989) presumes that the first (5′) AUG in a sequence should encode the translational initiator methionine. Hence, the upstream AUGs should act as a translational start, with the potential for influencing expression of the downstream ER coding region.

The translational start of the two uORFs begin in the regions not shared by the two transcripts (Fig. 1). The upstream AUG of the ER proximal promoter transcript provides the potential translational start of a 20 codon uORF that is in-frame with the main ER translational start AUG but which ends, due to a UGA terminator codon, 60 nt 5′ to the main ER translational start. The human distal promoter transcript contains two uORFs. One of these, with 18 aa residues, begins in sequences that are unique to the distal promoter transcript but it shares five C-terminal codons with the uORF in the proximal promoter. The two uORFs share the same reading-frame (Fig. 1) (Keaveney et al., 1991) and are totally conserved at the protein level in the Japanese monkey (Kato et al., 1998). The prox-uORF encodes a peptide with a higher content of hydrophobic residues and a much higher calculated p*I* (Fig. 1C) due to the nature of the residues not shared with the potential translational product of the distal uORF.

We report here that there are differences in the translational potential of transcripts from the two major ER promoters. Data indicate that the proximal transcript uORF is poorly expressed, relative to the distal uORF, yet is an effective inhibitor of ER translation when present 5′ to the major ER translational start.

2. Materials and methods

2.1. Plasmid constructs

The green fluorescent protein (GFP) constructs utilized the pEGFP-N1 vector (GenBank U55762, Clontech, Palo Alto CA) with DNA fragments inserted upstream of the ATG translational start codon of the GFP cassette. An initial group of constructs, the *ER-GFP series* (Fig. 2), contained approximately 150 bp of ER-derived proximal (ProxER-GFP) and distal promoter transcript sequences (DisER-GFP). The ER-GFP constructs contained sequences of the ER transcripts from −7 relative to the initial base of the uORFs to 56 bp (18 codons) 3′ to the main ER translational start (see Figs. 1 and 2). ER sequences were generated by RT PCR using a human uterine RNA template (Clontech) prepared with poly-dT primer and MMLV reverse transcriptase (Life Technologies, Bethesda, MD). This template contained both the distal and proximal promoter transcripts. The PCR reactions utilized forward primers corresponding to the first 18 bases of distal or proximal transcript sequences shown in Fig. 1B Both products were generated in separate reactions, using Taq polymerase (Clontech), with a common reverse primer CT*GGATCC*TGGATCT GATGCAGTAGGGC corresponding to the shared sequence complementary to sequences within the major ER-ORF of the ER transcripts (nt 3040–3060 in Genbank entry HSERB5FR). The forward primers carried 5′ *Eco*RI sites, and the reverse primer carried a terminal *Bam*HI site (italicized) to facilitate insertion into the GFP expression cassette. The *Bam*HI site was positioned to maintain the reading frame of the main ER-ORF into the GFP sequence. Utilization of the major ER-ORF translational start increased the size of the GFP cassette by 25 codons; 7 derived from polylinker sequences and 18 authentic codons corresponding to the ER N-terminal region.

Mutations eliminating the uORFs were introduced to sequences by use of modified oligonucleotide forward primers and PCR using the uterine derived template. Bases altered were the initial residue of the ATG of each uORF (A to C) giving m1aDisER-GFP and m1ProxER-GFP. A second, m1bDisER-GFP, uORF start mutant construct (ATG to AAG) was prepared for the distal ER-GFP. A proximal ER-GFP construct, m2ProxER-GFP, expressing a truncated uORF was prepared using a forward primer where the last base of codon three (TGC; cysteine, Fig. 1B) was changed from C to A, generating a TGA termination codon. The template for this reaction was a ProxER-GFP plasmid construct.

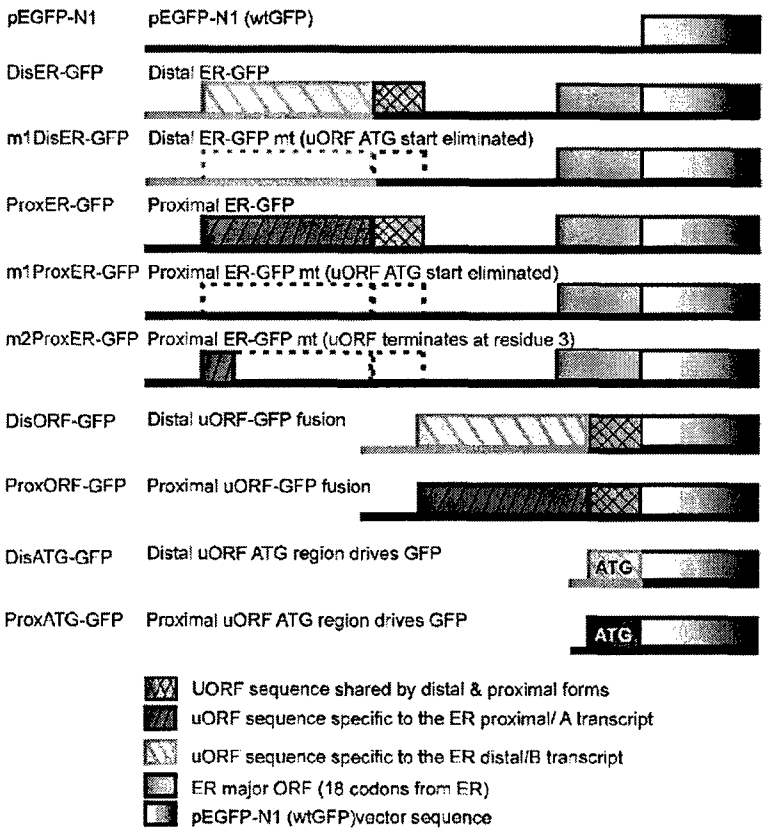

Fig. 2. Schematic diagram of ER sequences in the GFP expression cassette of pEGFP-N1 regions of ER distal and proximal promoter transcripts were inserted ahead of the GFP cassette of pEGFP-N1, resulting in modified transcripts generated from a strong CMV promoter in the vector. The *ER-GFP* constructs contained approximately 150 bp of ER-derived proximal and distal promoter transcript sequences from −7 relative to the initial base of the uORFs to 56 bp (18 codons) 3′ to the main ER translational start (see Fig. 1). Mutations of both of the uORF sequences (ER-GFP mt constructs) were made either by eliminating the uORF by modifying the upstream translational start and by introducing, for the proximal transcript construct, a premature termination signal. The *uORF-GFP fusion* constructs contained the uORF sequences in-frame to the GFP cassette of pEGFP-N1 (see Fig. 1 with no intervening termination signal. Initiation occurs from the uORF translational initiation codons and flanking sequence (out to −7) are included in constructs. The *uORF ATG-GFP* constructs contained only the ER sequences regarded as critical parts of the uORF translational initiation region, i.e. sequences −7 to +6 relative to the ATGs (see Fig. 1 ahead of and in-frame with the GFP cassette of pEGFP-N1).

The inserts of a second group of constructs, the upstream *ORF-GFP fusion series* (Fig. 2) consisted of the proximal or distal uORF sequences fused in-frame to the GFP cassette and utilized the AUG translational start region of the respective ER uORFs (see Fig. 1). These constructs express a fusion of the uORF peptides to GFP and lack all sequences of the major ER-ORF. The uORF fragments were generated by PCR on a uterine cDNA template using the same forward primers as used for ER-GFP series. The common reverse primer CT*GGATCC*CGGAAACCGGCGGGCCACC corresponded to the complement of the sequences for the five shared C-terminal amino acid codons (but no terminator) of the two upstream peptides, and two preceding bases (Fig. 1B). The reverse primer carried a terminal *Bam*HI site (italicized) positioned to allow insertion to pEGFP-N1 in-frame with the GFP cassette. The inserted fragments increased the size of the GFP cassette by 18 or 20 codons derived from the distal and proximal promoter transcript ORFs, with an additional 7 codons being gained from pEGFP-N1 poly-linker sequences between the uORFs and the original GFP translational start AUG.

A third group of constructs, the *uORF ATG-GFP series*, contained a copy of the proximal or distal upstream ORF translational start regions (−7 to +6, the first 13 bases of distal and proximal transcript upstream sequences shown in Fig. 1B) initiating GFP translation directly, with no other ER-derived sequences (Fig. 2). The annealed oligonucleotides had Bgl II and Hind III compatible overhangs to allow insertion into cut pEGFP-N1 vector. The sequences introduced a new AUG in-frame upstream of and in-frame with the GFP cassette. Use of the inserted translational start motifs increased the size of the GFP protein by addition of the two initial ER uORF codons and 19 extra codons from the vector sequences between the new and original GFP start codons.

A series of cell transfections for immunoblot and RNA analysis were performed with the ER-related GFP fusion constructs and fusions of GFP and an ORF encoding the ~20 kDa HEM45 peptide (Pentecost, 1998). The fusion pro-

tein provides an invariant reference control that is detected by the same antisera used to detect GFP. The HEM45-GFP fusion protein has a molecular weight of ~40 kDa and is well separated from GFP and ER-GFP fusions in Western immunoblots. HEM45 cDNA ORF sequences were placed 5′ to GFP in pEGFP-N1. The HEM45 ORF cassette was amplified by PCR using primers that included *Xho*I and *Bam*HI sites for directional cloning. The HEM45 translational start region was modified to maximize the strength of the initiation and the translational termination signal eliminated to generate a fusion of the HEM45 and GFP ORFs.

Plasmid constructs were prepared by equilibrium centrifugation twice in cesium chloride gradients or using the Qiagen (Valencia, CA) Maxiprep system. All DNAs in a single experiment were prepared by the same methodology. Fidelity of ER-derived regions of DNA constructs was confirmed by sequencing. Multiple batches of DNA were isolated from separate bacterial colonies and used in HeLa cell transfections for flow cytometry. This minimized the possibility that DNA quality or unrecognized mutations in vectors or inserts could influence results.

2.2. Cell culture and transfection

Cell transfection was performed with the HeLa line. DNA was generally introduced by lipofection using Lipofectin (Life Technologies Inc, Gaithersburg, MD) on cells plated at 270,000 cells per 35 mm diameter well in DMEM with 10% donor calf serum (Life Technologies) (DC10) on the previous day. Typically, 2 μg of GFP construct was used with total DNA adjusted to 4 μg using pBSK when cells were to be analyzed by flow cytometry or subsequently used for microscopy. Carrier pBSK was replaced with the HEM45-GFP fusion construct when cells were to be analyzed by immunoblot. DNA was incubated with 14 μl lipid in 100 μl DMEM/ 2% UltraSer SF (IBF Biotechnics, France) for 30 min prior to application to cells in 1 ml DMEM/ 2% UltraSer SF. Typically, 1 ml DC10 was added after 5 h at 37 °C giving a final serum concentration of 5%. Cells were washed after further incubation overnight and media changed to 2% UltraSer in DMEM. Cells were harvested for analysis at the times indicated in figures, 24–72 h after the final media change.

2.3. Flow cytometry

GFP expression was measured using quantitative analysis by flow cytometry in a Becton-Dickinson FACScan. Cells monolayers were harvested by trypsinization, and typically analyzed after fixation in 0.4% *para*-formaldehyde-PBS for at least 4 h. Alternatively, cells were fixed in 70% ethanol or analyzed immediately without fixation. Fixed cells were spun down and resuspended in PBS for analysis. Analysis was restricted to single cells; debris and clumped cells were gated out based on forward and side scatter. In addition we restricted analysis to cells showing greater fluorescence than the inherent auto-fluorescence determined with untransfected cells. All samples in a specific experiment were analyzed together, under identical FACScan settings.

Presented data is based on the mean of fluorescence intensity (MFI) of analyzed cultures. The arithmetic mean and standard error of grouped sample MFIs was subsequently determined and is presented as a measure of fluorescence representing GFP expression from constructs in cells.

2.4. Western immunoblot analysis

Cells for Western immunoblot analysis were transiently transfected in 35 mm wells as described above. Wells were PBS washed and cells were lysed in situ using a modified gel loading solution containing SDS (Fasco et al., 2000). Samples (20 μg) were analyzed on 10% acrylamide NuPage gels (Invitrogen) and blotted to Millipore PVDF membrane. Blocked blots were incubated with a 1:100 dilution of a goat anti-GFP-peptide antibody (SantaCruz Biotechnology, Santa Cruz, CA) and washed as described. Pierce (Rockford, IL) HRP-conjugated donkey anti-goat IgG (SantaCruz BioTechnology) was used as secondary antibody and detection was by chemi-luminescence using the Pierce 'super-signal' system. The Western immunoblots showed greater changes than the flow analysis. This is largely because with weak expressing constructs more cells are gated out in the flow analysis; fluorescence looks like the autofluorescence in control cells, and we collect data only from cells with higher expression.

2.5. Analysis of GFP RNA and protein levels

For analysis of relative RNA and protein expression, HeLa cells were plated at 400,000 cells per 35 mm well in DC10 and transfected the next day. Plasmid DNA was introduced using Lipofectamine 2000 (Life Technologies Inc, Gaithersburg, MD). One microgram of each GFP construct and of the reference HEM45-GFP construct were used, with total DNA adjusted to 4 μg/well using pBSK. Media were changed the next morning and cells were harvested by trypsinization after a further 48 h. Cells were suspended in PBS and equal aliquots used for RNA and protein preparation.

RNA from transfected cells was prepared using the RNeasy mini kit (Qiagen Valencia, CA). The on-column DNase I digestion step was used to eliminate the residual plasmid DNA. The Qiagen (Valencia, CA) One-Step Kit supplemented with Syber Green I (Molecular Probes, Eugene, OR) was employed to generate cDNAs and perform quantitative PCR in a LightCycler (Roche, Indianapolis, IN). Reactions were 15 μl and 75 ng RNA was included. A 30 min incubation at 50 °C was used to synthesize cDNA. This was followed by heating for 15 min at 95 °C to inactivate the reverse transcriptase and activate the Taq polymerase. The number of amplification cycles was 45, and the cycling times for denaturation (95 °C), annealing (60 °C) and extension (72 °C) were 15, 15, and 30 s respectively. Fluorescence was determined during a 5 s pause in ramping, at 85 °C, after each extension step.

Primer sets amplifying fragments specific for ER-GFP or HEM45-GFP were designed using Primer 3 PCR primer selection program (Whitehead Institute, MIT). A common reverse primer, 5′AAGTCGTGCTGCTTCATGTG 3′ was used as both RNA targets contain GFP sequences. Forward primers were selected that lay in the unique regions of each transcript. These were 5′CATGACCCTCCACACCAAA3′ for ER-GFP and 5′CAAGAGCATCCAGAACAGCC3′ for HEM45-GFP. The products were 321 and 402 bp, respectively. The forward ER primer begins at +6 in the major ER-ORF. PCR reactions without the reverse transcription step were used to test for carry-through plasmid DNA. The reactions with the reverse transcription step had crossover numbers at least 3.5 cycles greater than for the no reverse transcription controls; signal from carry-through plasmid was <10% of the total. RNA levels were calculated by inclusion of an 8.5 attomole plasmid standard sample in each LightCycler run and from stored standard curves originally generated by PCR of serial dilutions of the plasmid constructs.

Protein samples were prepared as described above. Samples were analyzed on SDS polyacrylamide gels (15%) and transferred to PVDF membrane. Blocked blots were incubated with a 1:250 dilution of goat polyclonal anti-GFP-peptide antibody (Santa Cruz Biotechnology, Santa Cruz, CA) and washed as described above.

3. Results

We examined the capacity of the 5′ untranslated regions and AUG translational start signals of the ER coding regions to support reporter expression using a GFP reporter (see construct summary in Fig. 2). Studies utilized flow-cytometry, protein immunoblotting, RNA quantitation and fluorescence microscopy as analytical tools and were generally carried out using transiently transfected HeLa cells.

ER-GFP transcripts of the constructs in pEGFP-N1 were from a strong CMV promoter, since these studies focus on the post transcriptional regulatory influence of the sequences of the transcripts, *not* regulation of the ER promoters. Our constructs were designed to probe the relevance of these transcript sequences to ER translation.

3.1. Modification of the proximal ER transcript uORF affects expression from the ER-ORF

In an initial experimental series we made *ER-GFP fusion* constructs (see Fig. 2) in which the GFP protein would be generated from an ER-GFP fusion transcript in which the natural AUG region of the major ER coding region provided the translational start. In these ProxER-GFP and DisER-GFP constructs, the upstream uORFs were present in their natural relationship to the main ER translational start and had the potential to influence translation of the ER-GFP fusion. All but ~45 bp in the 5′ regions of the ER sequences are identical in these constructs. Each ER transcript fragment began 7 nt prior to the short 5′ uORFs; this allowed us to include the principal translational start sequences (Kozak, 1987a) around the uORF AUGs (see Figs. 1 and 2). It also enabled us to mutate several of the uORF codons by changes to PCR primers. DNA fragments for the main ER AUG and for 17 complete following codons (56 bp) were fused in-frame to GFP sequences (see Figs. 1 and 2); constructs were designed for translation to begin from the main ER translational start and continue into the GFP protein.

The ProxER-GFP constructs supported reduced expression as compared to expression from the parent pEGFP-N1 construct (Fig. 3); this was significant at the 0.05 level by Student's paired *t*-test. The ER-GFP constructs should express a GFP fusion protein that is slightly larger than the parent GFP due to initiation of translation at the AUG of the main ER coding region, introducing an extra 25 residues (18 codons from ER and 7 from polylinker ahead of the GFP ATG). This was tested by immunoblotting with anti-GFP anti-sera in order to prove that the major ER translational start was utilized. A size increase of the ProxER-GFP fusion protein (Fig. 4) as compared to GFP from the parent pEGFP-N1 vector confirmed use of the ER translational start in place of the downstream GFP AUG.

The role of the uORFs in ER proximal transcript translation was probed by the smallest possible nucleic acid alteration with maximal effect on the ORF: the uORF ATG was mutated to CTG, eliminating translational start (m1ProxER-GFP). The single base mutation in m1ProxER-GFP resulted in a marked increase in the expressed ER-GFP signal, restoring expression to levels statistically indistinguishable by flow cytometry (Fig. 3A) from those of the wt-GFP construct pEGFP-N1.

Similar results were seen in Western immunoblots. We included a reference construct in cell transfections intended for Western immunoblot analysis to prove that the changes were not artifacts of transfection efficiency. The reference construct was a fusion of GFP to a second ORF for HEM45. The expressed fusion was detected by GFP antisera as a 40 kDa protein and relative expression was calculated for reference and reporter band densities. A strong increase in *intensity* of signal in Western immunoblots upon eliminating the translational initiator, relative to the level of cotransfected HEM45-GFP (Fig. 4), supports the role of the uORF translational start in *regulating* downstream expression of the ER-GFP fusion in the proximal promoter transcripts. The *molecular weight* of the ER-GFP fusion product was unaffected by elimination of the uORF AUG as the upstream AUG does not provide the translational start of the ER-GFP fusion product.

The inhibitory effect eliminated by mutation of the translational start of the proximal transcript uORF could be due to loss of the proximal peptide, or to elimination of the AUG start or even to an RNA conformation effect. The role of features of the proximal ER transcript uORF was probed with a second mutation where the third base of codon 3 (see proximal peptide in Fig. 1B) of the uORF was mu-

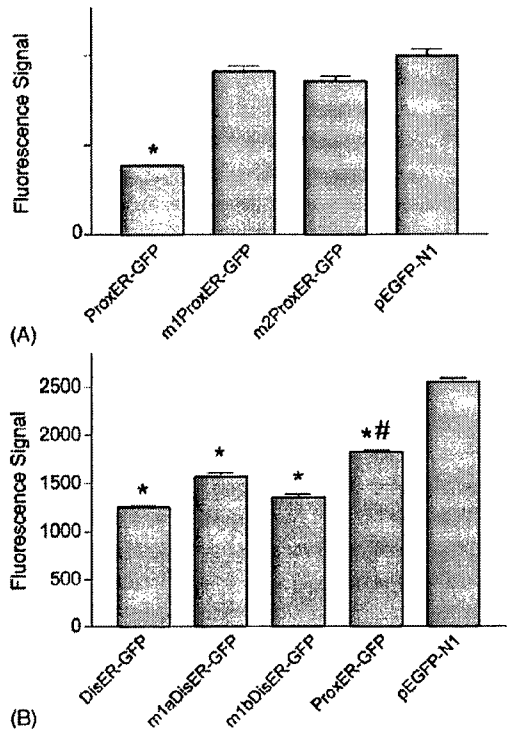

Fig. 3. GFP expression is affected by the uORF sequence of ER. (A) Analysis of regulation of GFP expression by ER proximal promoter transcript sequences: Cells were transfected with pEGFP-N1 or proximal ER-GFP derivatives (Fig. 2). Data is presented as the arithmetic mean and standard error for the mean fluorescence intensities (determined in a FACScan unit) of HeLa cells transiently transfected using Lipofectin with 2 μg GFP construct in 35 mm wells. Three transfected plates were used for each data set; separate DNA preparations were used for each plate. Cells were harvested 48 h after the replacement of transfection medium. (*) Expression levels in cells transfected with the ProxER-GFP constructs were statistically different from the pEGFP-N1 transfected cells (all statistics by Student's paired *t*-test, $p < 0.05$). Expression from the mutated proximal ER-GFP constructs was indistinguishable from that of the pEGFP-N1 parental vector. (B) Analysis of regulation of GFP expression by ER distal promoter transcript sequences and comparison to expression from ProxER-GFP constructs: HeLa cells were transfected with pEGFP-N1 or indicated ER-GFP derivatives (Fig. 2). The cells were harvested 34 h after transfection, formaldehyde fixed and analyzed as described above. The arithmetic means (and standard error) for the mean fluorescent intensity of gated cells is shown.(*) Expression levels in cells transfected with these constructs were statistically different from the pEGFP-N1 transfected cells. Mutation of the upstream translational start of the distal ER-GFP constructs had no statistically significant effect. The three distal constructs were not significantly different from each other. (#) Expression in cells carrying the proxER-GFP construct was statistically different from those cells transfected with the DisER-GFP construct (all statistics by Student's paired *t*-test, $p < 0.05$).

tated. We introduced a premature termination signal (TGC-Cys TGA-stop, Fig. 2; m2ProxER-GFP). This mutation left the uORF AUG intact, potentially allowing translational initiation, but the reading frame then prematurely ends at the introduced termination codon to generate a minimal translational product (Fig. 2). This mutation again eliminated the inhibitory effect of the proximal ER transcript 5′ untranslated region. The fluorescent signal measured by the FACScan in

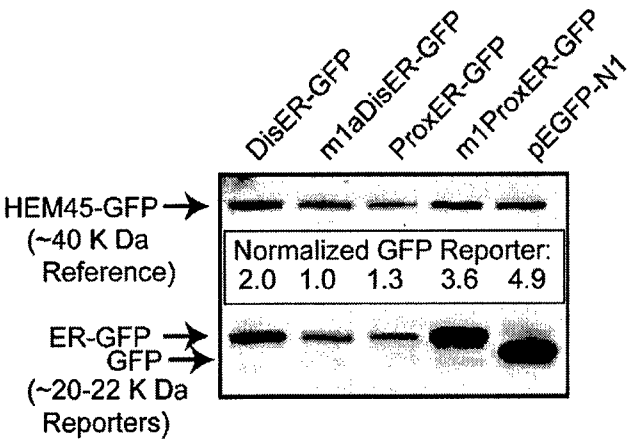

Fig. 4. Fusion of ER sequences to the GFP cassette of pEGFP-N1 alters the mass and can regulate expression levels of GFP protein detected by Western immunoblotting. HeLa cells were transfected (Fig. 3 and methods) with 2 μg of GFP constructs and 2 μg of the construct encoding HEM45-GFP using Lipofectin. Cells were lysed in situ 36 h after replacement of the transfection medium. Protein (20 μg) from lysed cells was analyzed in Western immunoblots using goat anti-GFP antisera and chemi-luminescent detection. The panel shows a blot of proteins from the transfected cells. Both the GFP reporter and the HEM45 fusion are detected by the antibody against GFP. The ER-GFP protein migrates as a 22 kDa protein and is slightly larger than the GFP alone due the extra ER residues. HEM45-GFP migrates as a 40 kDa protein. Expression of immuno-detected ER-GFP is clearly increased upon eliminating the uORF translational start from proximal promoter transcript ER-GFP constructs. This effect is not seen with the distal promoter transcript ER-GFP constructs. Densitometric analysis of the reference and reporter bands (inset) confirms these results and indicates that changes are not due to varying transfection efficiency.

cells transfected with the 'early-stop' construct (Fig. 3A) was equivalent to that of cells expressing pEGFP-N1 (wt-GFP) and the m1ProxER-GFP lacking the uORF initiator codon.

3.2. Elimination of the Prox-uORF affects protein expression, but not RNA levels, from constructs

An assay was established to determine GFP RNA levels in addition to protein levels in order to determine if effects of the Prox-uORF on downstream ER-GFP expression was translational. 'RealTime' PCR assays were performed in the Roche LightCycler to measure the levels of the ER-GFP mRNAs and the HEM45-GFP mRNAs. The assays used forward primers specific to the ER or HEM45 fragments which facilitated separate measurement of each transcript and again permitted cotransfection of test and normalizing constructs. RNA and protein were isolated from aliquots of trypsinized cells transfected with constructs (see methods) in order to allow direct comparison of protein and RNA levels. The data (Fig. 5) indicate that the levels of mRNA were similar from the ProxER-GFP construct and the m1ProxER-GFP constructs where the uORF translational start was eliminated. The limited (~20%) difference was attributable to transfection efficiency in the two sets of cells as it was also seen in the levels of HEM45

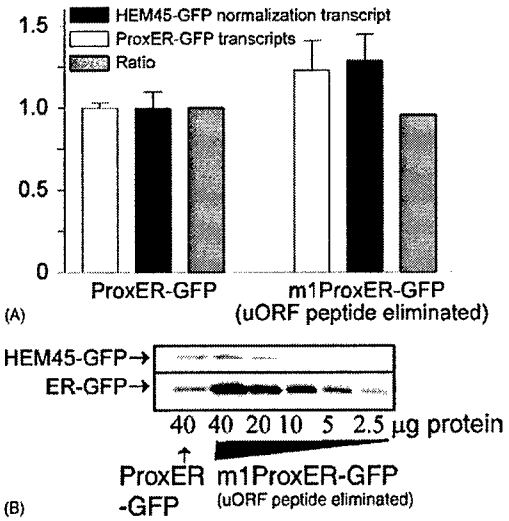

Fig. 5. Elimination of the proximal uORF affects ER-GFP protein expression without affecting mRNA expression. Cells were transfected with the normalizing HEM45-GFP construct together with either a ProxER-GFP construct or the derivative m1ProxER-GFP where the uORF translational start was eliminated. RNA and protein samples from the same cultures were analyzed. Panel A: the levels of ER-GFP and HEM45-GFP RNA expression were determined by a RealTime PCR assay. Each sample was analyzed in triplicate and the mean ± standard error presented. The data for ER-GFP and HEM45-GFP was first normalized to the mean for expression of the ProxER-GFP culture and level of ER-GFP RNA in each culture then expressed as a ratio to that for HEM45-GFP. Panel B: the levels of ER-GFP and HEM45-GFP protein expression were evaluated by Western immunoblotting with GFP antiserum. A series of dilutions of the m1ProxER-GFP sample was included to facilitate quantitation. The level of ER-GFP protein is clearly increased when the uORF translational start is eliminated, in contrast to lack of change at the RNA level.

RNAs in the samples. The presented data for both transcripts was normalized to levels in the ProxER-GFP. The absolute RNA levels in cells transfected with ProxER-GFP and HEM45-GFP constructs were 446 and 61 attomoles/μgRNA, respectively and for cells transfected with m1ProxER-GFP and the normalizing construct the RNA levels were 549 and 79 attomoles/μgRNA.

In contrast to data for RNA, there was a large difference in levels of GFP in ProxER-GFP and m1ProxER-GFP transfected cells, as determined by Western immunoblot (Fig. 5B). The levels of GFP were measured by Western immunoblot in cells transfected with the ProxER-GFP construct and m1ProxER-GFP. GFP levels were approximately eight-fold greater in the extract of cells transfected with the m1ProxER-GFP constructs where the tanslational start of the uORF peptide was abolished by mutation of the ATG to CTG. The levels of the normalizing HEM45-GFP construct changed less than two-fold between the two transfected cell populations. Quantitation was by matching signal from the ProxER-GFP transfected samples to serial dilutions of the m1ProxER-GFP samples as we found chemiluminescent detection to have limited linearity.

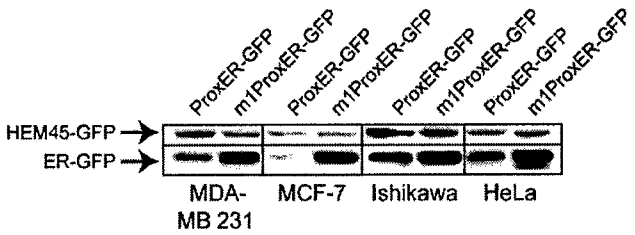

Fig. 6. The ER proximal transcript uORF affects downstream ER-GFP expression in a battery of cell lines. The indicated cell lines were transfected using lipofectamine 2000 and 2 μg of the HEM45-GFP reference control together with 2 μg of either a ProxER-GFP construct or the derivative m1ProxER-GFP where the uORF translational start was eliminated. The level of ER-GFP and HEM45-GFP protein expression was evaluated by Western immunoblotting with GFP antiserum. Data for each cell line was from a single gel, appropriate film exposures were used to detect the ER-GFP and the HEM45-GFP.

3.3. The proximal transcript uORF affects downstream initiation in a battery of cell lines

HeLa cells were used as a model system that is easily transfected, however the modulation of ER-ORF utilization by the upstream proximal transcript uORF was also seen in cell lines relevant to reproductive tract biology and breast cancer (Fig. 6). These cell lines included MDA-MB 231, an ER negative breast cancer line, the MCF-7 adenocarcinoma line expressing ER transcripts predominately from the proximal promoter and the uterine line Ishikawa where ER is transcribed from both the distal and proximal promoters.

DNA was introduced to cells using Lipofectamine 2000 with 2 μg each of the test GFP constructs and the HEM45-GFP reference. Western immunoblot analysis (Fig. 6) indicates that elimination of the uORF by mutation of the uORF translational start (m1ProxER-GFP) increased expression compared to the parental ER-GFP construct ProxER-GFP in each cell line.

3.4. The distal ER transcript uORF does not regulate downstream initiation

The expression of GFP from constructs was also reduced (Fig. 3B) compared to the pEGFP-N1 parent vector, when we included the upstream and start region of the distal transcript (DisER-GFP, Fig. 2). This was similar to, though greater than, reductions seen on inclusion of the proximal ER transcript sequences. However, mutation of the uORF to eliminate its translational start (m1aDisER-GFP, m1bDisER-GFP, Fig. 3B) had a limited effect on the level of expression of the distal ER-GFP fusion, in contrast to results for the ProxER-GFP constructs. By Student's *t*-test the expression from DisER-GFP constructs and the two derivatives with mutated translational start codons were all significantly less than that of expression from the parent pEGFP-N1 at the 0.05 level, but were not significantly different to each other. We

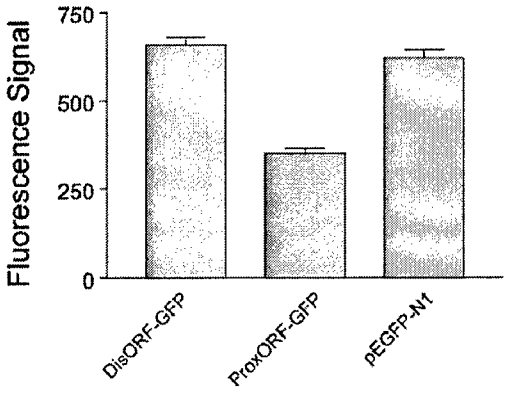

Fig. 7. A fusion of the proximal ER promoter transcript uORF to GFP is expressed poorly in cells, as compared to the parent pEGFP-N1 construct or a distal ER-ORF-GFP fusion. HeLa cells were transfected with 2 μg GFP constructs using Lipofectamine and GFP expression quantitated on a FACScan flow cytometer (see Fig. 3 and methods). Constructs used (Fig. 2) were the distal ORF-GFP fusion (distal), proximal ORF-GFP fusion (proximal), and the parental 'wild-type' pEGFP-N1 vector. Three transfected plates were used for each data set; separate DNA preparations were used for each well.

used two different mutations of the distal uORF translational start; ATG to CTG and to AAG. The use of non-AUG codons for translational initiation has been reported (Mehdi et al., 1990) but similar results with two different base changes virtually eliminated the chance of translational initiation of the distal uORF sequence from a non-AUG codon. These results were confirmed by Western blot analysis (Fig. 4) in separate experiments. The data indicate there are regulatory features which are specific to the unique regions of the ER proximal promoter transcript and similar properties are not shared by the distal ER promoter transcript fragment.

3.5. The ER upstream AUGs regions are functional translational entities

The mutations eliminating or truncating the uORF of the proximal ER transcripts relieved the suppression of GFP expression seen with ER-GFP constructs. We therefore made new types of constructs to probe the capacity of the uORF peptides to be expressed, and to determine the relative strengths of the uORF translational start regions in supporting peptide expression.

We made a new series of *ORF-GFP* constructs (Fig. 2) where the uORFs were fused in-frame to the GFP cassette, making a fusion protein whose translation initiated from the AUG regions of the ER uORFs; these constructs contained uORF sequences beginning at −7 relative to the A of the AUG but contained no sequences from the main ER coding region. GFP expression from these constructs measures the translational potential of the uORFs. HeLa cells were transiently transfected with the ORF-GFP constructs and the parent pEGFP-N1 construct. The ProxORF-GFP fusion was expressed at lower levels than the disORF-GFP fusion as measured both by flow cytometry (Fig. 7) and Western immunoblot-analysis (not shown). We achieved similar results with *ORF-ATG* constructs (Fig. 2) when we placed only the upstream ATG translational start regions (nt −7 to +4) ahead of GFP, eliminating the uORF peptides but initiating GFP translation from ER upstream translational start motifs. These studies indicated that the isolated proximal uORF translational start motif was very weak compared to the distal elements by both Western blot analysis (Fig. 8) and flow cytometry (mean fluorescence 417.37, S.E.M. 17.8, and 748.1 ± 32.5 respectively, $n=3$). Mutation of the proximal ORF-GFP translational start region at −3 and +4 to the consensus increased expression (data not shown).

The reduced mobility of the major band for the distal ATG-ORF construct in blots (Fig. 8) again clearly demonstrated the use of the added translational start in preference to the downstream GFP AUG. In these ORF-ATG constructs the size change came from polylinker sequences between the inserted translational start and the downstream GFP translational start codon. The presence of bands corresponding to the size of wt-GFP is variable and it is not clear if this is from a modification of the larger GFP or variable initiation at the original GFP AUG in pEGFP-N1. However, it is clear that translational start introduced to the ProxATG-GFP constructs strongly reduces all initiation. The weak initiation of expression from the ProxATG-GFP constructs was seen with three different batches of DNA isolated from different ligations events and *E. coli* colonies.

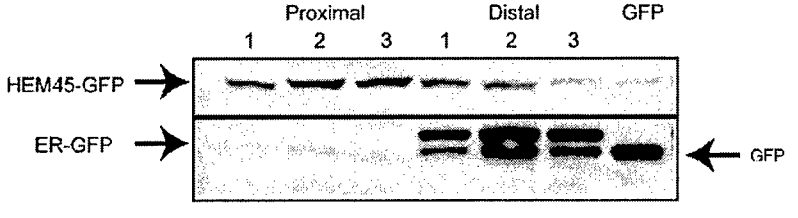

Fig. 8. Western immunoblotting confirms that the translational start region of the distal ER uORF is much stronger than that of the proximal promoter ER transcript uORF. Cells were transfected with uORF ATG-GFP constructs where distal and proximal promoter transcript sequences from −7 to +6 of the nucleotide sequence around the uORF translational start were placed ahead of the GFP ORF in pEGFP-N1. Three (1–3) DNA preparations from separate colonies were used in transfections for each construct design. Western immunoblot analysis for GFP was as described in Fig. 4. The upper panel represents signal to a cotransfected HEM45-GFP reference, the lower panels show bands from the uORF ATG-GFP fusion constructs or, in the far right lane, pEGFP-N1 (GFP).

4. Discussion

The proximal ER transcript upstream regions limited the capacity of an ER-GFP fusion (Fig. 2) to be expressed (Figs. 3 and 4). This suppression was clearly relieved by elimination of an upstream translational start. The change in GFP expression at the protein level measured in Fig. 5, without a similar change in RNA expression, upon elimination of the uORF translational start indicates the mechanism is translational rather than being an effect of the point mutation in m1ProxER-GFP on either mRNA stability or transcription.

The data, when considered together, indicate that the uORF of the ER proximal promoter transcript has effects on ER expression in its native context relative to the main ER translational start. The inhibitory effect is related to the encoded peptide product of the uORF. This is despite an apparently poor capacity of the peptide to be expressed (Figs. 7 and 8).

There was one prior study of translational control of ER (Kos et al., 2002). That study found no effect of the proximal transcript uORF on expression of a luciferase reporter, though the authors did find effects of the 5′ regions of a testis-specific ER transcript. The differences in results between our study and that of Kos et al., may be related to experimental details and design of reporter. The prior study included a larger upstream region of the ER proximal promoter than we used as the constructs here terminate immediately upstream of the uORF translational starts. However, only the initial three codons after the ER translational start were included in their luciferase reporter, and the native ER Kozak region was disrupted at −3 with a restriction site used for fragment insertion. We fused an 18 codon from the start of the main ER-ORF to our GFP reporter and maintained the integrity of the entire ER related region of constructs.

The extent of inhibitory action by the proximal peptide is comparable to that reported for uORF in the HER-2/neu oncogene (Child et al., 1999).

4.1. Translational regulation by the ER proximal transcript uORF requires more than an initiation site

Translational controls are poorly understood. The basic scanning model of eukaryotic translation (Kozak, 1989) and more recent mechanistic proposals (Jackson and Wickens, 1997) presume that the first (5′) AUG in a sequence should encode the translational initiator methionine, with 60S ribosomal subunits joining the scanning 40S unit to give the complete 80S complex. At its simplest, translational control is exerted because of the blocking of scanning; utilization of downstream AUG motifs requires either translational reinitiation, or that 'leaky scanning' has allowed some 40S complexes to pass over the upstream site without formation of a translational complex.

Leaky scanning appears to be a general phenomenon at any translational start that deviates from the maximally effective 'consensus' (Kozak, 1995). Re-initiation (Geballe, 1996) requires that the 40S subunit regain the range of cofactors that may have been lost in the formation of the 80S translational complex before the downstream codon can be utilized. In this model the translational start is the critical feature, and associated uORFs may be only a few codons long. The *S. cerevisiae GCN4* gene (Hinnebusch, 1996) provides a well characterized example, and this mechanism appears important for translational regulation of the HER-2/Neu oncogene by an AUG motif starting 29 bases upstream of the major translational start (Child et al., 1999). Increased spacing is generally considered to allow re-initiation, though results for Neu suggest it can occur with a minimal separation.

The distal transcript upstream AUG in isolation or as part of an uORF clearly provided a stronger translational start to GFP fusion constructs (Figs. 4 and 7) than did the proximal transcript upstream AUG region. This was not predictable from inspection of the sequences since both had deviations from the loose consensus, CGCCRCCATGG defined by Kozak (1987a), where strong sites have purines (R) at −3 relative to the AUG, and G at +4; the distal transcript upstream AUG lacks the purine at −3, and the proximal uORF translational start lacks the guanine at +4 (see Fig. 1B). An additional factor contributing to the weakness of the proximal uORF translational start may be the G at −3, since A is the favored purine. In contrast to expression characteristics, the proximal transcript uORF had functional effects since it was inhibitory and reduced ER expression from a downstream site. The distal transcript uORF had little or no effect despite its stronger expression.

Clearly a translational initiator is necessary for existence of a uORF, but the data indicate that the act of translational initiation is not the key feature leading to limited expression from the ER reading frame in ER proximal promoter transcripts.

4.2. Regulation of ER expression by the ER proximal transcript uORF

The ability to alter expression of GFP by truncating the uORF in addition to eliminating the translational start argues for a mechanism that requires the peptide of the uORF, rather than the effect being due to interaction of the uORF translational start motif with the ribosomal machinery to the detriment of downstream initiation. A single base mutation changed the uORF codon 3 Cysteine (Fig. 1B) to a stop signal. Premature termination of the proximal transcript upstream peptide relieved the suppression of expression of the ER-GFP fusion and had effects identical to the mutant eliminating the uORF translational start (Fig. 3). The effects of this second one base change also suggest that the results are not simply due to mutations affecting the RNA conformation, and hence translational capacity, of the ER proximal transcript 5′ regions. The general inhibition of GFP expression by the distal promoter transcript, unrelieved by elimination of the uORF, could be due to altered RNA conformation.

The organization of the uORFs within the ER proximal promoter transcript fits the tentative pattern emerging from studies of regulatory uORFs in other genes. Recent data indicate that re-initiation is possible following closure of uORFs of up to about 20 amino acids, hence it is possible to have uORFs in functional genes. At somewhat greater sizes there is loss of the capacity of the ribosomal machinery to re-initiate (Luukkonen et al., 1995). In addition, Kozak found that increasing the separation of two AUG motifs from 12 to 80 bases greatly increased expression from a downstream site (Kozak, 1987b). These observations may reflect the mechanisms of translational initiation, and the limitations this sets for modulation and control. The ER uORF translational starts are ~114 nt 5′ to the main ER translational start, the uORF stop signal is ~60 bases upstream of the main AUG. This distance is sufficient that ER could be derived either from reinitiation or from 'leaky scanning' past the upstream motif. Hence, the failure of the distal transcript upstream AUG to interfere with initiation is not surprising, underscoring the special properties of the proximal transcript.

4.3. Possible mechanisms for translational inhibition by the ER proximal transcript uORF

Other systems show a requirement for specific peptide sequences, generally with a *cis* role in regulation, either because of specific translational mechanisms or because of enhanced concentration in the translational region, i.e. within the ribosome. Approximately five examples of regulatory 5′ uORF sequences have been studied in detail. However, the exact mechanism of how translation control by specific uORFs and their peptides is achieved seems to be very variable. The studied uORFs lack conserved (shared) sequences (Geballe, 1996), and we have not been able to detect homology to ER uORFs. In one such example, the C-terminal prolyl codons are a key feature of the cytomegalovirus GP48 uORF (Cao and Geballe, 1998). The hydrolysis of prolyl-tRNA appears to occur at a low rate hence pausing the ribosomes on the mRNA upstream of the major GP48 ORF.

The ER distal and proximal uORFs share five C-terminal residues, hence it seems likely that the key differences between action of the two uORFs lie in the unique regions. However, it is possible that the shared regions do have a mechanistic role in the context of the complete proximal peptide. Two clear differences between the distal and proximal transcript upstream peptides are that the proximal transcript peptide has a much higher content of hydrophobic amino-acid residues and has a basic iso-electric point (Fig. 1C). It has been noted (Lovett and Rogers, 1996) that one of the few common features of regulatory upstream uORFs is that they are not acidic. We hypothesize this may be relevant to uORF peptide interactions with RNA and other negatively charged ribosomal components during translation and is supported by our finding that the inhibitory proximal transcript uORF encodes a basic peptide. The functionally silent distal peptide is acidic.

We do not yet fully understand how these data relate to in vivo regulation of ER. If the action of the uORF peptide is with the ribosomal machinery during the act of translation then it is likely that all cells that generate proximal promoter transcripts will have some degree of regulation, as was seen in Fig. 6 with a reporter construct. However, the extent of inhibition in specific cell environments and in normal versus tumor cells needs to be further evaluated. Using transgenic models, the expression of protein from the retinoic acid receptor RAR 2 transcript was strongly affected by a uORF only in heart and brain (Zimmer et al., 1994). The degree of influence of translational controls on ER may also vary with the menstrual cycle and may change at menopause as the levels of estrogen affect the levels of ER (Borras et al., 1994). Our model constructs contain only a small fraction of the ER regions and this may be a factor in the low expression from all the distal ER-GFP constructs analyzed. However, the data clearly indicate the potential for translational control of ER from the proximal promoter transcript. The combination of mRNA-derived translational controls together with multiple, alternative ER promoters under potentially different transcriptional controls provides a highly flexible regulatory system that we are only beginning to appreciate. A next step is to study effects of alternate transcript upstream regions on ER itself, in model systems and in human tumor samples.

Acknowledgments

These studies utilized the resources of the Wadsworth Center Molecular Genetics and Immunology cores. Supported in part by US Army BCRP contract DAMD17-01-1-0261 and -0529. Technical Assistance was provided by Alan Dupuis and Yili Lin.

References

Borras, M., Hardy, L., Lempereur, F., el Khissiin, A.H., Legros, N., Gol, W., Leclercq, G., 1994. Estradiol-induced down-regulation of estrogen receptor. Effect of various modulators of protein synthesis and expression. J. Steroid Biochem. Mol. Biol. 48, 325–336.

Cao, J., Geballe, A.P., 1998. Ribosomal release without peptidyl tRNA hydrolysis at translation termination in a eukaryotic system. RNA 4, 181–188.

Child, S.J., Miller, M.K., Geballe, A.P., 1999. Translational control by an upstream open reading frame in the HER-2/neu transcript. J. Biol. Chem. 274, 24335–24341.

Clark, G.M., Osborne, C.K., McGuire, W.L., 1984. Correlations between estrogen receptor, progesterone receptor, and patient characteristics in human breast cancer. J. Clin. Oncol. 2, 1102–1109.

Fasco, M.J., 1998. Estrogen receptor mRNA splice variants produced from the distal and proximal promoter transcripts. Mol. Cell. Endocrinol. 138, 51–59.

Fasco, M.J., Keyomarsi, K., Arcaro, K.F., Gierthy, J.F., 2000. Expression of an estrogen receptor variant protein in cell lines and tumors. Mol. Cell Endocrinol. 162, 167–180.

Fuqua, S.A., Wolf, D.M., 1995. Molecular aspects of estrogen receptor variants in breast cancer. Breast Cancer Res. Treat. 35, 233–241.

Geballe, A.P., 1996. Translational Control Mediated by Upstream AUG Codons.

Grandien, K., Berkenstam, A., Gustafsson, J.A., 1997. The estrogen receptor gene: promoter organization and expression. Int. J. Biochem. Cell Biol. 29, 1343–1369.

Hayashi, S., Imai, K., Suga, K., Kurihara, T., Higashi, Y., Nakachi, K., 1997. Two promoters in expression of estrogen receptor messenger RNA in human breast cancer. Carcinogenesis 18, 459–464.

Hinnebusch, A.G., 1996. Translational control of GCN4: gene-specific regualtion by phosphorylation of eIF2. In: Translational Control. CSH Laboratory Press.

Hori, M., Iwasaki, M., Shimazaki, J., Inagawa, S., Itabashi, M., 2000. Assessment of hypermethylated DNA in two promoter regions of the estrogen receptor alpha gene in human endometrial diseases. Gynecol. Oncol. 76, 89–96.

Jackson, R.J., Wickens, M., 1997. Translational controls impinging on the 5′-untranslated region and initiation factor proteins. Curr. Opin. Genet. Dev. 7, 233–241.

Kato, J., Hirata, S., Koh, T., Yamada-Mouri, N., Hoshi, K., Okinaga, S., 1998. The multiple untranslated first exons and promoters system of the oestrogen receptor gene in the brain and peripheral tissues of the rat and monkey and the developing rat cerebral cortex. J. Steroid Biochem. Mol. Biol. 65, 281–293.

Keaveney, M., Klug, J., Dawson, M.T., Nestor, P.V., Neilan, J.G., Forde, R.C., Gannon, F., 1991. Evidence for a previously unidentified upstream exon in the human oestrogen receptor gene. J. Mol. Endocrinol. 6, 111–115.

Kos, M., Denger, S., Reid, G., Gannon, F., 2002. Upstream open reading frames regulate the translation of the multiple mRNA variants of the estrogen receptor alpha. J. Biol. Chem. 277, 37131–37138.

Kozak, M., 1987a. At least six nucleotides preceding the AUG initiator codon enhance translation in mammalian cells. J. Mol. Biol. 196, 947–950.

Kozak, M., 1987b. Effects of intercistronic length on the efficiency of reinitiation by eucaryotic ribosomes. Mol. Cell. Biol. 7, 3438–3445.

Kozak, M., 1989. The scanning model for translation: an update. J. Cell Biol. 108, 229–241.

Kozak, M., 1995. Adherence to the first-AUG rule when a second AUG codon follows closely upon the first. Proc. Natl. Acad. Sci. USA 92, 7134.

Lovett, P.S., Rogers, E.J., 1996. Ribosome regulation by the nascent peptide. Microbiol. Rev. 60, 366–385.

Lucas, P.C., Granner, D.K., 1992. Hormone response domains in gene transcription. Annu. Rev. Biochem. 61, 1131–1173.

Luukkonen, B.G., Tan, W., Schwartz, S., 1995. Efficiency of reinitiation of translation on human immunodeficiency virus type 1 mRNAs is determined by the length of the upstream open reading frame and by intercistronic distance. J. Virol. 69, 4086–4094.

Mehdi, H., Ono, E., Gupta, K.C., 1990. Initiation of translation at CUG, GUG, and ACG codons in mammalian cells. Gene 91, 173–178.

Osborne, C.K., 1998. Steroid hormone receptors in breast cancer management. Breast Cancer Res. Treat. 51, 227–238.

Pentecost, B.T., 1998. Expression and estrogen regulation of the HEM45 MRNA in human tumor lines and in the rat uterus. J. Steroid Biochem. Mol. Biol. 64, 25–33.

Romain, S., Laine, B.C., Martin, P.M., Magdelenat, H., The EORTC Receptor Study Group, 1995. Steroid receptor distribution in 47 892 breast cancers. A collaborative study of 7 European laboratories. Eur. J. Cancer 31A, 411–417.

Weigel, R.J., Crooks, D.L., Iglehart, J.D., deConinck, E.C., 1995. Quantitative analysis of the transcriptional start sites of estrogen receptor in breast carcinoma. Cell Growth Diff. 6, 707–711.

Zimmer, A., Zimmer, A.M., Reynolds, K., 1994. Tissue specific expression of the retinoic acid receptor-beta 2: regulation by short open reading frames in the 5′-noncoding region. J. Cell Biol. 127, 1111–1119.

ELSEVIER

Molecular and Cellular Endocrinology 206 (2003) 33–47

MCE
Molecular and Cellular Endocrinology

www.elsevier.com/locate/mce

Phenotypic changes in MCF-7 cells during prolonged exposure to tamoxifen

Michael J. Fasco [a,b,*], Agita Amin [a,b], Brian T. Pentecost [a,b], Yi Yang [a], John F. Gierthy [a,b]

[a] *Laboratory of Human Toxicology and Molecular Epidemiology, Department of Environmental Disease Prevention, Wadsworth Center, New York State Department of Health, Albany, NY 12201, USA*

[b] *School of Public Health, The University at Albany, Department of Environmental Health and Toxicology, Albany, NY, USA*

Received 15 January 2003; accepted 25 June 2003

Abstract

MCF-7 breast tumor cells form multicellular nodules (foci) over a confluent monolayer in an estradiol (E2)-dependent, antiestrogen-sensitive reaction. A cell line cloned from MCF-7 that displays these phenotypes was probed to determine the effects of long term exposure to tamoxifen on the growth of foci, estrogen receptor alpha (ERα) status, and gene responsiveness to E2. In one of two experiments, a heterogeneous cell population emerged (TMX2) that over-expressed estrogen receptor alpha wild type mRNA (ERα mRNA) (~ 20-fold) missing exon 3 (ERΔ3 mRNA) and its corresponding protein (ERΔ3P). On a per mRNA to protein basis, ERΔ3P and wild-type ERα were equivalently expressed. Return of the TMX2 population to medium without tamoxifen eventually selected for a population that expressed predominately wild-type ERα, whereas TMX2 clones over expressing ERΔ3 mRNA and ERΔ3P retained this phenotype in tamoxifen-free media. In both experiments, expression of all ERα mRNAs and proteins declined to barely detectable levels during 6–12 months exposure, concomitant with a progressive increase in the ability of the cells to form foci independently of E2 or tamoxifen. Selection for these various populations suggests that tamoxifen can induce and/or support certain cellular changes that lead to altered ERα expression, E2-independent cell growth and resistance to antiestrogens.

Keywords: Human breast cancer; Tamoxifen; Estrogen receptor mRNA; Alternatively spliced estrogen receptor mRNAs; Estrogen receptor protein expression and estrogen receptor transcriptional regulation

1. Introduction

E2 and its cognate receptors, estrogen receptor alpha (ERα) and estrogen receptor beta (ERβ), play pivotal roles throughout the life span of a female in such essential processes as cell differentiation and growth, organ development, reproduction, and maintenance of bone density and the cardiovascular system. E2 also serves as a mitogen that enhances the growth of cancer cells in tissues associated with reproduction—cancer of the breast being the most prevalent among Western women, as well as the most intensively studied. In normal human breast epithelium, ERβ may be the prevailing receptor, but during carcinogenesis ERα emerges as the overwhelmingly predominant form Gustafsson and Warner (2000), Leygue et al. (1998) and Speirs et al. (1999).

Basic tenets of the current paradigm for E2-regulated cell growth (MacGregor and Jordan, 1998) are that circulating E2 enters the cell by passive transport, crosses the cytoplasm, and enters the nucleus, where it binds to ERα. Upon association with ligand, heat shock and other proteins bound to unliganded ERα are

Abbreviations: DC5, Dulbecco's minimum essential medium with supplements and 5% calf serum; DEPC, diethylpyrocarbonate; E2, estradiol; ERα, estrogen receptor alpha wild type protein; ERβ, estrogen receptor protein beta; EREs, estrogen response elements; ERα mRNA, estrogen receptor alpha wild type mRNA; ERΔn mRNA, estrogen receptor alpha mRNA missing exon n; ERΔnP, estrogen receptor alpha protein translated from ERΔn mRNA; RT-PCR, reverse transcription-polymerase chain reaction.

* Corresponding author. Tel.: +1-518-474-6192; fax: +1-518-486-1505.

E-mail address: fasco@wadsworth.org (M.J. Fasco).

0303-7207/03/$ - see front matter © 2003 Elsevier Ireland Ltd. All rights reserved.
doi:10.1016/S0303-7207(03)00256-9

released. ERα then dimerizes and binds to estrogen response elements (EREs) in the chromosomal DNA of responsive genes. Brown and co-workers (Shang et al., 2000) have recently demonstrated a stepwise assembly and cyclic grouping/ungrouping of E2-responsive transcriptional factors in MCF-7 cells. Their studies also suggested that the antiestrogenic compound, tamoxifen, caused recruitment of co-repressors instead of co-activators. In addition to binding to EREs, ERα-liganded dimers bind to proteins associated with AP-1 and SP-1 sites (Kushner et al., 2000; Paech et al., 1997; Wang et al., 1998; Porter et al., 1997) and unliganded ERα may participate in transcription via ternary complex formation with cyclin D1 and steroid receptor co-activators (Zwijsen et al., 1997, 1998). Given also the potential for ERα to form heterodimers with ERβ or other structurally different ERα proteins, and cross-talk between ERα with other protein synthetic pathways, unraveling the varied signaling and transcriptional mechanisms involved in the synthesis of proteins and growth factors that ultimately dictate E2-dependent growth in tumors is a formidable task.

Antiestrogens that bind to ERα and inhibit its growth function are classified into two groups. Type I antiestrogens possess both estrogenic and antiestrogenic activities in in vitro models; these are typically triphenylethylene compounds, represented by tamoxifen and its metabolites. Type II antiestrogens possess only antiestrogen activity and resemble E2 in structure. Type I and Type II antiestrogens have different effects on the two transcriptional activation function domains (AF-1 and AF-2) that reside in the N- and C-terminal regions of ERα (Metzger et al., 1995), respectively, and only Type II antiestrogens consistently down-regulate ERα protein levels (Dauvois et al., 1992). E2 can also promote the down-regulation of ERα protein, but its effect is cell context-dependent (Pink and Jordan, 1996). Tamoxifen has been the drug most commonly used in the treatment of ERα positive breast cancers because it selectively inhibits breast tissue ERα and may have beneficial effects on other receptor-positive tissues, such as bone (MacGregor and Jordan, 1998).

Breast tumors that arise following long term tamoxifen treatment are often resistant to its growth inhibitory effect. In a within-patient cohort of 72 women with breast cancer who were treated with tamoxifen, the following observations were made: (a) in most cases tamoxifen caused a reduction in tumor ERα concentration; (b) most of the initially ERα positive tumors that acquired resistance to tamoxifen during treatment maintained ERα expression; and (c) de novo resistant tumors tended to be ERα negative (Johnston et al., 1995). Several possible mechanisms for tamoxifen resistance in ERα positive breast tumors have been explored including alterations in E2 metabolism, malfunction of the metabolic pathways essential for receptor function, and receptor mutation, particularly involving the role of splice variant ERα proteins, but a causal association has not been demonstrated (MacGregor and Jordan, 1998).

ERα positive breast tumor cells deprived of E2 or exposed to antiestrogens for prolonged periods in culture eventually undergo phenotypic changes that allow them to proliferate under these normally growth-inhibitory conditions. Studies of cell lines displaying these phenotypes have provided insight into ERα function and mechanisms potentially responsible for the development of resistance to antiestrogens (Herman and Katzenellenbogen, 1996; Brunner et al., 1997; Katzenellenbogen et al., 1987). Under the culture conditions used, MCF-7 cells grow to a confluent monolayer at a rate that is essentially independent of E2. Growth beyond this checkpoint occurs only very slowly in the absence of E2, but in its presence multicellular structures (foci) form over the monolayer in a dose-dependent reaction that can be quantified (Gierthy et al., 1991). The formation of foci is inhibited by Type I and Type II antiestrogens. In this study we used a line cloned (clone 33) from the parental MCF-7 cells that displays these phenotypes (Gierthy et al., 1991). Changes in E2-dependent postconfluent cell growth, ERα status, and gene responsiveness to E2 in these cells during prolonged exposure to tamoxifen were monitored.

2. Materials and methods

2.1. Growth of MCF-7 cells

The MCF-7 cell clone 33 (Gierthy et al., 1991) was maintained in T-75 culture flasks in DC5 without and with tamoxifen (10^{-6} M; Sigma, St Louis, MO) added in DMSO (0.1% final concentration). Cells were suspended with trypsin (0.25%) and split 1 to 5 into fresh media every 3 days. Portions were assayed periodically for the formation of foci, and for ERα status.

2.2. MCF-7 focus assay

The MCF-7 focus assay, in which human breast cancer cells respond to E2 by producing multicellular nodules or foci on a confluent monolayer background, was conducted as previously described (Gierthy et al., 1991). Briefly, MCF-7 cells were suspended in DC5 after treatment with trypsin (0.25%), seeded into 24-well plastic tissue culture plates at a density of 1×10^5 cells/ml per well, and placed in a 37 °C, humidified, CO_2 incubator. Cells were re-fed at 24 h and every 3–4 days thereafter with 2 ml of DC5 containing various concentrations of E2 and tamoxifen in DMSO (0.1% final concentration). After 14 days the cultures were fixed

with formalin and stained with 1% Rhodamine B. The stained foci were counted using a New Brunswick Biotran II automated colony counter (Edison, NJ).

2.3. Whole-cell competitive ERα binding assay

The whole-cell ERα binding assay was similar to that previously reported (Gierthy et al., 1996). Briefly, MCF-7 cells suspended in DC5 were seeded into 24-well plates at a density of 5×10^5 cells/ml per well. Twenty-four hours later, the seeding medium was changed to DC5 containing [2,4,6,7,16,17-^{3}H] E2 (1.0 nM) and varying concentrations of unlabeled E2, and incubated at 37 °C for 3 h. The confluent cultures were then washed three-times with PBS, 300 μl of ethanol was added to each well for 20 min to solubilize the bound [^{3}H]E2, and the radioactivity in 200 μl of the ethanol extract was determined. To ensure that E2 binding in the TMX and TMX2 cell lines and clones was specific, the amount of bound [^{3}H] E2 in the presence of increasing concentrations of unlabeled E2 was determined and compared with the replacement profile obtained with the parent MCF-7.

2.4. Cloning of TMX2 cells

TMX2 cells in suspension were seeded into multiple 96-well plates at a concentration of 0.5–10 cells/0.4 ml of DC5 per well to ensure that a significant number of wells contained single cells. After 16 h of incubation to allow attachment, the wells were assessed by microscopic examination, and those containing no cells or more than one cell were rejected. After 1 week of continued incubation, the remaining wells were assessed for single colony formation and these wells were scored as clones. As the clones expanded to 100–200 cells, they were trypsin-suspended, centrifuged at $1000 \times g$ for 5 min, resuspended in 1 ml of DC5, and transferred to a 24-well plate well for further growth and analysis.

2.5. RNA extraction

RNA from T47D and the MCF-7 cell lines cultured in T75 flasks or 6-well plates was isolated with TRI reagent (Molecular Research Center, Cincinnati, OH) as described previously (Fasco, 1997, 1998). RNA pellets were dissolved in diethylpyrocarbonate (DEPC) water, and concentrations were calculated from the absorbance at 260 nm.

2.6. Real-time PCR

A Light Cycler® (Roche, Indianapolis, IN) was used with the Qiagen (Valencia, CA) One-Step Kit supplemented with Syber Green I (10 000 ×, Molecular Probes, Eugene OR). Master mixes were prepared at 4 °C and in multiples of 50 μl containing: 33 μl water; 10 μl of 5 × buffer (supplied); 2 μl of dNTP solution (supplied); 2 μl of enzyme mixture (supplied), 1 μl primer mixture (25 μM each); and 2 μl of Syber Green I (diluted 1/5000 with water). Aliquots (14.3 μl) were distributed into capillaries precooled to 4 °C, and total RNA was added in 0.75 μl. Unknown samples contained 0.1 μg total RNA per μl for all genes assayed except 28S, which was 0.001 μg total RNA per μl. The capillaries were spun just prior to reverse transcription-polymerase chain reaction (RT-PCR). RT was at 50 °C for 30 min followed by a 15 min at 95 °C heating step to inactivate the reverse transcriptases and activate the Taq polymerase. The number of amplification cycles was 45, and the cycling times for denaturation (95 °C), annealing (60 °C, except for PgR, which was 55 °C), and extension (72 °C) were, respectively, 15, 15 and 30 s. The ERα primer set used for real-time RT-PCR was: forward primer 5′-ATGATCAACTGGGCGAAGAG (exon 4; 1429–1448); reverse primer 5′-GATCTCCAC-CATGCCCTCTA(exon 6; 1613–1632) 204 bp (accession number NM_000125). ERβ primers were described by Vladusic et al. (2000). The 28S primers were from Simpson et al. (2000): forward primer 5′-TTGAAAATCCGGGGGAGAC; reverse primer 5′-ACATTGTTCCAACATGCCAG. The reverse PgR(AB) primer was from Fujimoto et al. (1998): forward primer 5′-TGCGAGGTCACCAGCTCTTG; reverse primer 5′-TTTGCCCTTCAGAAGCGGAC (321 bp). The pS2 primers were: forward primer 5′-TTGTGGTTTTCCTGGTGTCA; reverse primer 5′-GCAGATCCCTGCAGAAGTGT 156 bp (accession number XM_009779) and the HEM45 (Pentecost, 1998) primers were: forward primer 5′-GAGCGCCTCCTACACAAGAG; reverse primer 5′-AAGCCGAAAGCCTCTAGTCC 188 bp (accession number U88964). Standard curves for ERα, pS2, HEM45, and 28S were generated from 10-fold dilutions of total RNA isolated from MCF-7 cells prior to the initiation of the experiment. The PgR standard curve was constructed from T47D total RNA. These curves were stored and used throughout this study to allow calculation of relative changes in target mRNAs. A standard RNA was always included with the unknown samples to compensate for run to run variation. Fluorescence at the end of each amplification cycle was acquired at 5 °C below the start of the melting curve for each amplified target.

2.7. ERα mRNA splice variant compositions

The method was similar to that described previously (Fasco, 1997, 1998), except that a one-step RT-PCR kit (Qiagen) was used. Master mixtures were prepared as described for real-time RT-PCR, except that the Syber Green I was omitted and 50 μl reactions containing 2 μg

of total RNA were run in a PE 9600 thermocycler (Applied Biosystems, Foster City, CA). Primer sets within exons 1 and 5, exons 4 and 8, and exons 4 and 6 was used to determine the proportion of various components in the estrogen receptor alpha wild type mRNA (ERα mRNA) pool as reported previously (Fasco, 1997). Amplification conditions were the same as used for real-time RT-PCR, except that the extension at 72 °C was for 1 min, and the number of amplification cycles was 35. Quantitation of the DNA products was done with a P/ACE 2200 capillary electrophoresis unit (Beckman Instruments, Fullerton, CA) equipped with an argon ion laser and a 47 cm × 0.75 μm μSil-DNA column (J&W Scientific, Fulsom, CA) as described (Fasco et al., 1995). Primers spanning exon 3 were: 5′-GCTATGGAATCTGCCAAGGA (exon 2; 883–902) and 5′-AAGGCCAGGCTGTTCTTCTT (exon 4; 1264–1283) 401 bp (accession number NM_000125).

2.8. Nucleotide sequencing

DNAs obtained by RT and amplification of TMX2 mRNA with the exon 1–5 primer set were separated on a 2% agarose gel and the ethidium bromide staining band at approximately 780 bp was isolated using the QIAquick kit (Qiagen) and protocol. A 1 μl portion was re-amplified in a 50 μl reaction using the exon 1 to 5 primer set and the components supplied in a HotStart-Taq™ kit (Qiagen). The final magnesium concentration was 2.5 mM, and the concentration of each dNTP was 10 mM. The amplification conditions were as described above. The variant DNA was partially purified using a Qiaquick column (Qiagen) and cloned with a TA Cloning Kit (Clontech, Palo Alto, CA). Nucleotide sequencing of the insert-positive clones was done at the Wadsworth Center Molecular Genetics Core Facility, using a PE-Biosystems ABI PRISM 377XL automated DNA sequencer and universal M13 primers.

2.9. Western immunoblotting

Cells from the various lines were dissolved in SDS sample buffer without dye and 2-mercaptoethanol as described previously (Fasco et al., 2000). Protein concentrations were calculated with a BCA kit (Pierce, Rockford, IL). Protein separation was done on 10% Bis–Tris gels under reducing conditions in MOPS-SDS running buffer, according to the manufacturer's protocol (NuPage, Invitrogen, Carlsbad, CA). Separated proteins were transferred to an Immobilon-P membrane (Owl Separation Systems, Woburn, MA) using the NuPage apparatus and protocol. Other conditions were as described (Fasco et al., 2000). ERα specific antibodies were NCL-ER-6F11 (Nova Castra Laboratories, Newcastle, UK) and HC-20, H-184 and Ser118 (Santa Cruz Biotechnology Inc., Santa Cruz, CA), used at a 1/100 and 1/500, 1/200 and 1/100 dilution, respectively, in blocking buffer. The ERβ specific antibody was N-19 (Santa Cruz Biotechnology) used at a 1/250 dilution in blocking buffer. Species- and Cruz molecular weight-compatible horseradish-peroxidase labeled secondary antibodies were from Santa Cruz Biotechnology Inc.

2.10. ERE-Luc reporter

Estrogen receptor action was assessed using a firefly luciferase reporter system. The reporter construct (pERE-Luc) utilized a functional ERE as described in Pentecost et al. (1990), but it was placed upstream of the promoter–reporter cassette of pGL2-promoter. All DNA was prepared with the Qiagen maxi prep system. Cells were transfected in 24-well cluster plates using Lipofectamine 2000 (Invitrogen Life Technologies, Baltimore, MD). Cell extracts were prepared with passive lysis buffer and assayed with the dual-luciferase assay (Promega, Madison, WI). Fire fly luciferase activity was normalized to the Renilla luciferase activity from co-transfected pRL-CMV. pERE-Luc (180 ng) was combined with 20 ng pRL-CMV (Promega) and 300 ng pBluescript (Stratagene, La Jolla, CA) as carrier, to give 500 ng DNA for each well. This DNA was combined with 2 μl lipofectamine in 100 μl DMEM (phenol red-free). After 45 min this was added to cells plated the previous day at 125 000 cells/well. The cells were in 0.5 ml phenol red-free DMEM with stripped, de-lipidated serum (Sigma). The liposomes and media were aspirated after overnight (17 h) incubation and replaced with 2 ml DMEM (phenol red-free) containing serum replacement (Sigma), and the indicated level of E2 added with ethanol (0.1% final concentration). Cells were harvested after 47 h and the lysates were assayed in a luminometer (Berthold Instruments). Corrections were applied to data for background autofluorescence. Media and liposomes were made up as master mixes that were subsequently aliquoted to multiple wells to minimize variability.

3. Results

MCF-7 clone 33, previously selected for its dependence on E2 for formation of foci (Gierthy et al., 1991), was continuously exposed to tamoxifen (10^{-6} M) in DC5, a highly E2-deficient media ($< 10^{-11}$ M). Clone 33 was also maintained in DC5 without tamoxifen throughout as a control population. Cell populations were assayed periodically for ERα status (splice variant composition and quantity) and changes in the patterns of postconfluent focal growth. When changes were observed, a portion was frozen for future use. Other portions were transferred to and maintained in media

with or without tamoxifen. Two essentially identical experiments were conducted that started approximately 1 year apart. A box chart depicting the names of the cell populations used in this study, the approximate times when they were isolated, and under what culture conditions is presented in Fig. 1. Also in Fig. 1 are photographs illustrating the ability of the focus assay to detect postconfluent growth differences among different cell populations, and populations treated with E2 and antiestrogens. Panels A, B, and C show the E2-responsive parental MCF-7 cells cultured in, respectively: DC5 (E2-deficient environment); DC5 plus 10^{-10} M E2; and DC5 plus 10^{-10} M E2 plus 10^{-6} M raloxifene. Panels D, E, and F show the ERα negative TMX cells under the same culture conditions, except that in Panel F no E2 was added, and the antiestrogen

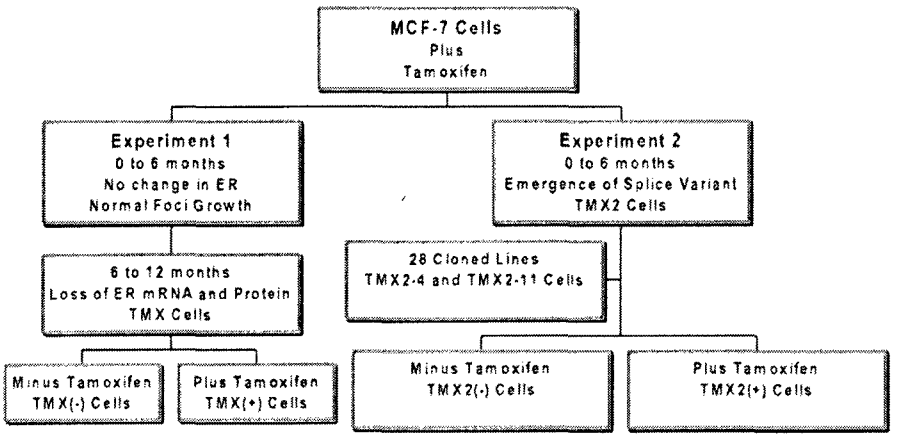

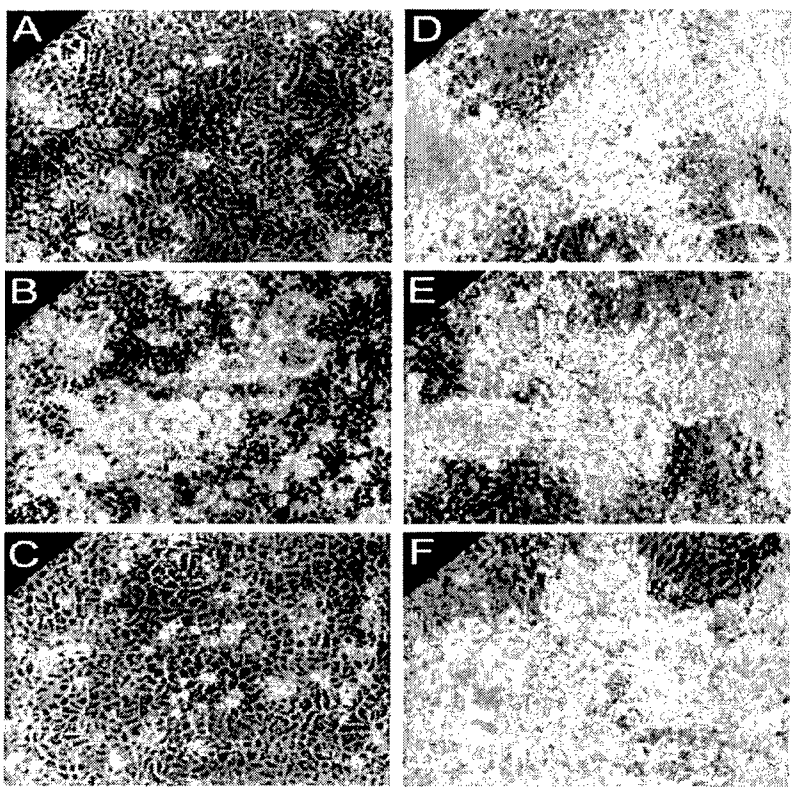

Fig. 1. Box chart showing the names of the various MCF-7 populations used in this study, when they were isolated and under what culture conditions. Phase contrast microscopy of 10-day postconfluent cell growth in the ERα positive MCF-7 parental cells and the ERα negative TMX(−) cell population. Cells showing as dark are the confluent monolayer; light areas are the foci. Panel A, MCF-7 parental cells in DC5 and thus without E2; panel B, MCF-7 parental cells in DC5 plus 10^{-10} M E2; panel C, MCF-7 parental cells in DC5 plus 10^{-10} M E2 and 10^{-6} M LY-156758 (raloxifene); panel D, ERα negative TMX(−) cells without E2; panel E, TMX(−) cells plus 10^{-10} M E2; panel F, TMX(−) cells plus 10^{-6} M tamoxifen. For growth conditions see Section 2.

was 10^{-6} M tamoxifen. The light gray areas are foci overgrowing the much darker appearing cells of the monolayer.

In the first of the two experiments, little change in ERα status was observed during the initial 6 months of culture in the presence of tamoxifen; a slight down-regulation of the ERα protein level did occur without any detectable change in the ERα mRNA splice variant pattern or the level of ERα mRNA. Subsequently, however, spontaneous (E2-independent) formation of foci began to increase. Concomitant with this phenotypic change was a progressive decrease in the expression levels of ERα and splice variant mRNAs and ERα. After approximately another 6 months, levels of ERα mRNA were just above the threshold for detection by RT-PCR, and ERα protein was undetectable in our Western immunoblot assay (Fig. 2). This ERα negative population (TMX), following transfer to media with tamoxifen (TMX(+)) or without tamoxifen (TMX(−)) more than 1 year ago, has not recovered any ERα mRNA or ERα expression nor has it undergone a reduction in the extent of E2-independent formation of foci. Postconfluent growth of foci in TMX occurs in the absence of E2, is not enhanced by E2, and is not inhibited by tamoxifen (Fig. 1).

In contrast to the first experiment, a pronounced change in ERα protein expression occurred in the second experiment during the initial 6 months of culture in tamoxifen. As shown in Fig. 2, two ERα proteins with approximate molecular masses of 66 and 61 kDa were recognized in TMX2 cells (see Fig. 1 box chart) by anti-ERα antibodies reactive against epitopes in the N-terminal (NCL-ER-6F11) and the extreme C-terminal regions (HC-20). Not shown are Western immunoblots demonstrating that ERα and the 61 kDa protein were also recognized by antibody H-184 (a polyclonal antibody raised against amino acids 2–185 of human ERα) and by Ser118 (raised against phosphorylated serine 118 of ERα). Reaction of both proteins with the latter antibody was greatly enhanced by exposing the cells to E2 (10^{-9} M) for 2 h before isolation of the cellular proteins. Recognition of the 61 kDa protein by all of these antibodies strongly suggests that the amino acids missing from the ERα sequence are internal and not at the N- and C-terminal regions.

Electropherograms of the DNAs amplified from cDNAs of the parental MCF-7 and TMX2 cells with a primer set spanning exons 1 to 5 are illustrated in the two upper graphs in Fig. 3. The DNA product amplified from those ERα cDNAs containing the complete exon 1–5 sequence (894 bp) is the major peak that elutes last in both electropherograms. The other major peak (777 bp) in the electropherogram of amplified TMX2 cDNA is missing only those nucleotides of exon 3 as established by nucleotide sequencing of TA clones containing the over-expressed DNA purified from an agarose gel. The variant portion of the ERα sequence obtained with the exon 1 to exon 5 primer set was (3′ end of exon 2) TATTCAA (**Δ exon 3**) GGGATACGAA (5′ end of exon 4).

Complete mRNA splicing profiles in the parental MCF-7, TMX, and TMX2 populations are presented in the bar graph of Fig. 3. The ERα mRNA splicing pattern in TMX was determined by RT-PCR before the ERα mRNA diminished below the detection threshold. As is evident from Fig. 3, TMX retained a mRNA splicing pattern that was very similar to that of parental MCF-7 with the predominant mRNA forms being wild type and that missing exon 7. In striking contrast is the TMX2 ERα mRNA pool that contains essentially equivalent amounts of ERα, ERΔ3 and ERΔ7 mRNAs. In TMX2 cells, the percent contribution of ERΔ3 mRNA expression to the total ERα mRNA pool is approximately 20-fold higher than in the other cell lines

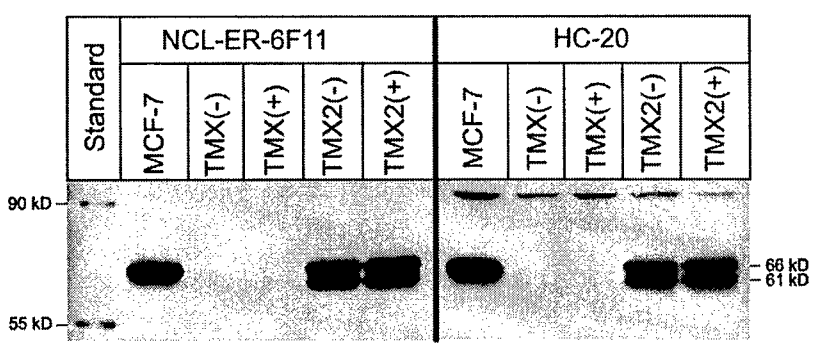

Fig. 2. Western immunoblots of various MCF-7 populations that developed during continuous exposure to tamoxifen (10^{-6} M). MCF-7 cells were continuously cultured in DC5 without tamoxifen. The NCL-ER-6F11 antibody recognizes the N-terminus of ERα and HC-20 recognizes amino acids in the extreme C-terminus. The ERα negative TMX cells that developed after approximately 1 year in tamoxifen presence were transferred to media without tamoxifen (TMX(−) cells) and with tamoxifen (TMX(+) cells) and assayed when they reached confluence. The TMX2 population at the end of 6 months in culture expressed high levels of ERα and a 61 kDa ERα protein. It was also split into media without tamoxifen (TMX2(−) cells) and with tamoxifen (TMX2(+) cells) and assayed at confluence. Each lane contained 20 μg of total protein. Other conditions were as described under Section 2.

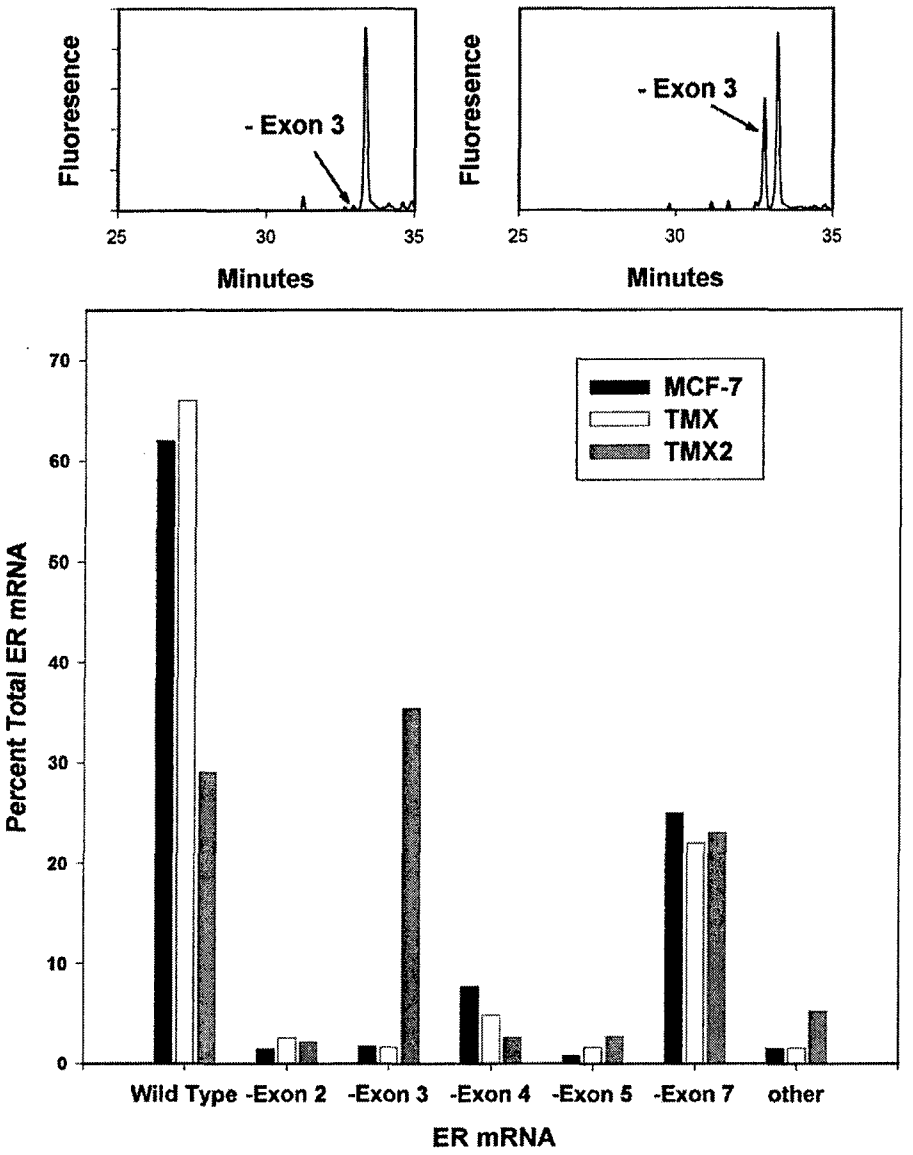

Fig. 3. ERα mRNA alternative mRNA splicing in parental MCF-7 and in TMX and TMX2. Top: electropherograms of MCF-7 (left) and TMX2 (right) DNAs amplified from ERα cDNA with the exon 1–5 primer set. The identity of the product missing exon 3 in the TMX2 cells was established by nucleotide sequencing. Bottom: bar graph of complete alternative ERα mRNA splicing patterns in MCF-7, TMX, and TMX2 constructed DNA fragments amplified with the exon 1–5 and exon 4–8 primer sets. The splicing pattern in TMX was obtained before the level of the ERα mRNA pool dropped below the analytical limit of the assay. Conditions were as described under Section 2.

(Fig. 3). This increase in ERΔ3 mRNA expression is accompanied by a nearly proportionate decrease in the expression of wild type ERα mRNA; the net effect on the ERα mRNA pool is that the percents of ERΔ3mRNA, ERΔ7mRNA and wild type ERα mRNA are nearly equivalent. Since expression of ERα protein and the 61 kDa ERα protein in these cells occurs to nearly the same extent (Fig. 2; TMX2(−) or TMX2(+) cell extracts), it follows that the two proteins are similarly expressed on a per-mRNA basis. This contrasts with ERΔ7P, whose expression is much less than that of ERα on an equivalent mRNA basis (Fasco et al., 2000).

Twenty-eight clones were isolated from TMX2 just after it was split into media with or without tamoxifen. A few clones expressed only ERα and one did not express any detectable receptor. All of the others expressed both ERα and the 61 kDa ERα protein in various proportions, with the majority expressing approximately equivalent amounts of the two. TMX2–4 was selected as representative of the heterogeneous TMX2 culture because it expressed approximately equal amounts of the two receptors. TMX2–11 was selected as a representative of 61 kDa ERα protein over-expression, having a 61 kDa ERα to ERα protein ratio of approximately 4:1. Fig. 4 qualitatively depicts the

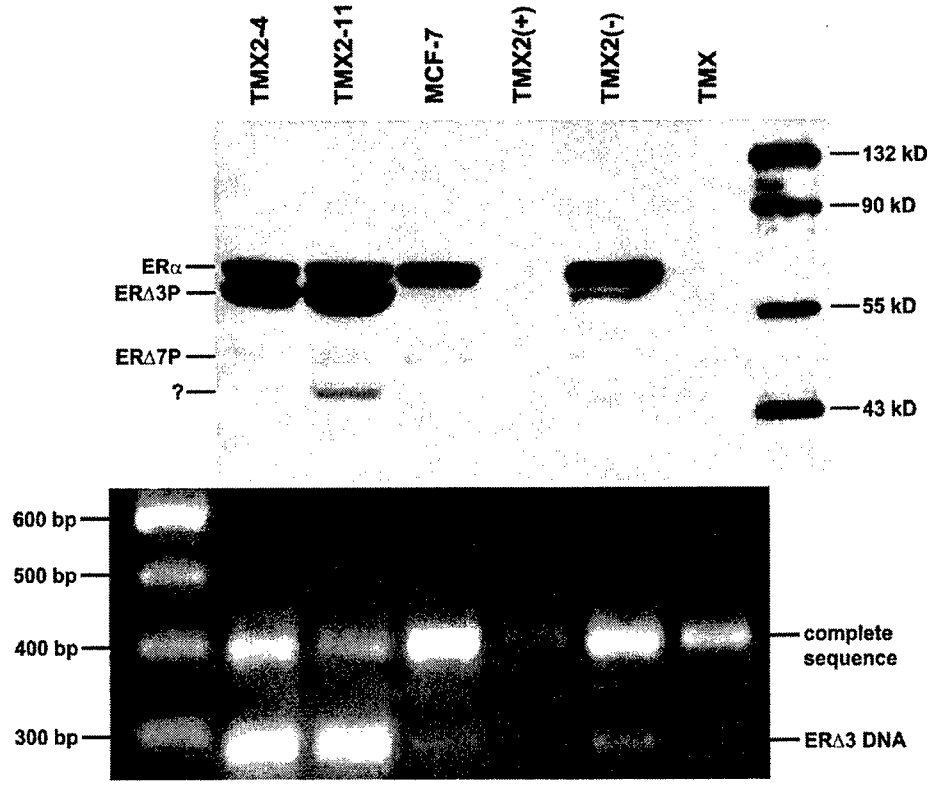

Fig. 4. Upper panel: Western immunoblot depicting receptor expression differences that occurred when the TMX2 cells previously exposed to tamoxifen for 6 months (see Fig. 1 box chart) were continued in culture in the presence (+) and absence (−) of tamoxifen (10^{-6} M) for an additional 6 months. Note the differences in the expression profiles of these cells compared with those in the TMX2(+) and TMX2(−) cells determined 6 months earlier (Fig. 2). The antibody was NCL-ER-6F11, and the total protein per lane was 20 μg. TMX was from the original ERα negative line and is included as an ERα negative reference. TMX-4 and TMX-11 are clones of TMX2 (Fig. 1 box chart) that had been cultured in the absence of tamoxifen for approximately the same length of time as TMX2(−) cells shown here. Bottom panel: RT-PCR of the RNAs from these cells using the exon 2 to 4 primer set are included so that the amount of ERΔ3 mRNA expression in the various samples can be compared with the amount of the 61 kDa protein expression (ERΔ3P). Experimental conditions were as described under Section 2.

relationship that exists between the expression ratio of the 61 kDa ERα protein to ERα protein (upper panel) and the expression ratio of the amplified ERΔ3 cDNA to complete sequence cDNA (lower panel) using primers located in exons 2 and 4. The fluorescence intensity of the complete sequence DNA band is derived from all the variant and wild type cDNA transcripts except for those missing primer locations in exons 2 or 4, which are not amplified, and those having enough internal nucleotide variation to produce DNAs that separate on an agarose gel. In this case, the internal variation was deletion of the nucleotides that comprise exon 3. As is evident, a highly positive correlation exists between the amount of ERΔ3 mRNA present in the ERα mRNA pool and the level of expression of the 61 kDa protein; consistent with the concept that the 61 kDa protein is translated from ERΔ3 mRNA.

Both of the TMX2 clones were transferred to and maintained in media without tamoxifen. Neither one has changed its levels of ERα and ERΔ3 mRNA or pattern of protein expression since its isolation and maintenance in media without tamoxifen over 6 months ago. In contrast, the heterogeneous TMX2 culture underwent significant change depending on whether it was cultured in the presence or absence of tamoxifen. In the absence of tamoxifen (TMX2(−)), a population of cells gradually emerged that expressed primarily ERα mRNA and protein: compare TMX2(−) with TMX2–4, whose ERα and ERΔ3P expression is representative of the heterogeneous TMX2 population, and with the parental MCF-7. In the continued presence of tamoxifen (TMX2(+)) all forms of ERα mRNA and protein eventually diminished to the extent that no forms of the latter were detectable by Western immunoblotting. As indicated from the amplified cDNA profile shown in the bottom panel of Fig. 4, few if any of the now ERα protein negative TMX2(+) cells over-express ERΔ3 mRNA as this splice variant is only a minor component relative to the complete exon 2 to 4 sequence obtained.

Other truncated ERα proteins were also detectable in the cell populations expressing ERα and ERΔ3P (Fig. 4). We demonstrated previously that the 52 kDa ERα protein in MCF-7 cells was ERΔ7P (Fasco et al., 2000). In both of the TMX2 clones, and particularly in

TMX2–11, another anti-ERα positive band was also detectable whose molecular mass was approximately 45 kDa. The amino acid sequence of this protein is not known, but it is probably linked to the exon 3 deletion since it is detectable only in the populations that over-express ERΔ3P.

A comparison of the E2-binding capability among the various populations is presented in Fig. 5. The lower panel in Fig. 5 illustrates the relative amounts of total (wild type plus splice variant) ERα mRNA among the cell populations as determined by real-time RT-PCR. The corresponding ERα and 61 kDa protein expression profiles are those depicted in Fig. 4. As expected, TMX and TMX2(+) cells, which had lost most of their ERα mRNA and ERα expression, also did not bind detectable E2. Each of the other populations bound the hormone efficiently, with TMX2–11 binding the most. Unlabeled E2 effectively competed for binding to the ERα protein(s) in a concentration-dependent manner that was very similar for all of the populations. Given some variation inherent in all the assays, relative differences between the cell populations at maximum (^{3}H)E2 binding (10^{-12} M unlabeled E2) closely approximate the relative levels of total ERα and ERΔ3P expression shown in Fig. 4 and the relative levels of their mRNA expression measured by real-time RT-PCR (Fig. 5. lower panel). Since the 61 kDa protein constitutes 50 and 80% of the total ERα expressed in TMX2–4 and TMX2–11 cells, respectively, E2 must bind to the 61 kDa protein and with an affinity comparable to that of the ERα. If this were not the case, E2 binding in these lines would be much less than in the parental MCF-7, which express only ERα.

To probe whether ERα function was significantly impaired by ERΔ3P, E2 effects on the endogenous ERα-regulated genes PgR, pS2 and HEM45 and on the non-regulated gene, 28S ribosomal RNA, were determined in all of the populations by real-time RT-PCR (Fig. 6). In the ERα positive cell lines MCF-7, TMX2(−), TMX2–4 and TMX2–11, all three E2-dependent genes were significantly up-regulated by E2 ($P \leq 0.01$ for all except HEM45 in TMX2(−) which was 0.015) as determined by paired students t-test. E2 did not significantly increase mRNA transcription of the 28S non-responsive gene in the various populations (P range = 0.10–0.65). Among the ERα negative lines, TMX cells showed a significant E2-dependent down-regulation of pS2 and HEM45, and the TMX2(+) cells a significant E2-dependent down-regulation of pS2. The actual differences were quite small, however, and given the fact that endogenous levels of pS2 are substantially reduced in the ERα negative lines, it is possible that these differences are only statistical. Irrespective, regulation was in the opposite direction of those genes known to up-regulated by E2. TMX2–4 and TMX2–11 were also transfected with a construct containing an ERE and luciferase reporter (ER-Luc), and their response to E2 compared with that of parental MCF-7 (Fig. 6). An E2 concentration of 10 pM elicited a maximal and highly significant (paired t-test $P \leq 0.05$) increase in luciferase activity in MCF-7 and in TMX2–4 and TMX2–11 cells.

The effect of E2 concentration on the formation of foci among the various populations is illustrated in the line graph of Fig. 7. The bar graph shows the effect of 10^{-10} M E2 with or without 10^{-6} M tamoxifen on the formation of foci. TMX and TMX2(+), which are nearly devoid of ERα mRNAs and proteins, readily formed foci in the absence of E2 and independently of the presence of exogenous E2 at any concentration. Tamoxifen had little, if any, effect on the postconfluent cell growth of TMX or TMX2(+). The extents of formation of foci by the parental MCF-7 and TMX2(−) lines, which express, respectively, exclusively ERα and predominately ERα with some ERΔ3P, were similar with respect to E2-dependence and inhibition by tamoxifen. Much different, however, were the postconfluent growth patterns in the TMX2–4 and TMX2–11 clones. TMX2–11, and particularly TMX2–4, required more E2 for the formation of foci than did the parent MCF-7. Tamoxifen was an effective inhibitor of the formation of foci in TMX2–11, and probably TMX2–4 as well, although the data for this clone are equivocal because the focal density with or without E2 was very low.

ERβ mRNA expression in the parental MCF-7 cells and all the other populations was similar and very low, being just above the detection threshold of detection in our real-time RT-PCR assay. No ERβ protein was detected by Western immunoblotting in any of the cell lines (data not shown).

4. Discussion

Carcinogenesis involves the alteration of many genes, eventually resulting in unregulated growth and aggressive behavior of cells. Cancers arising in reproductive tissue are often dependent upon hormones, such as E2, for sustained growth and, while much has been learned regarding hormone-dependent cell growth, much yet remains unexplained. A major contributor to our lack of knowledge in this area is a shortage of adequate in vitro models. In the media used, MCF-7 cells readily grow to confluence in an essentially E2-independent manner, but continue to grow beyond this checkpoint point only very slowly (Gierthy et al., 1988, 1996). Addition of physiological levels of E2 produces discrete, three-dimensional nodules of cellular overgrowth, termed foci, over the monolayer 3–4 days postconfluence. Their unique cellular structure readily permits quantitation of the number of foci per unit area by differential staining, thus assaying a highly complex growth process. The formation of foci is also sensitive to many xenoestrogens

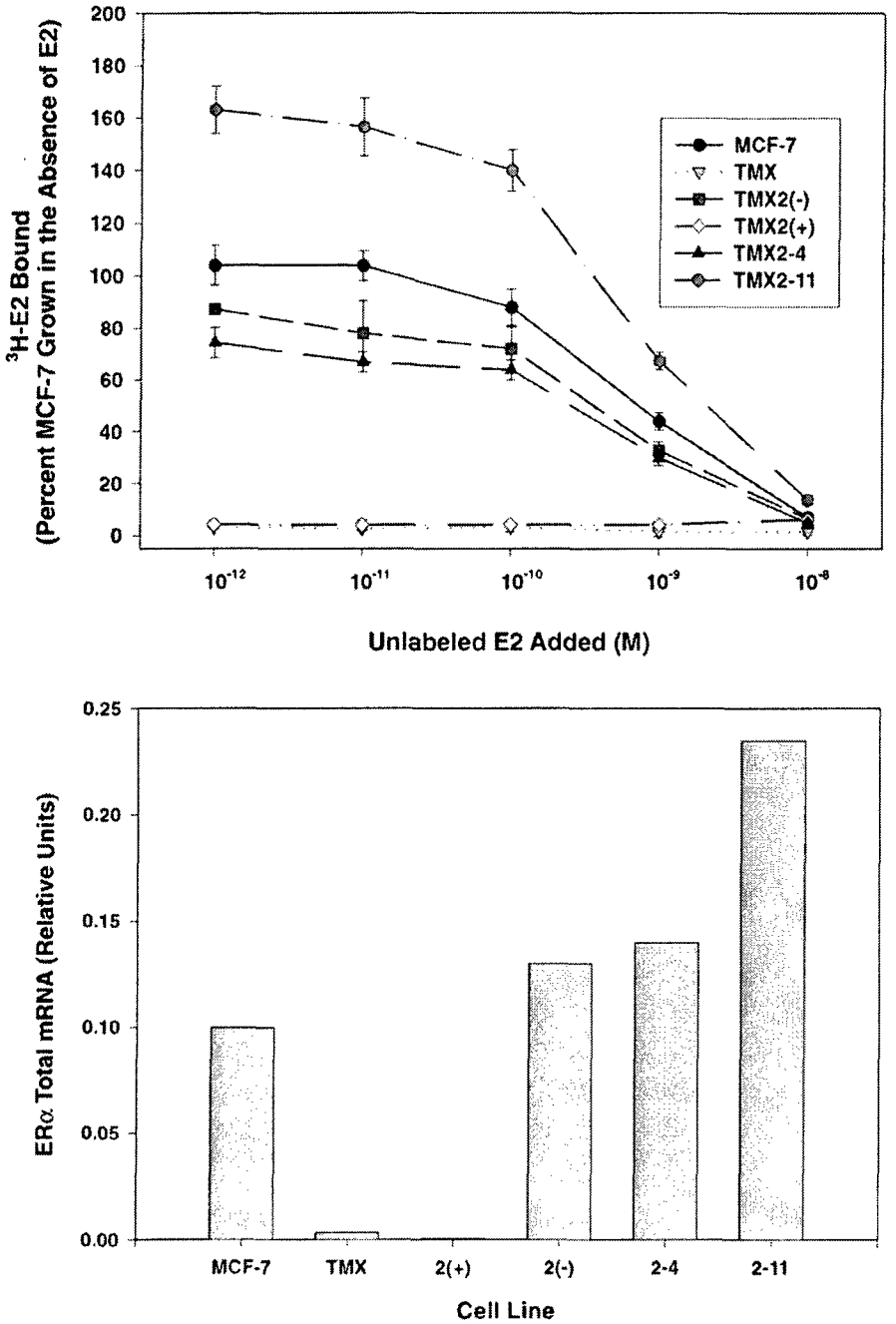

Fig. 5. Upper panel: comparison of whole-cell E2 binding among the various MCF-7 cell populations. Error bars are the SEM of four replicates. Lower panel: relative amounts of total ERα mRNA in the various MCF-7 cell populations excluding the contribution from alternatively spliced ERα mRNA variants missing exons 4 or 6, which comprise no more than 15% of the total ERα mRNA pool (see Fig. 3; -exon 4 plus forms contained in "other"). Values are the average of duplicate samples run as described under Section 2 for real-time RT-PCR of ERα mRNAs. Corresponding ERα protein expression is shown in the Western immunoblot in Fig. 4.

and xenoantiestrogens, and to Type I and Type II antiestrogens, thereby making the postconfluent cell growth of MCF-7 cells in vitro a useful model by which to probe physiologically relevant mechanisms of hormone-dependent growth and antiestrogen resistance (Gierthy et al., 1991, 1997; Arcaro et al., 1999; Mizejewski et al., 1996).

During prolonged exposure of the parental MCF-7 cells to tamoxifen, populations of cells emerged in which changes in the levels of ERα mRNA and ERα protein expression and in the growth of foci could be readily detected without the aid of cloning. In two separate, but essentially identical experiments, both similar and markedly disparate changes occurred, despite the fact

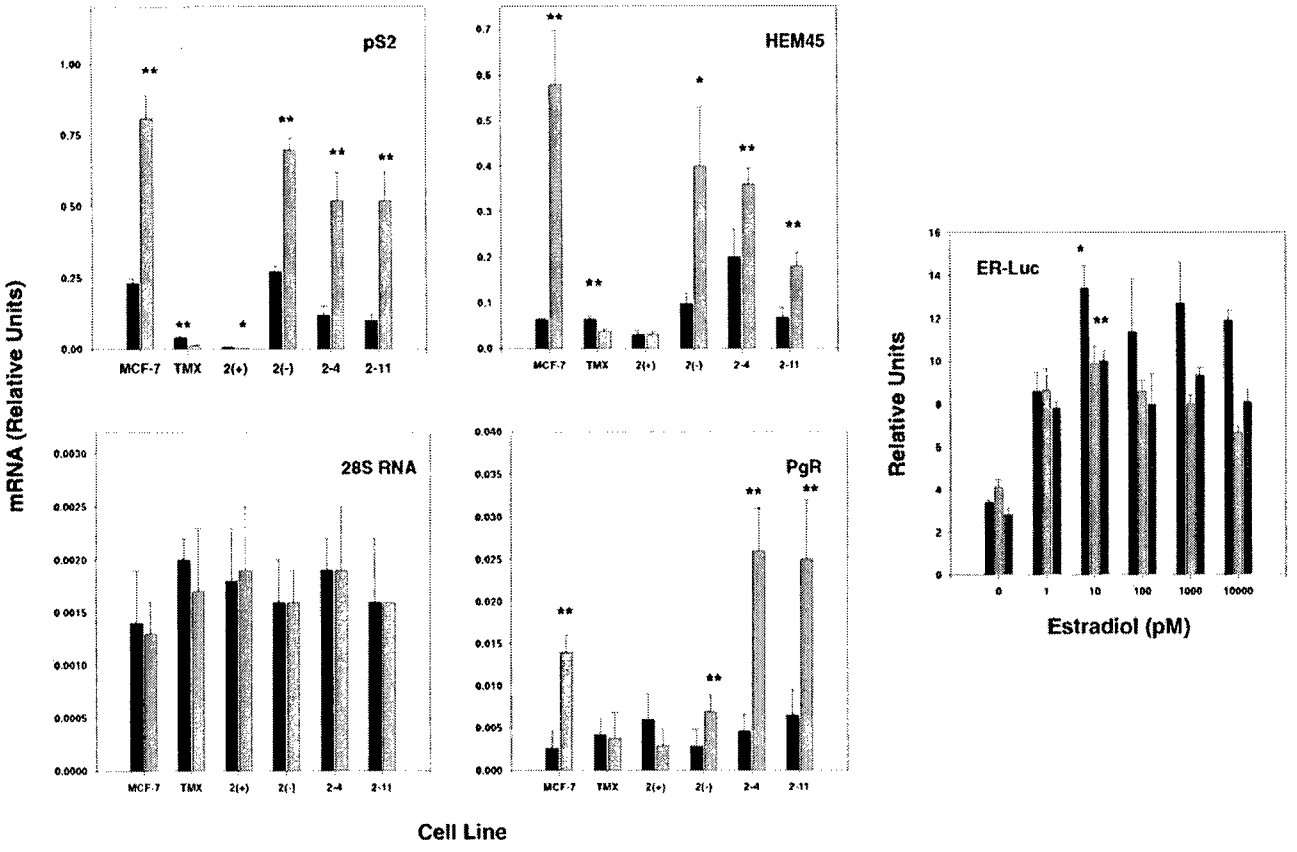

Fig. 6. Comparison of E2 deprivation (DC5 media only—dark bars) vs. 24 h E2 exposure (10^{-9} M—gray bars) on mRNA levels of the E2-dependent genes PgR, pS2, and HEM45 and the E2-independent gene 28S among the various cell populations. Values are the mean±S.D. of two separate experiments containing duplicate samples. Significance was determined by paired t-test between the DC5 versus E2 exposed samples: $P \leq 0.05$ and ≤ 0.01 are represented by 1 and 2 stars, respectively. Second experiment samples for 28S in the E2-treated 2–11 cells were lost, hence the absence of an error bar. Conditions for real-time RT-PCR were as described under Section 2. ERα and ERΔ3P protein expression is that shown in the Western immunoblot of Fig. 4. Names designated with a 2- are abbreviations for TMX2. Also included in the figure is a comparison of the ability of E2 to activate a transfected construct containing an ERE and luciferase reporter (ER-Luc) in the parental MCF-7 cells (black bars) and the ERΔ3P-expressing clones TMX2–4 (light grey bars) and TMX2–11 (dark grey bars). Values are the S.E.M. of triplicate assays. Statistical comparison by paired t-test (* = $P \leq 0.05$) is shown only for the three cell lines not exposed to E2 vs. the same cells exposed to 10 pM E2. Experimental conditions for preparation of the construct and for the assay of luciferase activity were as described under Section 2.

that the same initial cell population was used for each experiment. The MCF-7 parental line used here was originally derived from a single cell several years ago. Throughout these experiments clone 33 was maintained in DC5 (a highly E2 deficient environment of $< 10^{-11}$ M) as a control population. Although cells cultured in an E2 deficient environment for prolonged periods can undergo phenotypic changes (Pink et al., 1995, 1996), no detectable changes in the overall E2-dependency on the postconfluent growth of foci or on ERα mRNA and protein expression occurred during the 2–3 year course of these experiments. Recent subcloning of the parental MCF-7 cell line did demonstrate that a few of the clones exhibited abnormal E2 dependency on the growth of foci, but none exhibited the phenotypes that developed during prolonged exposure to tamoxifen.

In the first of our two tamoxifen exposure experiments, little change occurred in the composition of the ERα mRNA wild type and splice variant pool or in the expression of their corresponding proteins during the first 6 months. By the end of 12 months, however, a pronounced reduction in the expression levels of ERα mRNA and protein had occurred. In the second experiment, cells maintained in media containing tamoxifen also eventually lost ERα mRNA and ERα expression while acquiring the ability to form foci independently of the presence of E2 or tamoxifen. These TMX and TMX2(+) ERα negative populations (Fig. 1) have retained these phenotypes since their transfer to tamoxifen-free media many months ago. One clone isolated from the heterogeneous TMX2 population also lacks detectable ERα proteins and forms foci independently of the presence of E2 and tamoxifen (data not shown), adding support to the observation that ERα loss associates with enhanced rates of postconfluent cell growth in the MCF-7 model. Oesterreich

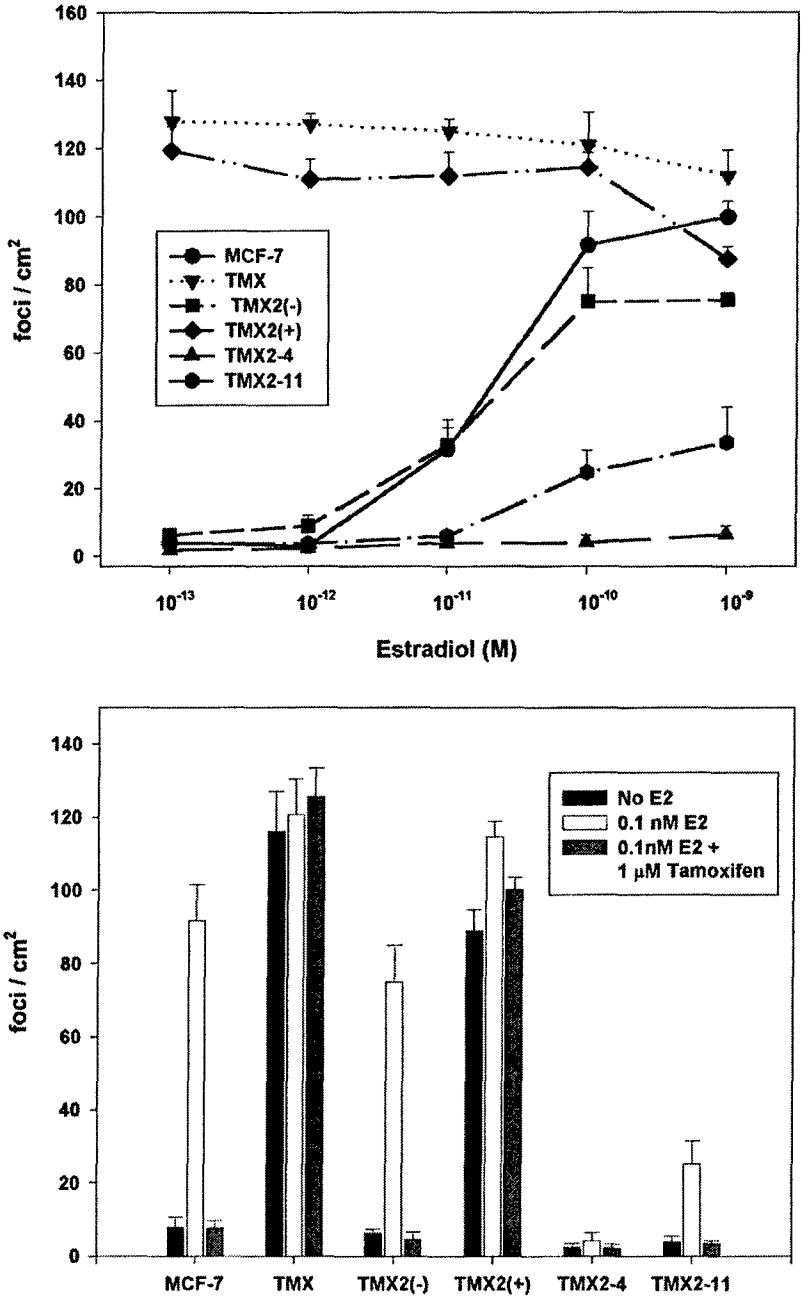

Fig. 7. Sensitivity of foci formation to the presence of E2 and tamoxifen among the various MCF-7 cell populations. Upper panel: comparison of postconfluent formation of foci by the various cell populations as a function of E2 concentration. ERα protein expression is that shown in the Western immunoblot of Fig. 4. Bottom panel: comparison of tamoxifen (10^{-6} M) inhibition of E2 (10^{-10} M) induction of postconfluent formation of foci among the various cell populations. Error bars are the S.E.M. of four replicates. Experimental conditions for the focus assay were as described under Section 2.

et al. (2001) also found that ERα negative MCF-7 clones (isolated from cultures deprived of E2) exhibited increased basal cell growth relative to the parent MCF-7 population, and that E2 was not a growth stimulant. These hormone-independent and tamoxifen-insensitive growth characteristics in the ERα negative cells thus mimic the more uncontrolled and aggressive growth phenotypes associated with ERα negative breast tumors and may provide useful models to uncover novel cellular pathways associated with this phenotype.

During the first 6 months of the second of the two exposure experiments, a novel population (TMX2) emerged that over-expressed a 61 kDa ERα protein and an ERα mRNA that was demonstrated by nucleotide sequencing to be missing exon 3. Several subsequent studies detailed in Section 3 provided compelling

evidence that the 61 kDa ERα protein is missing the 39 internal amino acids encoded by exon 3. The two designations of 61 kDa protein and ERΔ3P are, therefore, interchangeable throughout this text.

Many alternatively spliced ERα mRNA variants have been described (Poola et al., 2000; Murphy et al., 1997; Dowsett et al., 1997), but only in a few instances have expression of their corresponding proteins been detected. ERΔ5P and ERΔ4P were detected in breast tumors and ovarian normal and tumor tissue extracts, respectively (Desai et al., 1997; Park et al., 1996). A 77 kDa ERα expressed from ERα mRNA containing duplications in exons 6 and 7 is also expressed in an MCF-7 cell clone that grows optimally in the absence of E2 (Pink et al., 1996). ERΔ7P is expressed in the ERα positive breast tumor cell lines MCF-7, T47D, and ZR-75, and in some ERα-positive tissues and tumors (Fasco et al., 2000). To our knowledge, this study records the first time that ERΔ3P has been detected as a naturally occurring variant. Particularly striking is that its amount in many of the clones isolated exceeds the amount of ERα.

The isolation of cell populations expressing various ERΔ3P/ERα ratios in a normally regulated cellular environment provides a unique opportunity to examine the effects of ERΔ3P expression on a variety of E2-dependent processes. Of the identified ERα splice variants, ERΔ3P most resembles ERα, missing only 39 amino acids in the DNA binding domain. Because ERΔ3P efficiently binds E2, it possesses the potential to form liganded heterodimers with ERα and ERβ or homodimers that could possess dominant negative or dominant positive transcriptional activities or affect cross-talk pathways. Cells expressing exclusively ERΔ3P could also be used to probe transcriptional events of ERα, that are not dependent on its DNA binding domain. Most importantly, steady-state ratios of ERΔ3P/ERΔ3 mRNA are equivalent to those of ERα demonstrating that this receptor form is not a target for a reduced rate of synthesis and/or enhanced degradation as occurs with ERΔ7P (Fasco et al., 2000). ERΔ3 mRNA has been found in normal breast epithelium (Erenburg et al., 1997) and in a variety of ERα positive cell lines and breast tumors (Poola et al., 2000; Poola and Speirs, 2001). If the level of ERΔ3 mRNA expression is sufficient to support translation, it is probable that ERΔ3P is also expressed in these tissues and tumors.

Cell lines that over-express ERΔ3P also offer a means to evaluate how a naturally expressed ERα variant affects E2-dependent reactions compared with ERΔ3P expressed in cells from a transfected gene. In the two ERΔ3P expressing clones studied here, whose ERΔ3P to ERα ratios were approximately 1:1 and 4:1, E2 effectively up-regulated the endogenous E2-dependent genes PgR, pS2 and HEM45 and a luciferase reporter containing an ERE, demonstrating that ERΔ3P does not possess strong dominant negative activity against ERα. In contrast, ERΔ3P expressed from a transfected gene exhibited strong dominant negative activity against a similar ERE construct (Bollig and Miksicek, 2000) and MCF-7 cells expressing ERΔ3P from a transfected gene exhibited reduced anchorage-independent growth as well as a 93% reduction in E2 mediated pS2 up-regulation (Erenburg et al., 1997). A unique and not well understood aspect of E2-regulated cell growth is that some of the E2-dependent pathways are subject to "uncoupling", such as occurs in the ERα positive/PgR negative breast tumor phenotype. Based on the studies presented here, installation of ERα or any its variants by transfection does not ensure restoration of the actual E2-dependent receptor functions that normally occur within a cell. Indeed, in only one published study have ERα-transfected cells been isolated that exhibit an E2-dependent, positive growth response and this occurrence was from a MCF-7 cell clone that had lost its receptor during long-term E2 withdrawal (Oesterreich et al., 2001). ERα-negative cells transfected with ERα are normally growth-inhibited by E2 (Zajchowski et al., 1993; Shao et al., 1997).

The cellular phenotypes responsible for the emergence of cells that over-express ERΔ3P in an environment deficient in E2 and rich in the agonist/antagonist tamoxifen are an enigma. Culture of the TMX2–4 and TMX2–11 clones in E2-deficient, tamoxifen-free media for a prolonged period has not altered their ERΔ3P/ERα expression demonstrating that ERΔ3P expression is not epigenetic, but due to a stable genomic modification. When the heterogeneous TMX2 population was transferred to the same medium, ERΔ3P over expressing cells essentially disappeared and a population emerged that expressed primarily wild-type ERα; suggesting that ERΔ3P over expressing cells somehow require tamoxifen for their survival in a mixed cell milieu. However, in the TMX2–4 and TMX-11 clones examined, postconfluent cell growth of foci was inhibited by tamoxifen and required much higher levels of E2 than the parent cells. Additionally, no obvious correlation exists between the ability of E2 to support postconfluent cell growth and the presence of ERΔ3P. TMX2–11 cells expresses nearly twice as much ERα and ERΔ3P combined than do TMX2–4 cells, and ERΔ3P/ERα at a proportion approximately 1.5 times higher, yet the TMX2–4 cells are much less responsive to E2 with respect to the growth of foci. Preliminary studies with the other clones co-expressing ERΔ3P and ERα at various concentrations and proportions (data not shown) have similarly failed to indicate that a relationship exists between the E2-dependent growth of foci and the presence of ERΔ3P. A transcriptionally functional receptor does apparently exist in the TMX2–4 and TMX2–11 clones, however, because E2 up-regulated all the E2-dependent

genes examined as efficiently as it does in the parent MCF-7 cells (Fig. 6). From a mechanistic perspective, therefore, it appears that factors other than, or in addition to, the expression of ERΔ3P might be involved in the responses observed and more in-depth studies regarding the role of ERΔ3P in E2-dependent transcription and the cellular pathways that participate in E2-regulated growth are required. Whether ERΔ3P overexpression also occurs in breast tumors, and particularly in the tumors of patients who have received tamoxifen for a prolonged period or whose ERα positive tumors have become tamoxifen resistant also awaits future study.

In summary, prolonged exposure to tamoxifen produced ERα protein expression and cell-survival and growth changes in our MCF-7 cell line that were detectable without the aid of cloning. ERΔ3P was identified as an over expressed protein in a heterogeneous cell population cultured in an E2-deficient medium containing tamoxifen. Return of this population to media without tamoxifen resulted in a marked reduction in ERΔ3P over expressing cells, but a similar reversion did not occur with ERΔ3P over expressing cells that were cloned from the TMX2 population. Cloned TMX2 cells naturally over expressing ERΔ3P were E2-responsive toward three endogenous E2-dependent genes, and toward an ERE construct demonstrating that ERΔ3P is a not a strong dominant negative inhibitor of ERα transcriptional activity as had been suggested by transfection studies. Paradoxically, however, these clones require much higher levels of E2 to attain focus formation compared with the parental MCF-7 population. Of the populations examined in the tamoxifen exposure experiments, only those that had lost ERα mRNA and protein expression were tamoxifen-resistant in the focus assay. These populations also formed foci independently of E2.

Acknowledgements

Portions of this work were supported by grants DAMD17-10-0261 (B.T.P.) Department of Defense, Breast Cancer Research Program and 2R42ES09467 (J.F.G.).

References

Arcaro, K.F., Yi, L., Seegal, R.F., Vakharia, D.D., Yang, Y., Spink, D.C., Brosch, K., Gierthy, J.F., 1999. 2,2′,6,6′-Tetrachlorobiphenyl is estrogenic in vitro and in vivo. J. Cell. Biochem. 72, 94–102.

Bollig, A., Miksicek, R.J., 2000. An estrogen receptor-alpha splicing variant mediates both positive and negative effects on gene transcription. Mol. Endocrinol. 14, 634–649.

Brunner, N., Boysen, B., Jirus, S., Skaar, T.C., Holst-Hansen, C., Lippman, J., Frandsen, T., Spang-Thomsen, M., Fuqua, S.A., Clarke, R., 1997. MCF7/LCC9: an antiestrogen-resistant MCF-7 variant in which acquired resistance to the steroidal antiestrogen ICI 182780 confers an early cross-resistance to the nonsteroidal antiestrogen tamoxifen. Cancer Res. 57, 3486–3493.

Dauvois, S., Danielian, P.S., White, R., Parker, M.G., 1992. Antiestrogen ICI 164384 reduces cellular estrogen receptor content by increasing its turnover. Proc. Natl. Acad. Sci. USA 89, 4037–4041.

Desai, A.J., Luqmani, Y.A., Walters, J.E., Coope, R.C., Dagg, B., Gomm, J.J., Pace, P.E., Rees, C.N., Thirunavukkarasu, V., Shousha, S., Groome, N.P., Coombes, R., Ali, S., 1997. Presence of exon 5-deleted oestrogen receptor in human breast cancer: functional analysis and clinical significance. Br. J. Cancer 75, 1173–1184.

Dowsett, M., Daffada, A., Chan, C.M., Johnston, S.R., 1997. Oestrogen receptor mutants and variants in breast cancer [Review]. Eur. J. Cancer 33, 1177–1183.

Erenburg, I., Schachter, B., Lopez, R., Ossowski, L., 1997. Loss of an estrogen receptor isoform (ER alpha delta 3) in breast cancer and the consequences of its reexpression: interference with estrogen-stimulated properties of malignant transformation. Mol. Endocrinol. 11, 2004–2015.

Fasco, M.J., 1997. Quantitation of estrogen receptor mRNA and its alternatively spliced mRNAs in breast tumor cells and tissues. Anal. Biochem. 245, 167–178.

Fasco, M.J., 1998. Estrogen receptor mRNA splice variants produced from the distal and proximal promoter transcripts. Mol. Cell. Endocrinol. 138, 51–59.

Fasco, M.J., Treanor, C.P., Spivack, S., Figge, H.L., Kaminsky, L.S., 1995. Quantitative RNA-polymerase chain reaction-DNA analysis by capillary electrophoresis and laser-induced fluorescence. Anal. Biochem. 224, 140–147.

Fasco, M.J., Keyomarsi, K., Arcaro, K.F., Gierthy, J.F., 2000. Erratum to "Expression of an estrogen receptor alpha variant protein in cell lines and tumors". Mol. Cell. Endocrinol. 166, 155–169.

Fujimoto, J., Hirose, R., Ichigo, S., Sakaguchi, H., Li, Y., Tamaya, T., 1998. Expression of progesterone receptor form A and B mRNAs in uterine leiomyoma. Tumour Biol. 19, 126–131.

Gierthy, J.F., Lincoln, D.W., Kampcik, S.J., Dickerman, H.W., Bradlow, H.L., Niwa, T., Swaneck, G.E., 1988. Enhancement of 2- and 16 alpha-estradiol hydroxylation in MCF-7 human breast cancer cells by 2,3,7,8-tetrachlorodibenzo-P-dioxin. Biochem. Biophys. Res. Commun. 157, 515–520.

Gierthy, J.F., Lincoln, D.W., Roth, K.E., Bowser, S.S., Bennett, J.A., Bradley, L., Dickerman, H.W., 1991. Estrogen-stimulation of postconfluent cell accumulation and foci formation of human MCF-7 breast cancer cells. J. Cell. Biochem. 45, 177–187.

Gierthy, J.F., Spink, B.C., Figge, H.L., Pentecost, B.T., Spink, D.C., 1996. Effects of 2,3,7,8-tetrachlorodibenzo-p-dioxin, 12-O-tetradecanoylphorbol-13-acetate and 17 beta-estradiol on estrogen receptor regulation in MCF-7 human breast cancer cells. J. Cell. Biochem. 60, 173–184.

Gierthy, J.F., Arcaro, K.F., Floyd, M., 1997. Assessment of PCB estrogenicity in a human breast cancer cell line. Chemosphere 34, 1495–1505.

Gustafsson, J., Warner, M., 2000. Estrogen receptor beta in the breast: role in estrogen responsiveness and development of breast cancer. J. Steroid Biochem. Mol. Biol. 74, 245–248.

Herman, M.E., Katzenellenbogen, B.S., 1996. Response-specific antiestrogen resistance in a newly characterized MCF-7 human breast cancer cell line resulting from long-term exposure to trans-hydroxytamoxifen. J. Steroid Biochem. Mol. Biol. 59, 121–134.

Johnston, S.R., Saccani-Jotti, G., Smith, I.E., Salter, J., Newby, J., Coppen, M., Ebbs, S.R., Dowsett, M., 1995. Changes in estrogen receptor, progesterone receptor, and pS2 expression in tamoxifen-resistant human breast cancer. Cancer Res. 55, 3331–3338.

Katzenellenbogen, B.S., Kendra, K.L., Norman, M.J., Berthois, Y., 1987. Proliferation, hormonal responsiveness, and estrogen receptor content of MCF-7 human breast cancer cells grown in the short-term and long-term absence of estrogens. Cancer Res. 47, 4355–4360.

Kushner, P.J., Agard, D.A., Greene, G.L., Scanlan, T.S., Shiau, A.K., Uht, R.M., Webb, P., 2000. Estrogen receptor pathways to AP-1. J. Steroid Biochem. Mol. Biol. 74, 311–317.

Leygue, E., Dotzlaw, H., Watson, P.H., Murphy, L.C., 1998. Altered estrogen receptor alpha and beta messenger RNA expression during human breast tumorigenesis. Cancer Res. 58, 3197–3201.

MacGregor, J.I., Jordan, V.C., 1998. Basic guide to the mechanisms of antiestrogen action [Review 539 refs]. Pharmacol. Rev. 50, 151–196.

Metzger, D., Berry, M., Ali, S., Chambon, P., 1995. Effect of antagonists on DNA binding properties of the human estrogen receptor in vitro and in vivo. Mol. Endocrinol. 9, 579–591.

Mizejewski, G.J., Dias, J.A., Hauer, C.R., Henrikson, K.P., Gierthy, J., 1996. Alpha-fetoprotein derived synthetic peptides: assay of an estrogen-modifying regulatory segment. Mol. Cell. Endocrinol. 118, 15–23.

Murphy, L.C., Dotzlaw, H., Leygue, E., Douglas, D., Coutts, A., Watson, P.H., 1997. Estrogen receptor variants and mutations [Review]. J. Steroid Biochem. Mol. Biol. 62, 363–372.

Oesterreich, S., Zhang, P., Guler, R.L., Sun, X., Curran, E.M., Welshons, W.V., Osborne, C.K., Lee, A.V., 2001. Re-expression of estrogen receptor alpha in estrogen receptor alpha-negative MCF-7 cells restores both estrogen and insulin-like growth factor-mediated signaling and growth. Cancer Res. 61, 5771–5777.

Paech, K., Webb, P., Kuiper, G.G., Nilsson, S., Gustafsson, J., Kushner, P.J., Scanlan, T.S., 1997. Differential ligand activation of estrogen receptors ERalpha and ERbeta at AP1 sites. Science 277, 1508–1510.

Park, W., Choi, J.J., Hwang, E.S., Lee, J.H., 1996. Identification of a variant estrogen receptor lacking exon 4 and its coexpression with wild-type estrogen receptor in ovarian carcinomas. Clin. Cancer Res. 2, 2029–2035.

Pentecost, B.T., 1998. Expression and estrogen regulation of the HEM45 mRNA in human tumor lines and in the rat uterus. J. Steroid Biochem. Mol. Biol. 64, 25–33.

Pentecost, B.T., Mattheiss, L., Dickerman, H.W., Kumar, S.A., 1990. Estrogen regulation of creatine kinase-B in the rat uterus. Mol. Endocrinol. 4, 1000–1010.

Pink, J.J., Jordan, V.C., 1996. Models of estrogen receptor regulation by estrogens and antiestrogens in breast cancer cell lines. Cancer Res. 56, 2321–2330.

Pink, J.J., Jiang, S.Y., Fritsch, M., Jordan, V.C., 1995. An estrogen-independent MCF-7 breast cancer cell line which contains a novel 80-kilodalton estrogen receptor-related protein. Cancer Res. 55, 2583–2590.

Pink, J.J., Wu, S.Q., Wolf, D.M., Bilimoria, M.M., Jordan, V.C., 1996. A novel 80 kDa human estrogen receptor containing a duplication of exons 6 and 7. Nucleic Acids Res. 24, 962–969.

Poola, I., Speirs, V., 2001. Expression of alternatively spliced estrogen receptor alpha mRNAs is increased in breast cancer tissues. J. Steroid Biochem. Mol. Biol. 78, 459–469.

Poola, I., Koduria, S., Chatraa, S., Clarkec, R., 2000. Identification of twenty alternatively spliced estrogen receptor alpha mRNAs in breast cancer cell lines and tumors using splice targeted primer approach. J. Steroid Biochem. Mol. Biol. 72, 249–258.

Porter, W., Saville, B., Hoivik, D., Safe, S., 1997. Functional synergy between the transcription factor Sp1 and the estrogen receptor. Mol. Endocrinol. 11, 1569–1580.

Shang, Y., Hu, X., Direnzo, J., Lazar, M.A., Brown, M., 2000. Cofactor dynamics and sufficiency in estrogen receptor-regulated transcription. Cell 103, 843–852.

Shao, Z., Jiang, M., Yu, L., Han, Q., Shen, Z., 1997. Estrogen receptor-negative breast cancer cells transfected with estrogen receptor exhibit decreased tumour progression and sensitivity to growth inhibition by estrogen. Chin. Med. Sci. J. 12, 11–14.

Simpson, D.A., Feeney, S., Boyle, C., Stitt, A.W., 2000. Retinal VEGF mRNA measured by SYBR green I fluorescence: a versatile approach to quantitative PCR. Mol. Vis. 6, 178–183.

Speirs, V., Parkes, A.T., Kerin, M.J., Walton, D.S., Carleton, P.J., Fox, J.N., Atkin, S.L., 1999. Coexpression of estrogen receptor alpha and beta: poor prognostic factors in human breast cancer. Cancer Res. 59, 525–528.

Vladusic, E.A., Hornby, A.E., Guerra-Vladusic, F.K., Lakins, J., Lupu, R., 2000. Expression and regulation of estrogen receptor beta in human breast tumors and cell lines. Oncol. Rep. 2000, 157–167.

Wang, F., Hoivik, D., Pollenz, R., Safe, S., 1998. Functional and physical interactions between the estrogen receptor Sp1 and nuclear aryl hydrocarbon receptor complexes. Nucl. Acids Res. 26, 3044–3052.

Zajchowski, D.A., Sager, R., Webster, L., 1993. Estrogen inhibits the growth of estrogen receptor-negative, but not estrogen receptor-positive, human mammary epithelial cells expressing a recombinant estrogen receptor. Cancer Res. 53, 5004–5011.

Zwijsen, R.M.L., Wientjens, E., Klompmaker, R., Vandersman, J., Bernards, R., Michalides, R.J.A.M., 1997. Cdk-independent activation of estrogen receptor by cyclin D1. Cell 88, 405–415.

Zwijsen, R.M.L., Buckle, R.S., Hijmans, E.M., Loomans, C.J.M., Bernards, R., 1998. Ligand-independent recruitment of steroid receptor coactivators to estrogen receptor by cyclin D1. Genes Dev. 12, 3488–3498.